

Summer 8-2022

Engineering of Ideal Systems for the Study and Direction of Stem Cell Asymmetrical Division and Fate Determination

Martina Zamponi
Old Dominion University, martinazamponi98@gmail.com

Follow this and additional works at: https://digitalcommons.odu.edu/biomedengineering_etds



Part of the [Biology Commons](#), [Cell Biology Commons](#), [Cellular and Molecular Physiology Commons](#), and the [Molecular, Cellular, and Tissue Engineering Commons](#)

Recommended Citation

Zamponi, Martina. "Engineering of Ideal Systems for the Study and Direction of Stem Cell Asymmetrical Division and Fate Determination" (2022). Doctor of Philosophy (PhD), Dissertation, Electrical & Computer Engineering, Old Dominion University, DOI: 10.25777/h30r-et74
https://digitalcommons.odu.edu/biomedengineering_etds/21

This Dissertation is brought to you for free and open access by the Biomedical Engineering at ODU Digital Commons. It has been accepted for inclusion in Biomedical Engineering Theses & Dissertations by an authorized administrator of ODU Digital Commons. For more information, please contact digitalcommons@odu.edu.

ENGINEERING OF IDEAL SYSTEMS FOR THE STUDY AND DIRECTION OF STEM
CELL ASYMMETRICAL DIVISION AND FATE DETERMINATION

by

Martina Zamponi

B.S. May 2017, Old Dominion University

M.S. August 2018, Old Dominion University

A Dissertation Submitted to the Faculty of
Old Dominion University in Partial Fulfillment of the
Requirements for the Degree of

DOCTOR OF PHILOSOPHY
BIOMEDICAL ENGINEERING
OLD DOMINION UNIVERSITY

August 2022

Approved by:

Robert Bruno (Co-Chair)

Venkat Maruthamuthu (Co-Chair)

Patrick Sachs (Co-Chair)

Michel Audette (Member)

ABSTRACT

ENGINEERING OF IDEAL SYSTEMS FOR THE STUDY AND DIRECTION OF STEM CELL ASYMMETRICAL DIVISION AND FATE DETERMINATION

Martina Zamponi

Old Dominion University, 2022

Co-Directors: Dr. Robert Bruno

Dr. Patrick Sachs

The cellular microenvironment varies significantly across tissues, and it is constituted by both resident cells and the macromolecules they are exposed to. Cues that the cells receive from the microenvironment, as well as the signaling transmitted to it, affect their physiology and behavior. This notion is valid in the context of stem cells, which are susceptible to biochemical and biomechanical signaling exchanged with the microenvironment, and which plays a fundamental role in establishing fate determination and cell differentiation events. The definition of the molecular mechanisms that drive stem cell asymmetrical division, and how these are modulated by microenvironmental signaling, is challenging. Important findings have been described in recent years, corroborating the idea that external stimuli play a fundamental role in development and stem cell physiology. However, speedy progress is hindered by the lack of adequate and highly efficient tools for the study of cellular mechanisms at the single cell level and within a defined and highly controllable environment.

The work presented in this dissertation focuses on the engineering of ideal techniques for the study of the processes that define stem cell asymmetrical division and fate determination, devising systems that overcome the current limitations of this research field. The first goal of this project was the engineering of a 3D bioprinting system in combination with tissue-specific substrates for the establishment of a biomimetic, highly accurate, three-dimensional cell culture system for the study of extracellular matrix impact

on stem cell physiology. Particular focus was posed on the development of an optimal system for the study of the influence of a brain-specific environment on embryonic and neural stem cells' differentiation potential. The second goal of this project was the optimization of a system for the delivery of single cells or single cell – single beads complexes into three-dimensional substrates to enable the performance of high throughput experiments at the single cell resolution. Particular focus was posed on the development of an optimal system for the study of asymmetrical stem cell division driven by discrete signals.

Copyright, 2022, by Martina Zamponi, All Rights Reserved.

ACKNOWLEDGMENTS

The realization of this dissertation would not have been possible without the continuous help and support of those around me. First, I want to thank my family for being by my side on every occasion, always believing in my potential and providing unconditional support. I would like to thank Pete and Megan for always being available to talk, help and collaborate. I would also like to thank the other students in the laboratory, with whom I have shared the highs and lows that were a natural part of my research journey: Julie, Xavier and Mackenzie. I am grateful for my committee members Dr. Michel Audette and Dr. Venkat Maruthamuthu. They agreed to join my advisory committee despite the advanced stage of my program and were extremely supportive and open minded to allow me to meet my departmental requirements. Lastly, I would like to thank my advisors Dr. Patrick Sachs and Dr. Robert Bruno. They always cared for my personal and academic success and have guided me through the graduate research process to achieve my potential and prepared me well for my future endeavors.

TABLE OF CONTENTS

	Page
LIST OF FIGURES.....	vii
Chapter	
I. INTRODUCTION	1
STEM CELLS	1
ASYMMETRIC DIVISION	4
STEM CELL MICROENVIRONMENT AND DIFFERENTIATION	8
TRADITIONAL METHODS FOR STEM CELL RESEARCH.....	18
NOVEL METHODS AND TECHNOLOGIES FOR STEM CELL RESEARCH.....	21
PROJECT AIMS	25
II. EFFECTS OF A BRAIN EXTRACELLULAR MATRIX-DERIVED 3D CELL CULTURE SYSTEM ON STEM CELL CULTURE AND DIFFERENTIATION	28
INTRODUCTION	28
RESULTS	30
MATERIALS AND METHODS.....	72
DISCUSSION	82
CONCLUSION.....	86
III. ENGINEERING OF A BIOPRINTING SYSTEM FOR THE STUDY OF IMMOBILIZED - GROWTH FACTOR DRIVEN ASYMMETRICAL STEM CELL DIVISION	87
INTRODUCTION	87

METERIALS AND METHODS	89
RESULTS	98
DISCUSSION	113
CONCLUSION	115
IV. DISCUSSION	116
BIBLIOGRAPHY	120
VITA	131

LIST OF FIGURES

Figure	Page
1. Stem Cell Potency	3
2. Intrinsic and Extrinsic Forces in Asymmetrical Division	5
3. Canonical WNT Pathway	7
4. Biomechanical Signaling in Embryonic Development	12
5. Production and Characterization of Porcine Brain Derived Hydrogels	33
6. Characterization of Mouse and Human Pluripotent Stem Cell and Neural Stem Cell Lines	36-37
7. Survival and Differentiation Potential of Mouse and Human Neural Stem Cell Lines on Brain ECM Coated Plates	41-43
8. Short-term General Neural Differentiation of Human and Mouse Neural Stem Cells on Brain ECM Coated Plates	45-48
9. Long-term General Neural Differentiation of Human and Mouse Neural Stem Cells on Brain ECM Coated Plates	49-51
10. 3D Bioprinting System for the Delivery of Cells Within Biomimetic Substrates	56
11. Three-dimensional Cell Culture of Mouse Embryonic Stem Cells in Brain ECM Substrates.....	57-58
12. Neural Organoids Formation from Mouse Embryonic Stem Cells in Brain ECM Substrates.....	59-61
13. Three-dimensional Cell Culture of Mouse Neural Stem Cells in Brain ECM Substrates.....	62-64
14. Biocompatibility of Tissue-Specific Hydrogels and Suitability to Promote Cell Survival and Proliferation <i>in vivo</i>	67-71
15. 3D Bioprinting Setup and Optimal Needle Shape for Injection of Individual Cells....	91
16. Immunostaining in Three-dimensional Substrates	97
17. Empirical Determination of the Optimal Extrusion Value for Single-Cell Injections	100
18. Printing, Survival and Proliferation of Individual Cells in Two-dimensional and Three- dimensional Substrates.....	104

Figure	Page
19. Nuclear Staining of Individual Cells in Three-dimensional Substrates	105
20. Printing, Survival and Proliferation of Single Cell-Single Bead Complexes in Three-dimensional Substrates.....	108
21. Localized Wnt3a is Not Sufficient for the Orientation of Asymmetrical Stem Cell Division in Mouse Embryonic Stem Cells.....	111-112

CHAPTER I INTRODUCTION

The cellular microenvironment has been shown to play an essential role in various cellular processes, such as stem cell fate determination and cell differentiation [1-4]. The *in vivo* histological organization, the biochemical composition of the environment, as well as the external forces to which they are subjected, influence stem cell physiology and behavior.

The work presented here develops ideal models for the study of the impact of a cellular microenvironment on stem cell differentiation and fate determination. The first goal of this project was the engineering of a 3D bioprinting system in combination with tissue-specific substrates to establish a biomimetic, highly accurate, three-dimensional cell culture system for the study of extracellular matrix impact on stem cell physiology. Particular focus was posed on the development of an optimal system for the study of the influence of a brain-specific environment on embryonic and neural stem cells' differentiation potential. The second goal of this project was the optimization of a system for the delivery of single cells or single cell – single beads complexes into three-dimensional substrates to enable the performance of high throughput experiments at the single cell resolution. Particular focus was posed on the development of an optimal system for the study of asymmetrical stem cell division driven by discrete signals.

Stem Cells

Differentiation is the process that allows the generation of cellular diversity via the formation of specialized, terminally differentiated cell types. It is characterized by an interruption of the cell cycle and the development of each cell's characteristic structures and functional properties [5]. The undifferentiated cells from which all the different types of somatic cells of the organism originate are known as stem cells. Stem cells are identified based on their differentiation potential, an attribute known as “potency”, which defines the diversity of cell types that a single stem cell can subsequently generate. They can be classified as either totipotent, pluripotent, multipotent, oligopotent or unipotent stem cells [6]. Totipotent stem cells can divide and differentiate into any cells of an organism, including those found in the four extraembryonic tissues. This property allows

for the formation of a developing embryo and the associated placenta after fertilization, all arising from a single totipotent cell.

Pluripotency is defined as the ability of a cell to differentiate into another cell belonging to any of the three germ layers (endoderm, mesoderm, or ectoderm), a defining property of embryonic stem cells (ESCs). Any adult cell can arise from pluripotent cells; however, on their own, they lack the ability to organize into an embryo able to successfully develop. *In vivo*, the presence of ESCs is transient [7] and localized to the inner cell mass of the pre-implantation embryo [8]. Cells with the same properties as ESCs can be generated *in vitro* starting from somatic ones and are known as induced pluripotent stem cells (iPSC). Multipotent stem cells are found in developed tissue and can only generate cell types with specificity restricted to the tissue in which they are located, playing fundamental roles in organogenesis and regeneration [9-11]. Stem cells with restricted potency compared to ESCs that are found in the developed organism are also referred to as adult stem cells. An example is provided by hematopoietic stem cells, found in bone marrow and responsible for the formation of the cell lineages circulating in the blood, or neural stem cells, responsible for the formation of neurons and the supporting glial cells present in the nervous system [12]. In contrast, oligopotent stem cells can only differentiate into a few, closely related mature cell types [11]. An example is myeloid stem cells, which are themselves derived from hematopoietic stem cells, and can only further differentiate into cells of the lymphatic system [13]. Finally, unipotent cells can only produce one cell type, while retaining their ability to divide into new stem cells over many generations. These are found in tissue types that regenerate on a regular basis, such as skin, and are fundamental in tissue repair processes [14]. While making this classification, it is important to consider that the potency of cells is likely only understandable within the specific context of their microenvironment, as changing the location of a cell within the organism can drastically affect its differentiation potential [15, 16]. Figure 1 shows a visual representation of stem cell potency, in which stem cells with higher differentiation potential can “branch out” further and originate many different cell types compared to cells of lower potency.

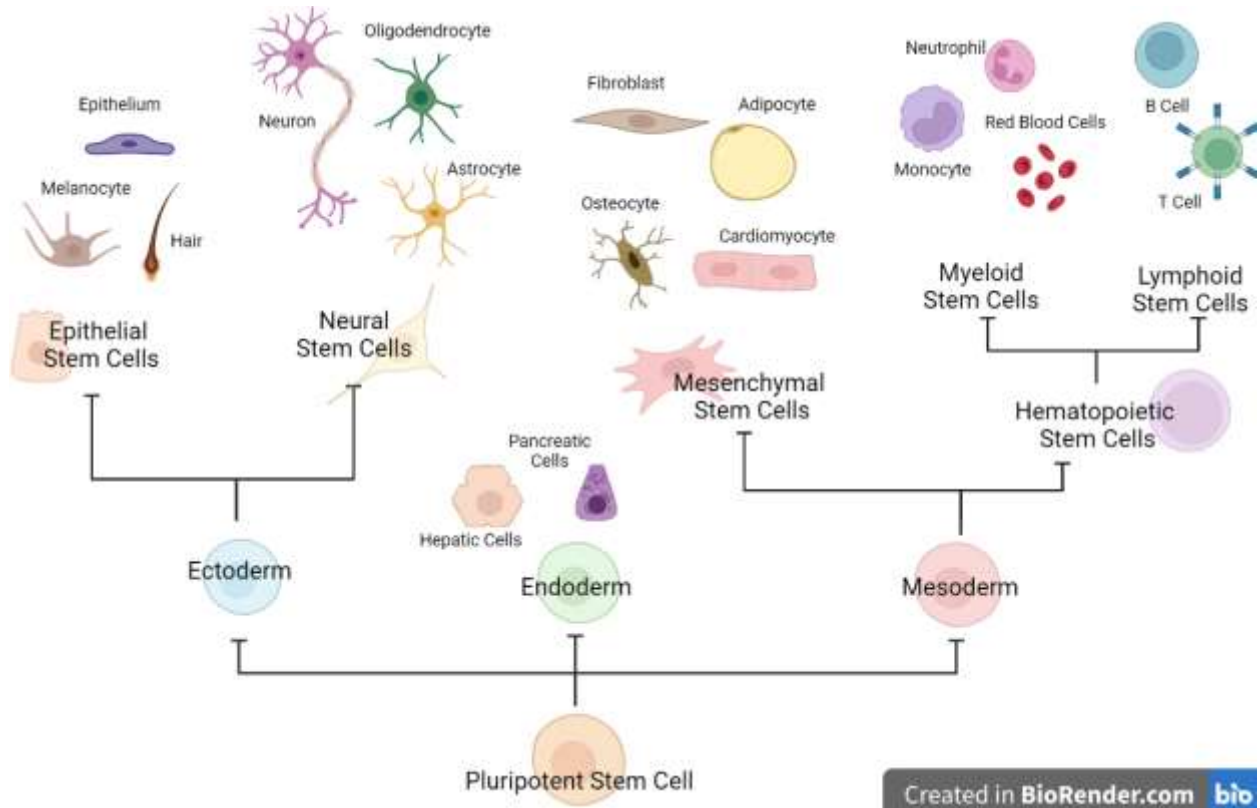


Figure 1: Stem cell potency. Stem cells with higher differentiation potential can “branch out” into many differentiate layers, in contrast to cells further down their differentiation path.

Asymmetric Division

The mechanism that allows stem cells to maintain a state of self-renewal and at the same time allows them to differentiate into mature cells is known as asymmetric cell division. Symmetric cell division results in the formation of two identical daughter cells while stem cell asymmetric division creates two daughter cells directed towards different fates, a new stem cell and a differentiated one. The process of asymmetric division can be initiated by two main mechanism types, intrinsic and extrinsic ones (Figure 2). In the first case, the formation of two different daughter cells is initiated following the polarization of intracellular fate determinants [17]. The segregation of protein and signaling pathways components prior to cell division is a determinant of the mitotic spindle orientation, ultimately affecting the asymmetrical inheritance of intracellular components [18]. An example of an intrinsic asymmetry in the division process is provided by the centrosome inheritance. Only one daughter cell inherits a maternal centriole, leading to the two daughter cells possessing centrosome-components with different ages. The maternal centrosome (containing the original centriole) possesses unique structures from the newly formed centrosome, which also provides superior organizing abilities, resulting in asymmetrical localization of proteins and divergence in the molecular composition of mother and daughter centrioles prior to cell division [19, 20].

Extracellular factors presented asymmetrically to the daughter cells may also promote cell differentiation or quiescence, giving rise to daughter cells of different fates [17, 21]. Such factors are constituted by signaling molecules found in the local microenvironment in which the stem cells reside and which can activate downstream transcriptional pathways that lead to cell division and differentiation. The orientation of the stem cells within the tissue microenvironment defines the localization of transcription factors relative to the cells, ultimately influencing the orientation of the cell division event and the daughter cells' fates.

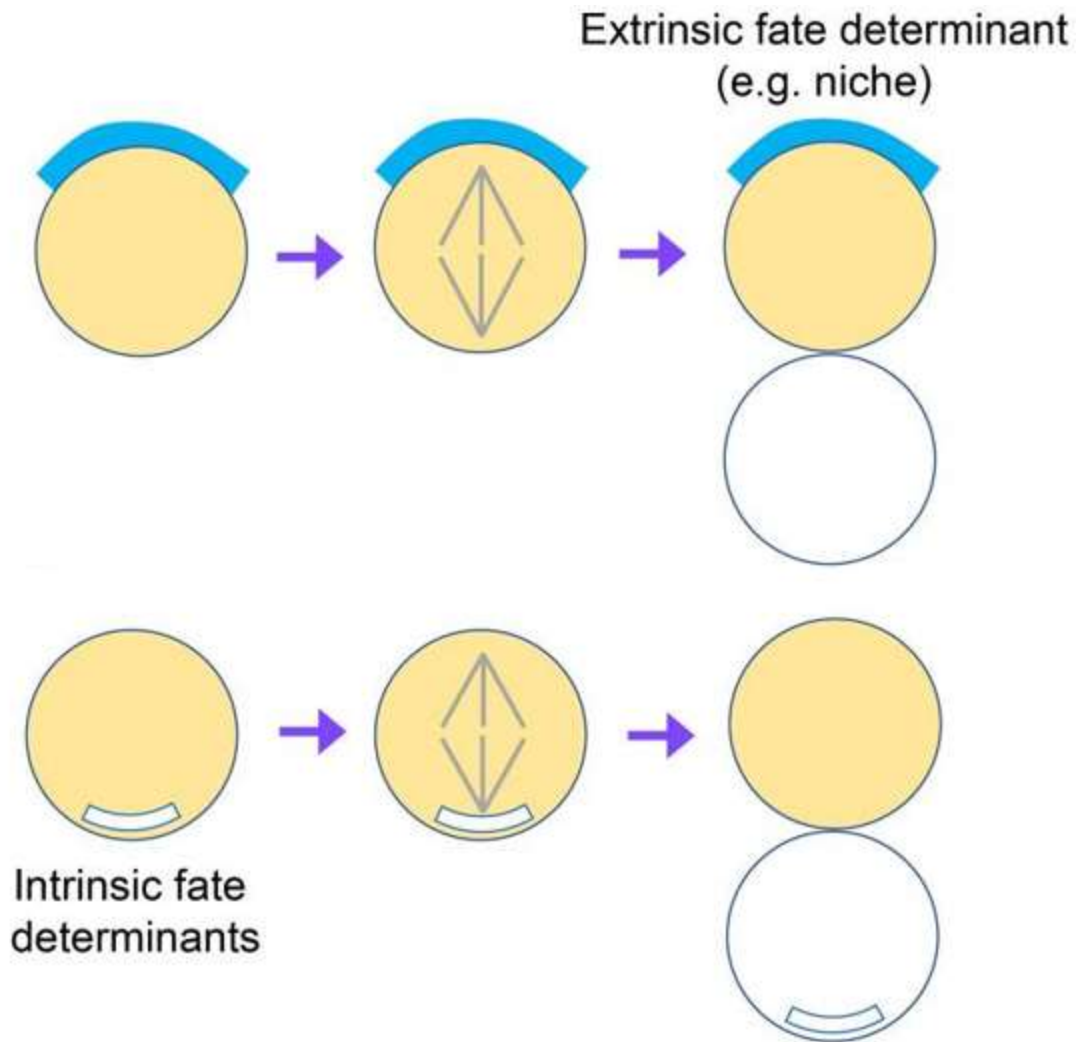


Figure 2: Intrinsic and Extrinsic Forces in Asymmetrical Division. Representation of intrinsically and extrinsically driven asymmetrical division of stem cells. When the fate determinant is intrinsic, their localization within the cell determined the fate of the daughter cells. When the fate determinant is extrinsic, the way in which it interacts with the mother stem cell affects the orientation of the cell division process, determining the fate of each daughter cell. Figure adapted from Venkei et al. [17], PMC6219723.

One of the growth factors that have been widely recognized to affect the determination of stem cell fate is the WNT class of proteins [22]. WNT proteins can affect cell function through two main signaling pathways categories: canonical and non-canonical. Their distinction resides in the notion that canonical pathways are β -catenin dependent, while non-canonical pathways are not. Although both classes of WNT pathways are associated with a plethora of cellular functions, the canonical ones have been found to affect stem cell division and fate determination. Under normal conditions, and in absence of environmental WNT, intracellular β -catenin is degraded by a protein complex consisting of Axin, glycogen synthase kinase-3 (GSK-3), casein kinase 1 (CK1) and adenomatous polyposis coli (APC) [23] (Figure 3). When WNT is present in the environment, it binds to the cell surface protein Frizzled (FZD) and low-density lipoprotein receptor-related protein (LRP5/6). The newly formed complex recruits the Axin and Disheveled proteins, which in turn displace the other components to which they are associated for the β -catenin degradation process. Relocation of the destruction complex towards the cell membrane results in the loss of its functionality and a consequent accumulation of intracellular β -catenin. At this point, the protein can relocate to the cellular nucleus, where it forms a complex with transcription factors to activate the transcription of WNT target genes [22, 24]. In mouse embryonic stem cell models, WNT signaling has been shown to be an essential and limiting factor in regulating the transition from pluripotent embryonic stem cells to epiblast stem cells, a cell type in which the epigenetic machinery that supports the differentiation towards embryonic cell types is activated [25]. More specifically, in the context of asymmetric stem cell division, localization of WNT growth factors have been shown to promote the maintenance of a pluripotent state, while allowing for differentiation of the distal daughter cell [26].

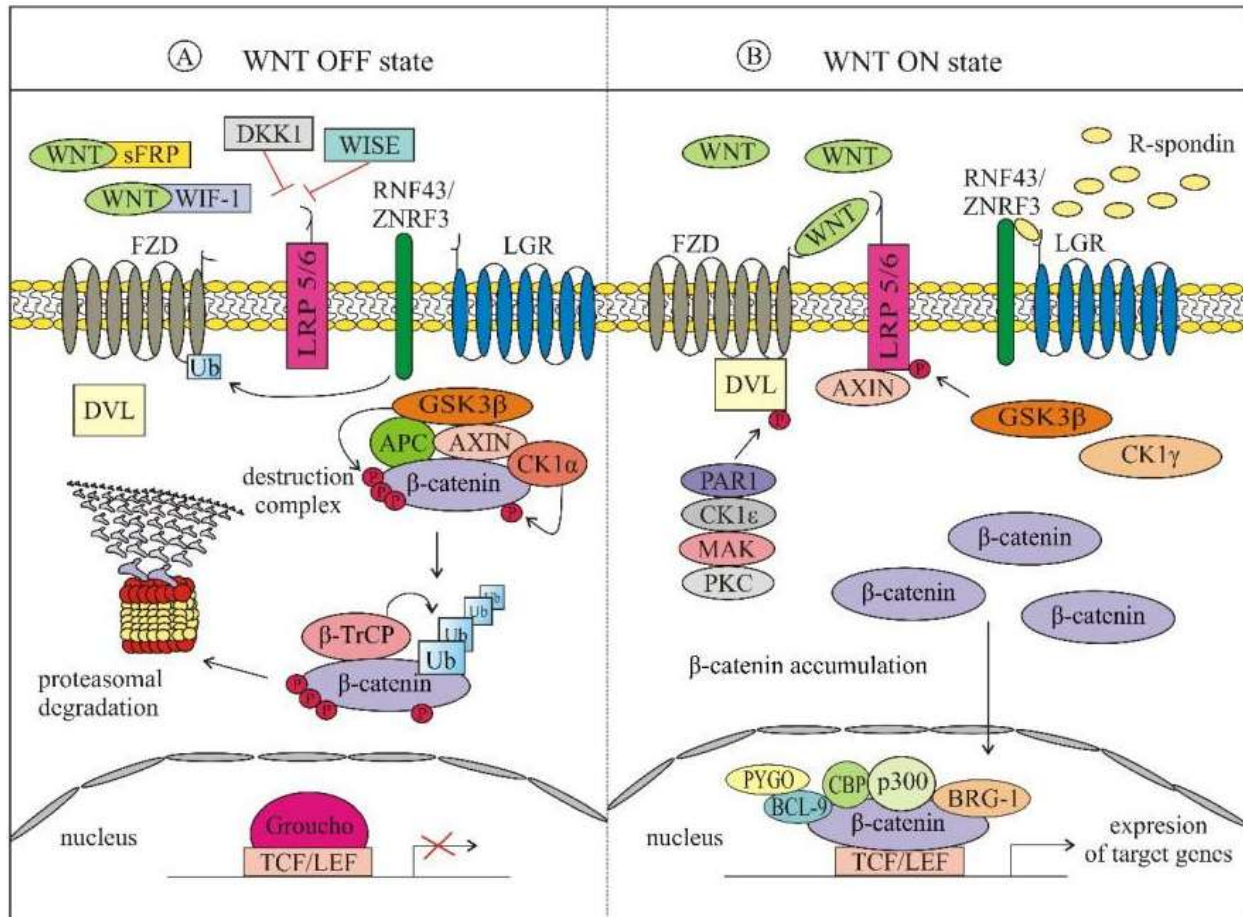


Figure 3: The Canonical WNT Pathway. (A) In absence of WNT, β -catenin is not accumulated and transcription of Wnt target genes does not occur. (B) Environmental WNT binds to surface proteins LRP and FZD, ultimately resulting in the intracellular accumulation of β -catenin, which in turns activates the transcription of WNT target genes inside the nucleus. Figure adapted from Gajos-Mischnewics et al, PMC7402324 [27].

Stem Cell Microenvironment and Differentiation

The Stem Cell Niche

Adult stem cells reside within different tissues of developed organisms and allow us to maintain local tissue homeostasis. The unique location in which stem cells are found within the tissue is known as a stem cell niche, a concept first postulated by Schofield in 1978. He defined a “niche” as the *in vivo* microenvironment in which the cells are physically located and receive and exchange stimuli that influence their fate [28]. The stem cell microenvironment is comprised of a parenchymal cell, stromal cells, and extracellular matrix proteins, signaling molecules, as well as any other stem or differentiated cells that reside in the same area [15 148]. The stimuli that the stem cells receive within the niche include cell-cell and cell-matrix interactions and are responsible for the activation and repression of genes and transcription. They allow for the maintenance of stem cells in a quiescent state, in which division does not occur but the regular functioning of the cell cycle can be triggered by normal physiological stimuli, and the proliferative potential of the stem cells is preserved [29-31]. Stem cell niches possess an intrinsic plasticity that allows them to coordinate the stem cells’ behavior to maintain the homeostasis of the tissue in which they are located [30, 32]. In fact, removal of cells from the niche would result in loss of stemness and self-renewal capacity, as well as initiation of differentiation [15, 33].

Extracellular Matrix

One major constituent of the cellular microenvironment is the extracellular matrix (ECM). The ECM is a three-dimensional architectural network comprised of proteins and macromolecules secreted by the tissue resident cells. The molecular composition of the matrix is extremely variable and unique, to support the specific functions of each tissue [31]. The coordination and cooperation of the various ECM components provide for structural integrity of tissue as well as allowing for cellular attachment. It is a widely accepted concept that the ECM plays a great role in the regulation of cellular physiology, motility, survival, differentiation, and attachment. Thus, it is a key player in the maintenance of local tissue homeostasis [34, 35].

The mammalian ECM is constituted by over 300 different types of proteins, which are collectively known as the matrisome. The main macromolecular components found in human ECM are collagens, proteoglycans (PGs) and glycosaminoglycans (GAGs), elastin and elastic fibers, laminins, fibronectin, and other proteins/glycoproteins such as matricellular proteins [35]. Collagens are the most abundant proteins in the human body. Within the ECM they are a fibrous type of protein composed of three polypeptide α chains that form a triple helical structure. There are 28 distinct types of collagens which can organize into fibrils, fibers, networks, matrices, or other three-dimensional structures. Types I, II and III collagen are largely abundant in the ECM. In general, collagen fibers are stiff and provide non-linear responses to stimuli, conferring strength and structure to the ECM [36, 37, Karamanos, 2021 #1164]. Glycosaminoglycans are negatively charged polysaccharide compounds constituted of repeating disaccharides units. The four primary categories of glycosaminoglycans are heparin/heparan sulfate, chondroitin sulfate/dermatan sulfate, keratan sulfate, and hyaluronic acid, and are distinguished based on their core disaccharide units. In the context of the extracellular matrix, this class of macromolecules plays a role in structural scaffolding and cell signaling [38]. Proteoglycans are compounds formed by a core protein covalently bound to a glycosaminoglycan, and can be classified into intracellular, cell-surface, pericellular and extracellular proteoglycans [39]. The negatively charged glycosaminoglycan chains allow sequestering water within the ECM providing for tissue hydration, resistance to compression forces, and trapping of growth factors within the matrix. Elastic fibers are abundant in the ECM of tissues that are subjected to repeated stretching, such as blood vessels, lungs, and heart. Elastin is the protein responsible for imparting elasticity to the matrix, and it interacts with the proteins fibrillin and microfibril-associated glycoprotein-1 for proper network assembly. Elastic fibers are produced during development to gradually decompose during adulthood and, in addition to their structural function, they participate in cell signaling and growth factors storage in the matrix [35, 36]. Finally, fibronectin is a macromolecule secreted in the form of dimers bound together by disulfide bonds, and it possesses binding sites for other ECM components. It is a critical component that supports cell migration and attachment as it plays a role in the organization of the actin cytoskeleton [36, 40, 41]. Fibronectin plays a key role in the initiation, progression, and

maturation of matrix assembly, as well as being a fundamental component in wound healing processes.

The ECM is a highly dynamic environment, and its continuous remodeling is now understood to be a fundamental part of normal organism development and homeostasis. The concept of matrix remodeling refers to the balance between matrix production and secretion from the tissues' cells, as well as its alteration and degradation, all necessary for proper tissue function. Specific enzymes, such as metalloproteinases, are responsible for the controlled degradation of ECM, which allows for branching morphogenesis during organism development as well as leading to the release of growth factors trapped in the matrix [42]. Controlled remodeling of the ECM is also what allows for the physical and biochemical changes that occur during wound healing and tissue repair processes. Dysregulation of the ECM remodeling mechanisms can result in diseases, with tissue destruction in the event of hyperexpression of genes associated with proteinases production and tissue fibrosis in the event of excessive ECM production and accumulation. The key role of the ECM in normal tissue development is also demonstrated by embryonic lethality in the event of mutations in the genes that code for key protein components [43].

The role of the extracellular matrix in the maintenance of tissue homeostasis includes the facilitation of cell-cell and cell-matrix signaling to regulate cell motility, proliferation, and differentiation. Biomechanical and biochemical signals from the ECM affect the tendency of stem cells to proliferate, as well as their fate determination during cell differentiation.

Biomechanical Signaling in Stem Cell Differentiation Regulation

Mechanical signaling in the context of cell physiology refers to all the cues that the cells can sense following the application of a force. Stem cells during embryonic development and adulthood receive a plethora of mechanical signals from their niche, to which they respond through mechanosensing and mechanotransduction. These mechanical interactions, mediated by adhesion to the ECM and between cells, will ultimately affect the proliferation, organization, and differentiation potential of the stem cells by regulating intracellular signaling pathways [44]. The type of biomechanical cues

that affect stem cell physiology can be classified into two main categories: intrinsic and extrinsic forces. Intrinsic forces are generated by the cells and exerted on the external environment, while extrinsic forces are generated by the environment and perceived by the cells.

Biomechanical signaling is crucial for all stages of embryonic development (Figure 4). Intrinsic and extrinsic signals are fundamental for the formation of higher order structures. Moreover, the mechanical coupling between cells and ECM during early development enables the storage of information over time. Modulation of the ECM during early development can trigger changes in cell behavior and tissue organization at later stages [44]. During the pre-implantation stage, contractile mechanical cues lead to a transition of the embryo from a spherical to elongated shape, which consequently enable its specification and organization into the three germ layers [45]. At the early stages of embryonic development, cell-cell interactions, rather than cell-ECM ones, are prevalent as ECM production increases progressively with embryonal growth. Here, tensile and compressive forces, mostly generated by intracellular actomyosin, are responsible for the establishment of the embryo's anterior-posterior axis, while fluid shear forces are responsible for the establishment of its right-left patterning [44]. In later stages of embryonic development, higher amounts of extracellular matrix are produced by the cells and deposited in the environment, and cell-ECM interactions start playing a more important role in organogenesis and tissue development. Local ECM composition is essential in the determination of a cell's fate at this stage, as it allows the cells to put mechanical signals into a relevant context. The presence of mechanical forces, such as tensile forces derived from intrauterine breathing; shear forces originating from blood flow; and stress, strain and hydrostatic pressures, with the specific ECM context, allow for the expression of patterning genes and organogenesis initiation. [46-50].

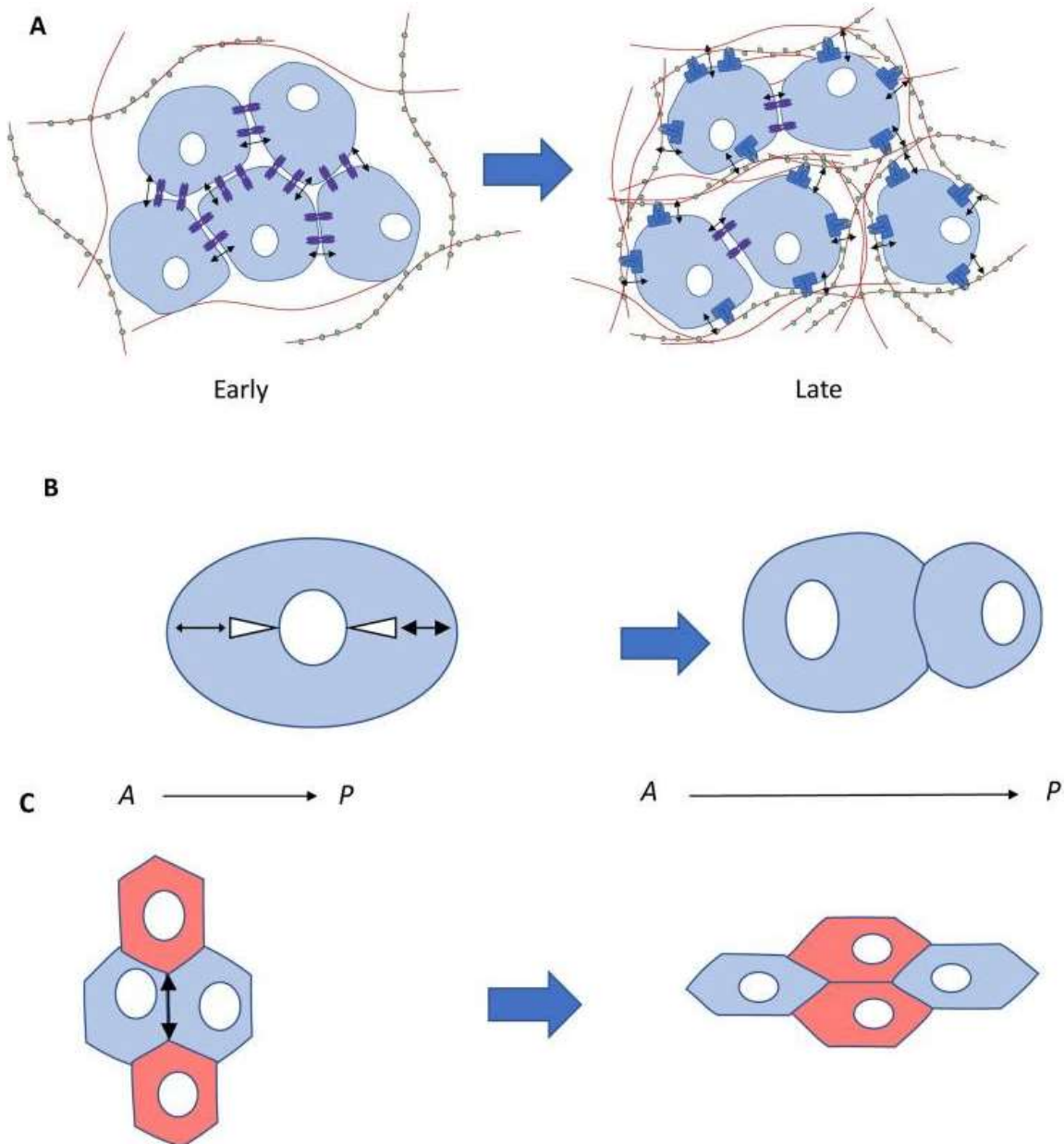


Figure 4: Biomechanical signaling affects all stages of organism development. (A) At earlier stages of development, the organism produces lower levels of ECM, therefore cell-cell interactions are the most significant. Throughout development, ECM is secreted, and cell-ECM interactions become more relevant. (B) Tensile and compressive forces, mostly generated by intracellular actomyosin, are responsible for the establishment of the embryo's anterior-posterior axis. (C) Fluid shear forces are responsible for the

establishment of its right-left patterning. Figure adapted from Vining et al, PMC5803560 [44].

Mechanotransduction and mechanosignaling are determinants of stem cells' proliferation, self-renewal, fate determination and differentiation also in the context of adult stem cells. The three types of interactions that affect adult stem cell physiology through biomechanical signaling are cell-cell, cell-substrate, and external stimuli.

Cell-cell contact entails interactions between cells of the same type (homotypic) or different ones (heterotypic), and it has been found to play a role in the maintenance of stem-cell character versus differentiation variably in different stem cell types. One example was reported by Tang et al. in 2010 in a study conducted on rat bone marrow mesenchymal stem cells (MSC) [51]. The authors plated MSCs in clusters of variable sizes and cultured the cells in either osteogenic or adipogenic media over the course of 6 days. Downstream assays were performed to evaluate the differentiation state of each cell cluster, and the authors reported that larger cell clusters exhibited a significantly higher degree of differentiation compared to smaller clusters or cells plated individually. The authors concluded that higher degrees of cell-cell contact favor mesenchymal stem cell differentiation and suggested a possible involvement of gap junctions, which form between cells in the process. In a second study published in 2017, Jiao et al. evaluated the proliferation and differentiation ability of mouse neural stem cells/neural progenitor cells (NSCs/NPCs) when cultured as single cells or in cell clusters [52]. They showed that NSCs/NPCs were able to proliferate more efficiently when plated as clusters (spheroids) compared to single cells, in which case viability was reduced. Moreover, NSCs/NPCs cultured as spheroids presented a predisposition to differentiate towards the neuronal cell type, while those plated as single cells tended to differentiate into astrocytes. The authors concluded that different cell aggregation states influence the survival and differentiation potential of mouse NSCs/NPCs and suggested a possible role of Cx45 gap junctions in this process. The results reported by each group are just two examples of the fact that cell-cell contact plays a role in the determination of stem cell survival and proliferation state, and that other factors such as environmental conditions and specific cell types affect these processes.

Cell substrate contact entails interactions between cells and the surrounding environment, constituted by extracellular matrix *in vivo*, and two or three-dimensional matrices *in vitro*. Mechanical properties of the substrate can alter the way in which

mechanical signals are perceived by the cells, and consequently impact the stem cell differentiation process. A first property that has been shown to strongly affect stem cell fate and behavior is extracellular matrix stiffness. Several studies conducted in recent years have provided evidence supporting the notion that the stiffness of the matrix alone can direct stem cell fate determination. Bone marrow mesenchymal stem cells (MSCs) are a class of stem cells that can differentiate into adipocytes, osteoblasts, myocytes, and chondrocytes. Park et al. demonstrated that the stiffness of the matrix utilized for MSCs culture can alone promote the differentiation into certain lineages over others, specifically with soft substrates promoting chondrogenic differentiation and stiff substrates promoting differentiation into smooth muscle cell [53]. Similarly, Engler et al. demonstrated that softer matrices promote neurogenic differentiation, stiffer matrices promote myogenic differentiation, and comparatively rigid ones promote osteogenic differentiation of mesenchymal stem cells [54]. The adaptation of softer matrices in the context of stem cell research has also been shown to provide a favorable environment for the successful reprogramming of MSC and the formation of more robust induced pluripotent stem cell colonies compared to stiffer substrates [55]. Similar studies have been performed to explore the role that substrate stiffness plays in neural stem cell differentiation. Saha et al. demonstrated that differentiation of mouse neural stem cells is affected by substrate stiffness, with softer substrates promoting neuronal differentiation and stiffer ones promoting astrocyte differentiation [56]. A second property of the substrates that can be taken into consideration is viscoelasticity, which defines its ability to flow and dissipate stress. A viscoelastic matrix has the potential to allow cells to reversibly change their shape, and this property has been implicated in adult stem cell differentiation. A study published by Chadhuri et al. demonstrated that MSCs cultured in substrates with faster relaxation times promoted osteogenic differentiation over adipogenic one [57].

The third type of stress that adult stem cells can be subjected to are those resulting from the application of external stimuli. One example of such is external loading. The effects of this type of stimulus on stem cell fate were studied in 2016 by Wang et al., who demonstrated that application of cyclical mechanical loading to MSCs in culture induced osteogenic differentiation [2]. A second type of external mechanical stimuli the cells can be subjected to is fluid shear stress. Based on two separate studies conducted in 2005

and 2006, Datta et al. showed that exposure to fluid shear stresses promotes calcium deposition rat MSCs [58, 59]. Mineral deposition is a fundamental step in the formation of new bone tissue, therefore the increase in calcium deposition was suggestive of the fact that shear stress influences the stem cell differentiation process, promoting osteogenic differentiation in MSCs.

The biochemical mechanisms that allow for the differentiation of stem cells down one preferential lineage in response to biomechanical stimuli have yet to be elucidated. The implication of different cellular components in directing the process has been the subject of much research. Some of the elements that have been hypothesized to take part in this process are focal adhesions, cellular cytoskeleton, Rho pathway and the cell nucleus. Focal adhesions (FA) are defined as the type of adhesive contact between cells and the extracellular matrix, or an alternate substrate. The formation of such structures is mediated by the transmembrane proteins, integrins. Following the attachment of the cells to their substrate, clusters of focal adhesions form, and signaling pathways are activated. Changes in the physical structure and characteristics of the substrate may affect the ability of cells to form focal adhesions. The variability of focal adhesions may alter the pattern of signaling activation and consequently affect stem cell fate determination [60]. The cell cytoskeleton is a complex network of protein filaments that extends across the cell, playing a fundamental role in cell proliferation, motion, and differentiation. Cytoskeletal contractility, regulated by components such as non-muscle myosin II and actin, enables the cells to perceive substrate stiffness. Additionally, the cytoskeleton regulates cell elongation and attachment to the substrate, regulating the cell's ability to establish focal adhesions. Combined, these properties allow for the regulation of stem cell differentiation in the patterns described in previous sections [60-62]. The Rho pathway is a signaling pathway mediated by the Rho family of GTPases. This class of molecules has been associated with the regulation of actin dynamics. The pathway has been directly linked to stem cell fate determination, as it is activated when osteogenic differentiation is initiated following application of mechanical forces, and it is inhibited in the contexts of adipogenic and chondrogenic differentiation [60, 61]. The nucleus is a final component of the cell that has been directly implicated in cell fate regulation in response to mechanical stimuli. Thanks to the intracellular cytoskeleton, the nucleus is directly

connected to the ECM, and mechanical stimuli are easily propagated. Additionally, expression levels of genes associated with stem cell differentiation have been found to be directly affected by mechanical stimuli [60, 62].

Biochemical Signaling in Stem Cell Differentiation Regulation

Biochemical signaling refers to the cues that cells can sense following the presence of a substance in their environment. The types of signaling that stem cells receive within the niche can be classified as autocrine, paracrine, and systemic signaling. Autocrine signaling refers to soluble signals produced by the stem cells and to which they respond. Various autocrine factors have been identified for different types of stem cells, and with variability across species [63]. In the case of human embryonic stem cells, Fgf2, TGF β /Activin, BMP, and WNT signaling factors are produced by embryonic stem cells and act directly for the maintenance of the pluripotent state or to prevent differentiation [64, 65]. Autocrine signaling is also involved in adult stem cell fate regulation. An example is provided by stem cells of the intestine which, under normal conditions, secrete WNT proteins, and inhibition of this process leads to stem cell differentiation [66].

Paracrine signaling refers to the signaling mediated by the release of soluble factors from cells, and to which neighboring cells respond (i.e. cells within the stem cell niche). The term paracrine is also used for signals released from a cell type, and to which that same cell type cannot respond, and which are therefore not responsible for cell self-regulation mechanisms [63]. Paracrine signaling between stem cells and their progeny is essential for the maintenance of the stem cell niche and preventing all cells from differentiating. This is the case for basal stem cells in the lung, where homeostasis is maintained through Notch ligand JAG2 mediated signaling [67]. This type of regulation has also been hypothesized to play an important role in tissue repair mechanisms. MSCs have been shown to produce and release cytokines, chemokines and growth factors that might be involved in the cardiac injury repair process [68], with increased production of these factors under hypoxic stress conditions [69]. The therapeutic potential of MSCs has also been explored in the context of wound injuries, where paracrine signals from the cells have been deemed responsible for the beneficial responses to injury such as

inflammation, angiogenesis and fibroproliferation [70]. Moreover, the secreted paracrine signals that aid in tissue repair seem to be tissue specific.

Lastly, systemic signals also affect stem cell physiology and behavior. A study by Belenguer et al. demonstrated that neural stem cells are responsive to peripherally induced inflammation through activation of tumor necrosis factor-dependent pathways [71]. Adult stem cells have been shown to respond to dietary fluctuations and systemic nutrient availability. In *Drosophila* models, follicle stem cell proliferation is directly correlated to the presence of a protein-rich diet by means of insulin signaling [72]. Mouse NSCs have been shown to be responsive to injury, with increased proliferation rates detected in neural cells surrounding the injury areas as well as peripheral ones [73].

Traditional Methods for Stem Cell Research

Despite meaningful advances in understanding stem cell physiology achieved in recent years, most mechanisms that drive stem cell fate determination and differentiation have yet to be uncovered. Laboratories across the world adopt many established techniques that constitute the foundation of stem cell research. Here, I will describe some of the most relevant ones for stem cell research contributions.

iPSC Models and Targeted Differentiation

Embryonic stem cells are an ideal model for the study of pluripotent stem cells and their *in vivo* mechanisms. However, the use of human ESCs models is often a complicated process for research laboratories, due to the high level of regulation surrounding their use. Cells with equivalent differentiation potential as ESCs can be generated *in vitro* starting from somatic cells and are known as induced pluripotent stem cells (iPSC) [74, 75]. This type of cell can be generated via the introduction of different combinations of transcription factors in the differentiated cells. This can be accomplished by using viral vectors (such as lentiviruses or non-integrating viruses), reprogramming factor mRNAs, microRNAs, minicircle vectors, via transposons cloned into piggyBac vectors, or using episomal plasmids [76]. A first successful set of factors was identified by Yamanaka's group, and consisted of OCT3/4, SOX2, C-MYC, and KLF4, while a second combination was reported by Thompson's group and consisted of the

reprogramming factors OCT3/4, SOX2, NANOG and LIN28 [15, 74, 75, 77]. The introduction of either combination of factors into mature cells results in the activation of the genes associated with pluripotency and the induction of the adult somatic cells from a mature, differentiated stage to an undifferentiated one.

Two-Dimensional Cell Culture

Traditional methods for the study of cellular mechanisms *in vitro* involve the use of monolayer cell culture. Conventional two-dimensional cell cultures rely on the adherence of primary or immortalized cells on the culture dish's flat surface, which provides the mechanical support needed by the cells. A culture of many different cell types is made possible by the ease with which nutrient media, optimized and supplemented with various exogenous components, can be delivered to the cells. Although characterization of the type and viability of cells as well as simplicity of culture maintenance are easily achieved, cells in two-dimensional cultures lose their natural *in vivo* histological organization, leading to the inaccurate representation of tissues' structures. The loss of polarization observed in cultured cells may lead to alterations in their behavior and in the way in which cells and other extracellular components in culture interact. In fact, the histological organization of a tissue is strictly related to its function and affects its biological functions and its biochemical specificities [78].

Three-Dimensional Cell Culture

Another approach to the study of cellular mechanisms and disease, while maintaining a high degree of accuracy, is represented by three-dimensional cell culture protocols. They overcome many of the structural limitations posed by monolayer culturing techniques while reducing the error margin associated with the development and interpretation of studies in animal models. Different methods can be adopted to culture cells three-dimensionally, consisting of spheroid cultures, natural or synthetic scaffolds, cell sheets and hydrogels. Three-dimensional cultures have so far been revealed to be efficient means for the development and testing of drugs, for the study of the physiology of cells and cell populations, including their behavior and interactions, and have had applications in regenerative medicine research [79, 80]. Three-dimensional cultures have

also been shown to promote the thriving of cell populations in culture. Their superiority to monolayer cell cultures resides in the cells' enhanced deposition of the ECM-components fundamental for cell movement and proliferation, as well as promoting integration of signaling pathways between cells, and ensuring a more natural response in drug studies [79, 80]. When considering the study of neural stem cell physiology and division processes *in vitro*, three-dimensional cultures represent an ideal approach, with some limitations. Typically, cell plating in three-dimensional environments occurs by either mixing a cell solution with the substrate prior to solidification, or manual injection of cell solutions within the three-dimensional substrates. Either method results in the random or approximate distribution of cells within the substrate, introducing limitations in the experimental design and in the ability to collect data. Random disposition of cells within a substrate makes it so that physiological and functional measurements are retrieved with difficulty, and neither plating method allows for repeatability of the experimental conditions with high accuracy.

Most often, the substrate used for a three-dimensional cell culture is not biomimetic, resulting in a system not accounting for the effect of different microenvironmental cues on the cell cultures' physiology and behavior. Hydrogels comprised of various starting materials have been successfully utilized for cell cultures and are a valuable research method as they allow the recapitulation of the three-dimensional cellular environment, allow for natural cell motility and self-organization, and allow for the introduction of proteins typically found in the ECM to mimic the *in vivo* biochemical environment. Some of the base materials commonly used for hydrogel fabrication are collagen I, alginate, gelatin, fibrin, polyacrylamide, polyethylene glycol or hyaluronic acid [81]. Alternatively, the commercially available matrices Matrigel[®], Geltrex[®], or equivalents, are substrates extracted from the Engelbreth-Holm-Swarm (EHS) mouse sarcoma that have been widely applied for the two-dimensional culture of stem cells as well as cells of the neural lineage. The EHS tumors are particularly rich in the type of proteins that constitute the basement membrane ECM, such as laminin, collagen IV, entactin, and different growth factors [82]. Matrigel is the substrate predominantly adopted by research facilities, and it has proven efficient for the 2D and 3D culture of cells of the neural lineage. However, its tumor-origin and its unlikelihood of ever receiving FDA

approval and therefore being utilized in a clinical setting raise concerns among researchers [83].

The systems described are sufficient, yet not ideal, for the establishment of three-dimensional cell culture models *in vitro*. Some of the limitations that researchers still encounter are given by the nature of the hydrogels which can only mimic the *in vivo* environment to a limited extent. Additionally, the traditional cell plating methods currently available do not allow for accurate reproduction of the same experimental conditions at different sites.

Animal Models

A last methodology of research that is commonly adopted at advanced stages of molecular biology and stem cell research projects is the use of animal models. Here, the inaccuracies encountered adopting monolayer cell cultures are overcome, as the cells and tissues studied are found in their natural disposition within the body. *In vivo* models also have the advantage of presenting all the conditions that are found in a living organism. However, known and unknown differences between animal and human physiology are significant limiting factors in the accuracy of such approaches. The effectiveness of drugs and treatments has been shown to be species specific, with identical approaches producing discordant results when administered to animal models versus humans, and therefore reducing the reliability of results [84]. An additional risk factor in the adoption of animal models is the high probability of errors in the design of preclinical studies to accurately represent a disease population, as well as errors in the results' interpretation [85]. Finally, animal models often present limitations in the experimental design, as the use of live models allows for minimal visualization of the experiment progression, as well as a limit on manipulation opportunities.

Novel Methods and Technologies for Stem Cell Research

Biomimetic Cell Culture Substrates

Novel methods of performing three-dimensional cell culture while at best recapitulating physiological conditions, envision the adoption of tissue-derived substrates. Tissues of interest are extracted from animal models and utilized to produce a substrate

suitable for cell culture and which mimics the environment of the given cell type *in vivo*. The process consists of extraction of the whole tissue and decellularization using a solution able to lyse the cells while preserving the extracellular matrix proteins intact. The decellularized product is then mechanically dispersed, lyophilized, enzymatically digested and neutralized, in order to obtain a self-gelling product able to solidify upon warming into a hydrogel. Slightly variable protocols have been developed and optimized by various laboratories, and substrates suitable for cell culture have been developed from a wide range of tissues, such as heart, liver, breast, central nervous system, and skin tissue [86-93].

This technique is currently employed in our laboratory, and substrates obtained from rat and human mammary tissues are manufactured for the study of the behavioral changes observed in breast cancer cell lines cultured in a healthy environment and along normal mammary cells. Our laboratory has shown that tissue specific ECMs of the breast have unique properties in supporting the development of mammary epithelial cells [88, 94]. We demonstrated that our decellularization protocol allows us to produce a self-gelling hydrogel, in which cells can be cultured in three dimensions and proliferate uninhibited. Moreover, we showed that mammary cells injected in human ECM-derived substrates form unique ductal branching structures and exhibited changes in protein and gene expression profiles, not observed in cells cultured in rat tail collagen or Geltrex[®] hydrogels.

Similarly, other laboratories have explored the use of tissue specific ECM for the culture of neural stem cells and neurons, demonstrating the possibility of manufacturing a substrate suitable for cell culture starting from animal brain tissue [89-91]. The adoption of a tissue-specific substrate derived from porcine brain was explored in this project to devise a highly biomimetic 3D culture model.

3D Bioprinting

One limitation of the current methods of three-dimensional cell culture studies is the inability to seed cells with high precision and repeatability. This pitfall has been previously addressed in our laboratory with the development of a custom 3D bioprinting device [95]. A commercially available 3D printer was modified to allow the injection of cell

solutions within three-dimensional substrates. The automation of the injection process allows us to determine an appropriate concentration of cell solution as well as extruded volume prior to every experiment, so that each injection site has a precise number of cells. A second advantage provided by the system is the fact that it is coordinate based, which, in combination with the injection of predetermined amounts of cells, allows for very high levels of reproducibility at each injection site. Finally, the 3D bioprinting system allows us to perform high throughput experiments at any desired resolution. The distance between injection sites and the number of injection sites per well can be adjusted to suit the needs of the experiment, allowing us to perform several hundreds of injections in a single experiment.

The system has been successfully adopted in our laboratory for the injection of mammary cells into three-dimensional substrates [95]. The 3D bioprinter allowed for the injection of a selected number of cells at a set distance. The growth pattern of the cells was followed over time, and through empirical studies it was possible to determine the optimal distance between injections that allowed enough space for the cells to grow, while still allowing the formation of ductal branching structures as the ones observed *in vivo*. Moreover, the cells injected within rat tail collagen and mammary substrates gave rise to tumoroids *in vitro*. The accessibility, high precision and automation advantages provided by the 3D bioprinting system render it a promising avenue for the future approach of three-dimensional cell culture.

Growth Factor Immobilization

Stem cell physiology and fate determination are affected by a plethora of biomechanical and biochemical signals that the cells send and receive from their environment. The mechanisms that drive these processes as well as the transcription factors that mediate them are mostly unknown. One of the contributing factors behind the lack of knowledge of the processes that drive asymmetrical stem cell division is the lack of ideal and accessible methods that enable studies at the single-cell resolution. One option for the study of the effects of localized transcription factors on the stem cell fate determination process is the use of protein immobilized onto microbeads. This allows for

the localization of transcription factors at a known position relative to the cells of interest, providing insights on the relevance of the physical location of proteins in this context.

The challenge of elucidating some of the mechanisms behind stem cell asymmetrical division was also taken on by Habib et al., who focused on the role of the WNT signaling pathway in the orientation of asymmetrical stem cell division [26]. Starting from the notion that the transcription factor WNT3A maintains the self-renewal property of various types of stem cells, including mouse embryonic stem cells [25], the authors first examined the effect of spatially localized WNT signals on mESCs, by immobilizing WNT proteins on microbeads. The Wnt3a signaling pathway operates through a β -catenin dependent mechanism. The authors observed that when an ES cell was in contact with a WNT3A conjugated bead, the components of the WNT/ β -catenin pathway are asymmetrically distributed close to the bead before division, and in the daughter cell proximal to the bead during and after division. The authors found that the presence of Wnt3a beads correlates with the asymmetric inheritance of centrosomes and that most daughter cells in contact with the bead inherited the centrosome with the older centriole. Additionally, it was found that the presence of WNT3A conjugated beads was associated with predominant orientation of the axis of mitotic division in line with the bead. Finally, after division, pluripotency genes were found to be preferentially expressed in the daughter cell proximal to WNT3A beads. The findings reported by Habib et al. suggest a potential mechanism for external control of asymmetrical stem cell division and differentiation. A spatially localized WNT signal can orient the mitotic division plane of stem cells, affect stem cell fate by orienting cell division, and position one cell away from signaling range and lead to its differentiation. Although the authors presented important results, the experimental setup they adopted was not ideal. To achieve single-cell/single-bead pairs, they plated cells at low density and released WNT-conjugated beads in the cell culture medium, relying on the chance that one bead would land and attach to one of the cells. This resulted in an extremely low efficiency of generation of single-cell/single-bead pairs, limiting the ability to perform high throughput experiments, requiring a high experimental volume to collect statistically significant data, and resulting in the use of a quite unreliable system. An optimization of this system to achieve single-cell/single-bead pairs to allow single-cell resolution studies was developed in this project.

Project Aims

The research efforts presented in this dissertation focus on the development of ideal techniques for the study of the effects of the microenvironment on stem cell physiology and behavior. Existing methodologies were engineered to develop novel cell culture systems that overcome the limitations of traditional methods for the study of stem cell physiology while being the most representative of *in vivo* conditions. The original systems presented enable the study of how different types of environmental manipulations can affect stem cell differentiation and fate determination.

To achieve this goal, two projects were carried out, herein referred to as Aim I and Aim II. In Aim I, a 3D bioprinter based system for the study of the effects of the extracellular matrix microenvironment on stem cell differentiation was developed. The effects of a brain-specific microenvironment on the differentiation potential of embryonic and neural stem cells were evaluated. In Aim II, a high throughput system for the study of asymmetrical stem cell division at a single cell resolution was developed. Particular focus was posed on the ability to study localized growth-factor driven asymmetrical division events.

Aim I: Effects of a Brain Extracellular Matrix-Derived 3D Cell Culture System on Stem Cell Culture and Differentiation

Traditional cell culture techniques are often poorly representative of the true conditions of cells within an organism. The development of biomimetic substrates that more closely represent the environment of specific tissues allows the creation of more accurate conditions in which to perform *in vitro* studies. Additionally, the application of such substrates to two-dimensional and three-dimensional cell culture provides insight into the potential effect that changes in the environment have on cellular behavior.

Aim I focused on the development of an ideal system for the study of the effects of tissue-specific microenvironment on stem cell culture and differentiation. A protocol for the generation of porcine brain extracellular matrix-derived hydrogels was optimized as part of my master's thesis, starting from previously developed protocols. The hydrogels represent a substrate highly representative of the environment specific to the tissues of the central nervous system. The substrate generated was then evaluated for its suitability

to promote cell survival in monolayer culture conditions, establishing its potential to be applied to *in vitro* research. I showed that the substrate is suitable for culture of human neural stem cells in two-dimensional conditions. Here, this investigation was developed further to determine the effects of the brain-specific substrate on the differentiation of human and mouse neural stem cells down the neural lineage.

Next, the system was evaluated for its ability to sustain the culture of stem cells in three-dimensional culture conditions. The effects of introducing a three-dimensional environment as well as the presence of a neural tissue-specific substrate on mouse embryonic and neural stem cells were evaluated. The tissue-specific hydrogels were used in combination with our 3D bioprinting system to produce neural organoids in an accessible and highly reproducible way. The influence of a brain-specific cellular microenvironment on the tendency of stem cells to spontaneously differentiate into the neural lineage was evaluated.

Finally, the biocompatibility of the brain-derived substrate and its role in promoting survival and proliferation of stem cells *in vivo* were evaluated. Moreover, the ability to transplant neural organoids previously generated using our 3D bioprinting system into mice models was assessed, along with the differentiation state of the transplanted organoids following incubation. Aim I provided important insights concerning the role that microenvironmental cues from the brain ECM have on the ability of embryonic and neural stem cells to differentiate into cells of the neural lineage. Moreover, I introduced an excellent method for the generation of neural organoids by utilizing the brain-specific hydrogels in combination with our 3D bioprinting system. This system allows us to easily produce a large number of organoids *in vitro*, with the potential of *in vivo* transplantation.

Aim II: Engineering of a Bioprinting System for the Study of Immobilized-Growth Factor Driven Asymmetrical Stem Cell Division

The physiological mechanisms that drive stem cell asymmetrical division are still mostly unknown. One of the driving factors behind the lack of available data is the absence of accessible pieces of equipment that enable the study of stem cell mechanisms in a biomimetic environment and at high resolution.

The development of Aim II focused on the optimization of an existing 3D bioprinter for the study of cellular processes at a single-cell resolution. In particular, the system was developed to enable the study of the effects of immobilized growth factors on the asymmetrical division process of single stem cells. A protocol that enabled the study of single cell-single beads complexes in a three-dimensional environment was developed. The protocol enabled the following: immobilization of single protein-bound beads to single cells; injection of bead-cell complexes into a three-dimensional substrate and with high efficiency; ability to visualize the same single cell-bead complex over time (localization of the complex); promotion of cell survival and proliferation of single cell-bead complexes over time; visualization of cell proliferation and transition from one to two (or more) cells; live imaging of proliferating cells; immunocytochemistry of the cell after proliferation for downstream analysis; and the ability to apply this protocol for high throughput experiments.

As part of Aim II, the developed protocols were applied to the study of molecular processes. The notions reported by Habib et al., in which asymmetrical division of mouse embryonic stem cells is influenced by localized WNT3A signaling, were evaluated with higher efficiency and in a three-dimensional cell context.

Overall, Aim II describes an ideal and efficient system for the study of cellular mechanisms at a single cell resolution, in a biomimetic setup and with high throughput.

CHAPTER II

EFFECTS OF A BRAIN EXTRACELLULAR MATRIX-DERIVED 3D CELL CULTURE SYSTEM ON STEM CELL CULTURE AND DIFFERENTIATION

Introduction

The microenvironment has been shown to play an essential role in various cellular processes, such as cell migration and differentiation [1-4]. The in vitro histological organization of tissues and the disposition of cells in a natural three-dimensional context affects the biological functions and biochemical specificities of the tissue itself [96, 97]. A major component of the cellular environment is the extracellular matrix (ECM), a three-dimensional network of resident cell-secreted macromolecules, in which components are specific to various tissues [88, 98]. The ECM is a fundamental determinant of cell behavior, engages in cell signaling and facilitates cell motility and structural organization [89, 99, 100]. In the context of stem cells, the local cellular environment defines the stem cell niche [15]. The niche represents the physical location of the stem cells in the adult organism, where they receive and exchange stimuli that influence their fate. Stem cell niches possess an intrinsic plasticity that allows them to coordinate stem cell behavior, enabling cells to keep a quiescent state or differentiate to maintain tissue homeostasis [32, 101].

Traditional substrates for two- and three-dimensional cell cultures comprise animal and tumor-derived matrices rich in basal proteins [81, 102, 103] [1, 15, 81]. These present various limitations, particularly in the context of human cells and tissue-specific research. The differences between animal and human physiologies, as well as the specificity of local tissue ECMs, render commercially available matrices only relatively biomimetic. The use of tissue specific ECMs, which allow a more faithful reproduction of the cellular in vitro environment, has been a developing field of research in recent years [Mollica, 2019 #797, 102, 103]. A few laboratories have successfully explored the potential to use central nervous system-derived hydrogels as a substrate for neural cell cultures [89-91]. However, the methodologies previously described mainly focus on the generation of a

substrate suitable to generate plate coatings for two-dimensional cell culture, as injectable solutions, or as supplements in a multi-component cell culture system [104-106].

The three-dimensional organization of the cells within their environment plays a role in their behavior and physiology, and when cells are seeded into three-dimensional hydrogel substrates in a non-controlled orientation, it is difficult to make predictions concerning cellular behaviors. To address this issue, our group has previously developed an accessible, coordinate-based, 3D-bioprinting system that allows for the placement of a controlled number of cells within predetermined locations of a three-dimensional substrate [94, 107, 108]. The system has successfully been applied to the formation and culture of mammary organoids within tissue-specific hydrogels and holds great promise for an application in the development of neural cell culture techniques.

In this article, we describe the combination of tissue-specific substrates with our custom 3D-bioprinting system for the establishment of a biomimetic neural cell culture system. We report an adaptation of available protocols to produce a self-gelling porcine brain-derived substrate able to support *in vitro* two- and three-dimensional neural and stem cell culture and differentiation. We describe the application of our custom 3D-bioprinting system for the precise placement of cells within the three-dimensional substrates, allowing for the easy performance of reproducible, high-throughput experiments. We finally establish the biocompatibility of our tissue-derived hydrogels for use in murine models, and we evaluate the ability of the tissue-specific hydrogels to promote stem cell survival and proliferation *in vivo*. Together the tissue-specific hydrogels combined with the 3D-bioprinting system allow for the easy generation of neural organoids in three-dimensional culture. We show that the brain tissue-derived ECM drives stem cell differentiation towards the neural lineage, resulting in unique morphologies without the inducing cell differentiation using culture medium. Our system allows for the generation of organoids that can be transplanted *in vivo* and supports continued growth and survival in the new environment.

Results

Fabrication of Brain ECM Derived Substrates.

The cellular microenvironment plays a key role in the maintenance of stem cell physiology and in fate determination. Mechanical and biochemical cues from the stem cell niche regulate stem cell physiology to maintain local tissue homeostasis. The *in vitro* study of the mechanisms that drive stem cell division and differentiation is hindered by the limited availability of biomimetic cell culture substrates that can accurately reproduce physiological conditions. To partly overcome this limitation that affects experimental design of *in vitro* stem cell studies, we developed a brain-tissue derived substrate that can promote cell culture in two- and three-dimensional conditions.

Previously published protocols have demonstrated the ability to generate tissue-specific substrates starting from central nervous system tissue [89-91]. We adapted and optimized such protocols to be able to obtain a biocompatible substrate able to sustain two- and three-dimensional cell culture. Porcine brains were carefully extracted from the heads of adult animals, and the blood-brain barrier, the meninges layers, and the blood vessels were removed to the best of our ability, shown in Figure 5A. The brain tissue was rinsed in sterile water, sliced and decellularized. The decellularization progress was marked by the tissue progressively turning white, as reported in Figure 5B. The decellularized tissue was then washed with sterile water, washed with isopropyl alcohol, and washed again in sterile water. The product, resuspended in sterile water, was frozen and lyophilized. An image of the lyophilized product is reported in Figure 5C. Then, the product was digested in a pepsin solution, as represented in Figure 5D. The digested acidic product was neutralized through dialysis against PBS and 1X ABAM, achieving a self-gelling product when placed above 4-8 °C, as represented in Figure 5E.

At each step of the decellularization process, samples were collected to define the efficiency of our protocol and characterize our product. Samples of native and decellularized tissue were collected, fixed, and stained with haematoxylin and eosin (H&E) to evaluate the presence of cellular nuclei in each, as reported in Figures 5F and 5G. Nuclei are visible in samples of whole brain tissue, confirming the presence of cells.

In the decellularized sample, cell nuclei are not visible, confirming the absence of whole cells and the efficiency of the decellularization protocol.

To further define the efficiency of the proposed protocol, we quantified the residual genomic DNA in the brain ECM derived hydrogels. The presence of genomic DNA in the final product was evaluated using the Quant-iT™ PicoGreen® dsDNA Reagent Kit. Seven samples were tested, one for every ECM batch produced. The average gDNA content for all the samples tested reduced by 71% compared to the native tissue. A second parameter of interest for the characterization of the porcine brain-derived substrates was the protein composition. The total protein concentration of each batch of brain-derived matrix was measured using the DCTM Protein Assay and comparing the brain-derived hydrogels to a serum albumin protein standard of known concentration (2.92 mg/mL). The hydrogels presented a total protein concentration between 6.4 and 14.1 mg/mL.

The hydrogels' protein content was also qualitatively evaluated through PAGE assay, shown in figure 5H. The product was run on a polyacrylamide gel and compared to Geltrex® matrix and a ladder positive control. The assay showed that the main protein components of the brain-derived product and those of the commercially available matrix are comparable. Geltrex® has been extensively characterized, and its main protein components are laminin, collagen IV and entactin. It is therefore possible to attribute the three major bands obtained performing PAGE assay of the Geltrex® matrix, and observed between 200-300 kDa, and 100-130 kDa, to such proteins. Multiple bands were also observed performing the assay respectively to the brain-derived matrix and confirming the preservation of intact proteins following the hydrogel-formation protocol. Bands were observed both in correspondence of those characteristic of Geltrex® and in additional locations that indicate smaller protein size. From this result it is possible to infer that the major protein components of the brain-derived product are laminin, collagen IV, and entactin, and that the product is also rich in smaller and yet unidentified proteins.

Our protocol presented an efficient method for the decellularization of porcine brains and the fabrication of self-gelling hydrogels. The final hydrogel product is characterized by the absence of whole cells while the ECM components are preserved.

The composition of the tissue-derived substrate presents the same principal components as commercially available matrices.

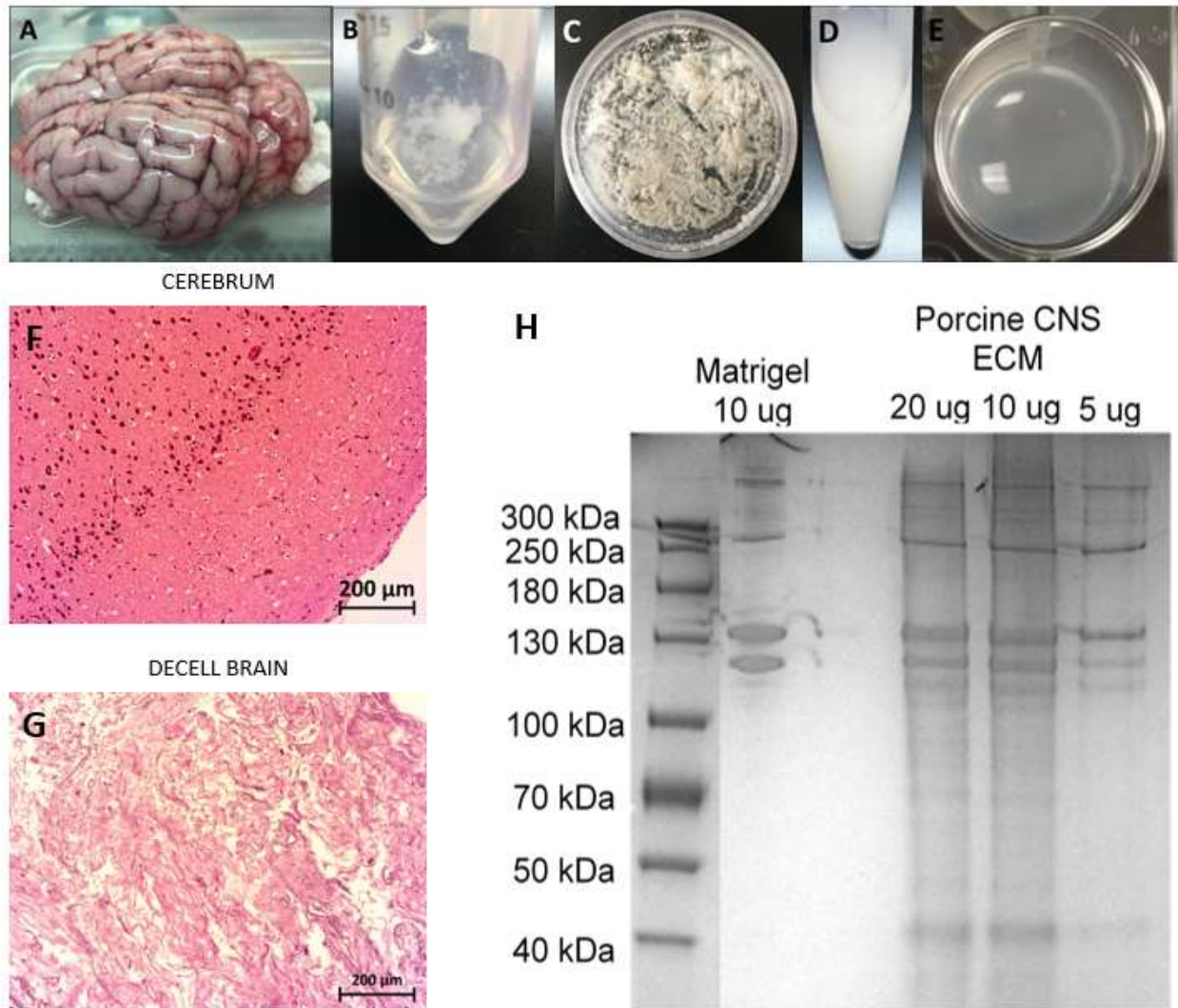


Figure 5: Production and Characterization of Brain-Derived Hydrogels. (A) Whole brain extracted from porcine head. In the figure, the Dura Mater was removed, while the Arachnoid and Pia Mater and the embedded blood vessels are depicted. (B) Decellularized brain tissue. (C) Lyophilized product obtained from the processing of a whole porcine brain. (D) Pepsin digestion process. (E) Hydrogel spontaneously formed after incubation of the final product at 37°C. (F) H&E staining of native brain, with visible cell nuclei. (G) H&E staining of decellularized brain, with cell nuclei not visible. (H) PAGE assay for the qualitative analysis of the hydrogel's protein content, compared to commercially available matrices.

Generation of Human and Mouse Neural Stem Cell Lines.

We investigated the suitability of our porcine brain ECM substrates for an application in biomedical research, starting from cell culture. To do so, we first generated and characterized human and mouse neural stem cell lines.

Human wild type induced pluripotent stem cells were successfully generated from the human fibroblast cell line bASC3. The stem cells (is-bASC3) were adapted to feeder free conditions and cultured on Geltrex® coated plates. Pluripotency of the stem cells was confirmed through TRA-1-60 live staining, a pluripotent specific marker. Colonies stained positively while the Geltrex® matrix did not stain, as shown in Figure 6A. This confirmed the identity of the is-bASC3 colonies and their suitability to be applied for the generation of cells of the neural lineage. After the is-bASC3 cells' identity and pluripotency were confirmed, colonies were used to generate a new human neural stem cell line: hNSC bASC3. The efficiency of the neural induction protocol was tested through immunocytochemistry staining assays, and the cell's identity was confirmed through positive staining for the NSC markers SOX2, NESTIN, SOX1 and PAX6. The newly generated cells presented uniform expression of the listed markers, as shown in Figure 6B.

Mouse embryonic stem cells of the GOlig2 reporter line were purchased from ATCC. The stem cells were adapted to feeder free conditions and cultured on Geltrex® coated plates. Pluripotency of the stem cells was confirmed through SSEA-1 live staining, a mouse pluripotent specific marker. Colonies stained positively, while the Geltrex® coating did not stain, as shown in Figure 6C. After the GOlig2 cells' identity and pluripotency were confirmed, colonies were used to generate a new mouse neural stem cell line: mNSC GOlig2. The efficiency of the neural induction protocol was tested through immunocytochemistry staining assays, and the cell's identity was confirmed through positive staining for the NSC markers SOX2, NESTIN, PAX3 and PAX6. The newly generated cells presented uniform expression of the listed markers, as shown in Figure 6D. The GOlig2 line is a GFP Olig gene reporter line, and the ability of the cells to express GFP upon Olig gene expression was confirmed via fluorescence imaging of the newly formed mouse neural stem cells.

Human and mouse pluripotent and neural stem cell lines were successfully generated and adapted to feeder-free culture conditions. The use of an Olig2 reporter line allows us to gain insight into the differentiation state of the cells in various culture conditions, while the use of a human cell line allows generation of a highly biomedically relevant model.

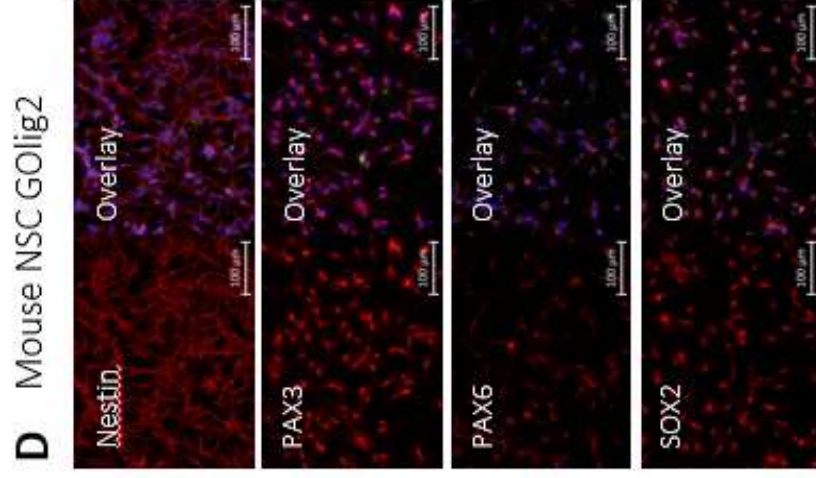
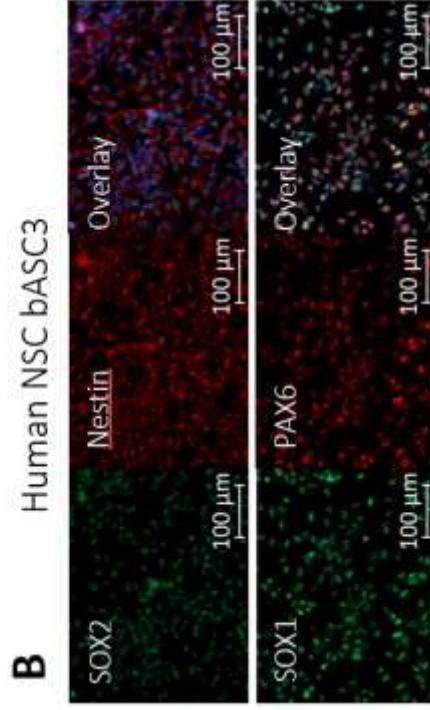


Figure 6: Characterization of pluripotent stem cells and neural stem cell lines. (A) Live staining of an is-bASC3 colony. Positive staining for TRA-1-60 confirms the pluripotency of the colony. Coincidence of the pluripotent region with the phase image of the colony indicates the absence of differentiated regions, and suitability of the colony to be expanded or adopted for the neural induction protocol. (B) Immunocytochemistry of hNSC bASC3 cells, confirming the identity of the newly formed human neural stem cell line. (C) Live staining of a G-Olig2 mESC colony. Positive staining for SSEA-1 confirms the pluripotency of the colony. Coincidence of the pluripotent region with the phase image of the colony indicates the absence of differentiated regions, and suitability of the colony to be expanded or adopted for the neural induction protocol. (D) Immunocytochemistry of mNSC G-Olig2 cells, confirming the identity of the newly formed mouse neural stem cell line.

Porcine Brain Matrix-Derived Substrate Promotes Neural Stem Cell Survival and Differentiation in Monolayer Culture Conditions.

The suitability of tissue-specific substrates to promote cell culture in two-dimensional conditions is a fundamental factor to consider. We tested the ability of the porcine brain-derived substrate to support two-dimensional cell culture and differentiation of stem cells. Cell culture plates and glass chamber slides were coated with 0.3 mg/mL porcine brain-derived matrix diluted in cold DMEM/F12.

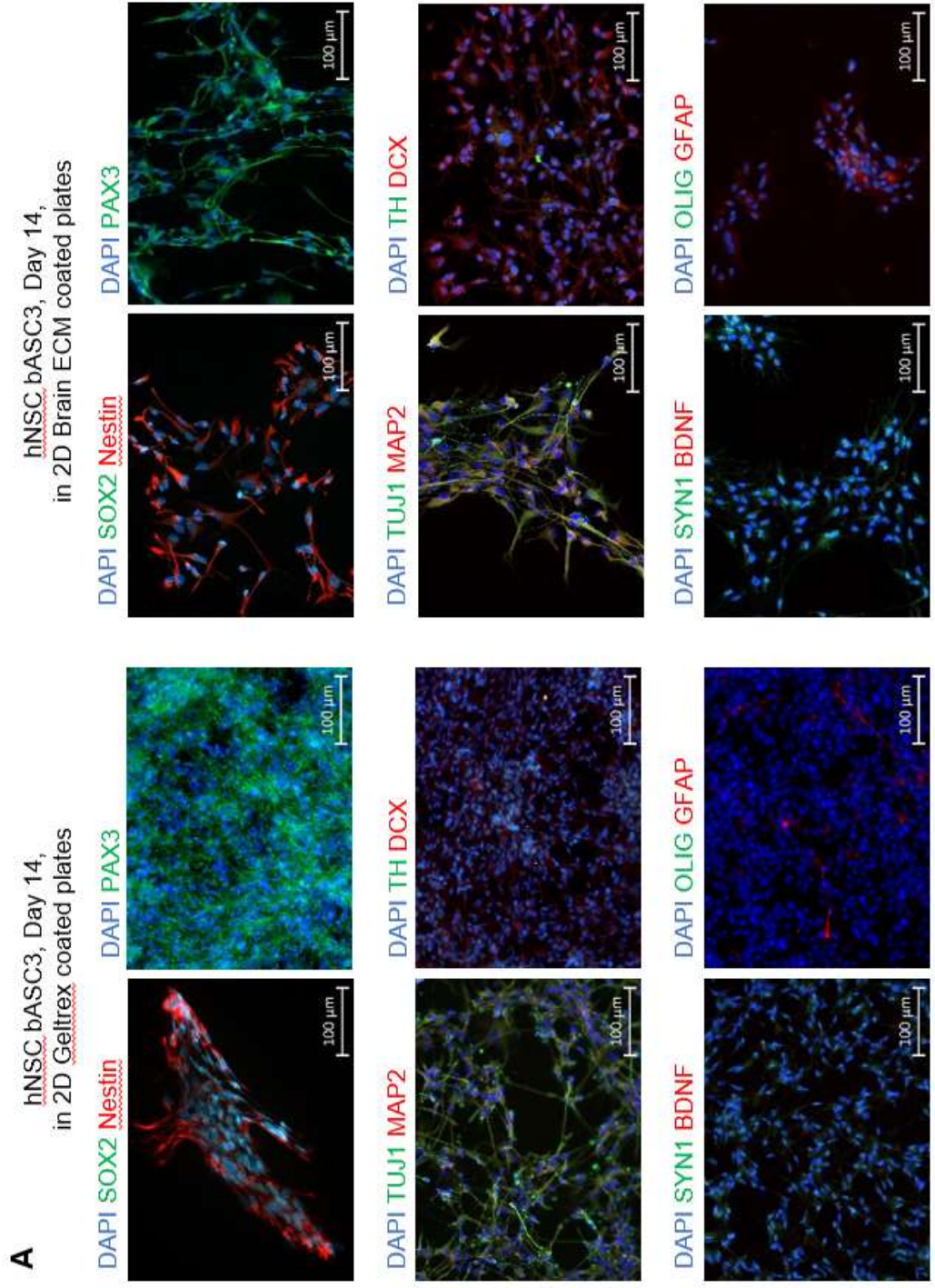
Mouse and human neural stem cells were cultured over a period of 14 days on brain matrix as well as Geltrex® coated plates. Cells were cultured in complete StemPro® NSC Serum Free Medium, completely replenished every other day. Cells were able to survive and proliferate on the brain ECM-coated plates comparably to the commercially available matrix. The ability of each substrate to promote maintenance of the neural stem cell character was evaluated via qPCR and immunocytochemistry (ICC) assays (Figure 7). The targets selected to assess the differentiation state of the cells in culture were PAX3 (ectoderm), SOX2 (pluripotency) Nestin (neural stem cell), Doublecortin (DCX, neuron), MAP2 (neuron), Beta III Tubulin (TUJ1/TUBB3, neuron), SYN1 (neuron), GALC/OLIG (oligodendrocyte), GFAP (astrocyte), BDNF (neuron). Pluripotency and NSC markers remained present over the 14-day period in both human and mouse NSCs. Human NSCs, presented elevated expression of the DCX early neuronal marker, which was significantly higher in cells grown on the brain ECM substrate, as well as slightly elevated mature neuron and oligodendrocyte markers. In contrast, mouse NSCs presented moderate changes in neuronal and glial markers expression and elevated expression of astrocyte marker, which was significantly higher in cells grown on Geltrex® coated plates. Overall, we demonstrated that the brain ECM-derived substrate is not only suitable for two-dimensional culture of neural stem cells, but it also affects the differentiation state of NSCs in monolayer culture conditions. Specifically, in the human NSC model the brain ECM substrate promoted expression of early neuronal markers, while in the mouse NSC model it had a protective effect against the elevated expression of glial cell markers.

Adult stem cell differentiation is influenced by mechanical and biochemical cues that the cells receive from their environment, with the overall goal of maintaining local

tissue homeostasis. We next investigated whether the presence of a tissue specific substrate could facilitate and/or influence the neural differentiation process in monolayer neural stem cell cultures. Mouse and human neural stem cells were seeded on Geltrex[®] and porcine brain matrix coated plates, and short term (7 days) and long term (30 days) neural differentiation was performed. The ability of each substrate to support neuronal differentiation was evaluated via qPCR and immunocytochemistry (ICC) assays (Figure 8, 9). The targets selected for ICC were PAX3, SOX2, Nestin, Doublecortin (DCX), MAP2, Beta III Tubulin, SYN1, GALC/OLIG, GFAP, BDNF. Human neural cells differentiated over 7-days presented elevated expression of neuronal and glial markers, as expected following application of the neural differentiation protocol. Expression of such markers was comparable between cells differentiated on Geltrex[®] and porcine brain matrix coated plates, with exception of the astrocyte marker, which was significantly more expressed in the latter condition. In the mouse model, elevated expression of the same markers was observed, with DCX being the marker more strongly present, but no significant differences across the two substrates were observed. Human and mouse neural cells differentiated over 30 days, presented elevated expression of neuronal and glial markers as expected following application of the neural differentiation protocol and in a comparable fashion across the two species. In both instances, neural cells differentiated on the brain ECM substrate showed a significant reduction in astrocyte markers expression compared to those differentiated on the commercially available matrix, suggesting a protective effect of the tissue-specific substrate in the differentiation towards supportive cell types. Overall, we demonstrated that the brain ECM-derived substrate is as suitable as commercially available matrices for the performance of neural lineage differentiation in monolayer culture conditions. We also demonstrated that the tissue specific substrate promotes the formation of supportive neural cell types in the short term in human models, while having a protective effect in the long term in both human and mouse models.

Monolayer cell culture conditions are widely adopted by researchers for *in vitro* studies thanks to the vast availability of established protocols and the fact that it is the most accessible method of cell culture for most laboratories. For the culture of pluripotent and neural stem cells in feeder-free conditions, the use of tumour-derived, commercially available matrices such as Matrigel and Geltrex[®] represents standard procedure. Here,

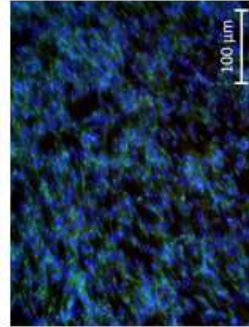
we demonstrate that our porcine brain-derived substrate can be utilized to coat cell culture plates and allow stem cell survival, proliferation and differentiation as efficiently as such products. We also demonstrate that our tissue-specific substrate does independently affect the differentiation state of neural stem and differentiated cells in monolayer culture.



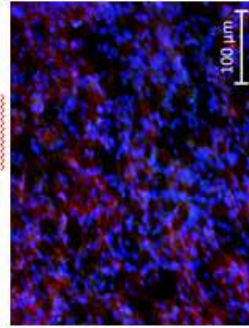
B

mNSC Golig2, Day 14, in 2D Geltrex® coated plates

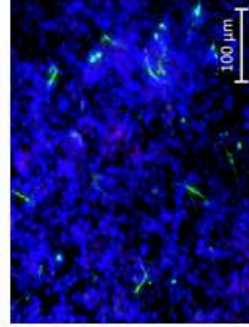
DAPI PAX3 SOX2



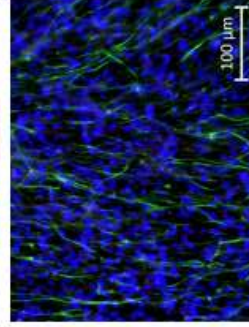
DAPI OLIG Nestin



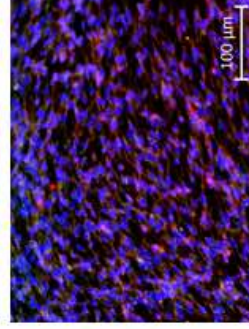
DAPI TUBB3 MAP2



DAPI GFAP BDNF

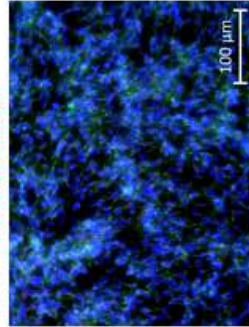


DAPI SYN1 DCX

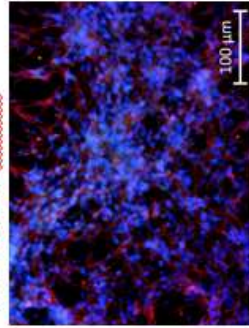


mNSC Golig2, Day 14, in 2D Brain ECM coated plates

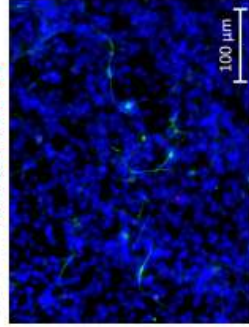
DAPI PAX3 SOX2



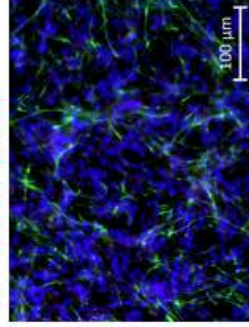
DAPI OLIG Nestin



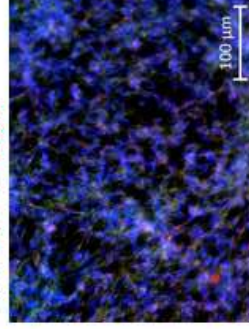
DAPI TUBB3 MAP2



DAPI GFAP BDNF



DAPI SYN1 DCX



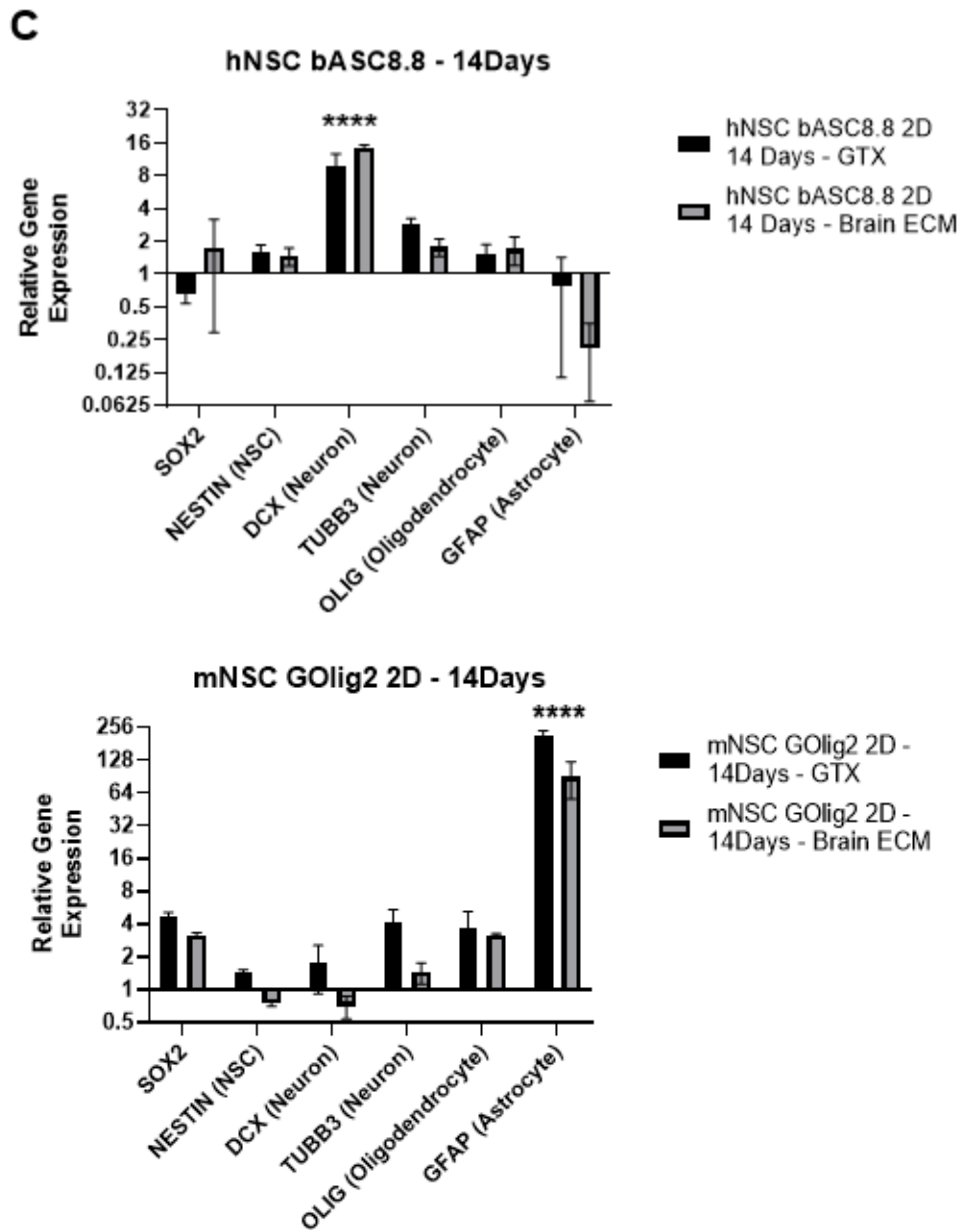
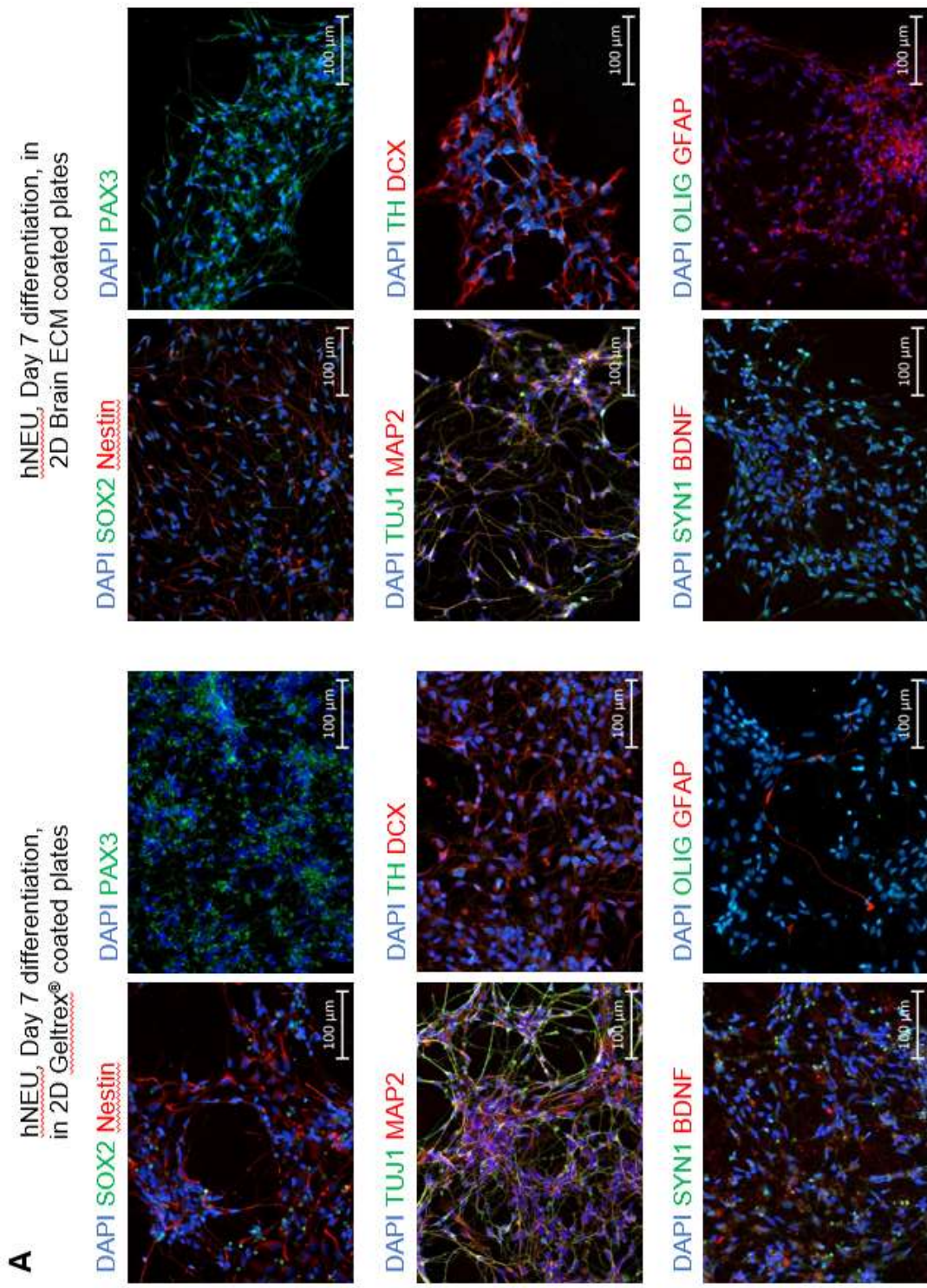


Figure 7: Survival and differentiation potential of mouse and human neural stem cells on Brain ECM coated plates. (A) Immunocytochemistry of Day 14 hNSC bASC3 grown on Geltrex® and Brain ECM coated plates. Cells grown in both substrates stained positively for NSC markers as well as early neural markers. (B) Immunocytochemistry of Day 14 mNSC GOlig2 grown on Geltrex® and Brain ECM coated plates. Cells grown in both substrates stained positively for NSC markers as well as early neural markers. (C)

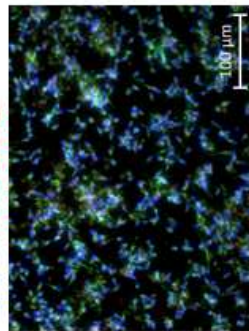
Relative gene expression of NSC and neural markers of hNSC bASC3 and mNSC GOlig2 cultured for 14 days on Geltrex and Brain ECM coated plates.



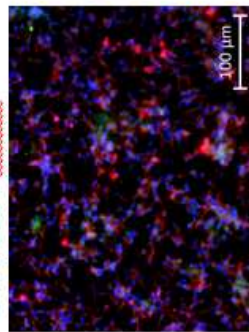
B

mNEU Golig2, Day 7, in 2D Geltrex® coated plates

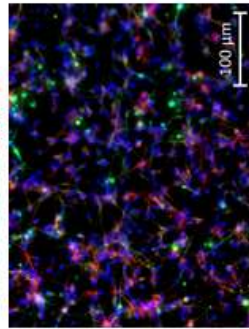
DAPI PAX3 SOX2



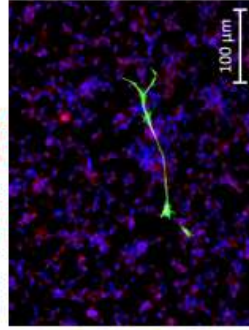
DAPI OLIG Nestin



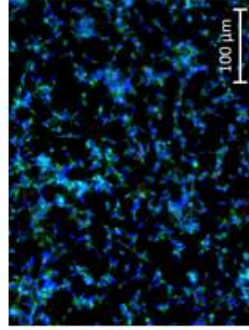
DAPI TUBB3 MAP2



DAPI GFAP DCX

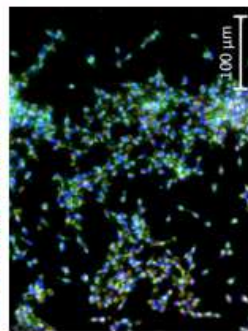


DAPI SYN1 BDNF

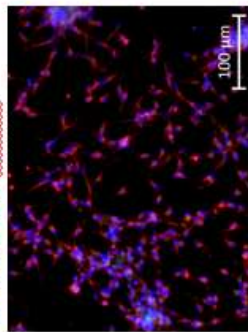


mNEU Golig2, Day 7, in 2D Brain ECM coated plates

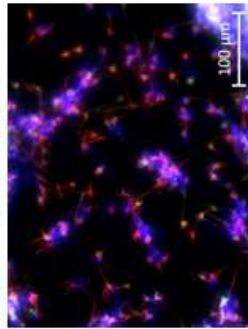
DAPI PAX3 SOX2



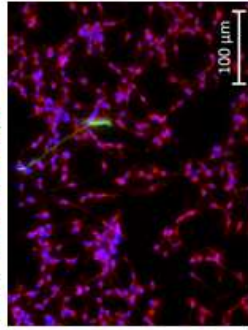
DAPI OLIG Nestin



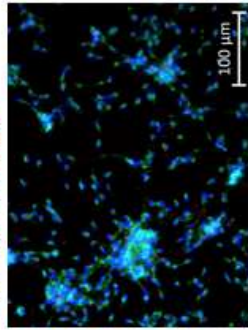
DAPI TUBB3 MAP2



DAPI GFAP DCX



DAPI SYN1 BDNF



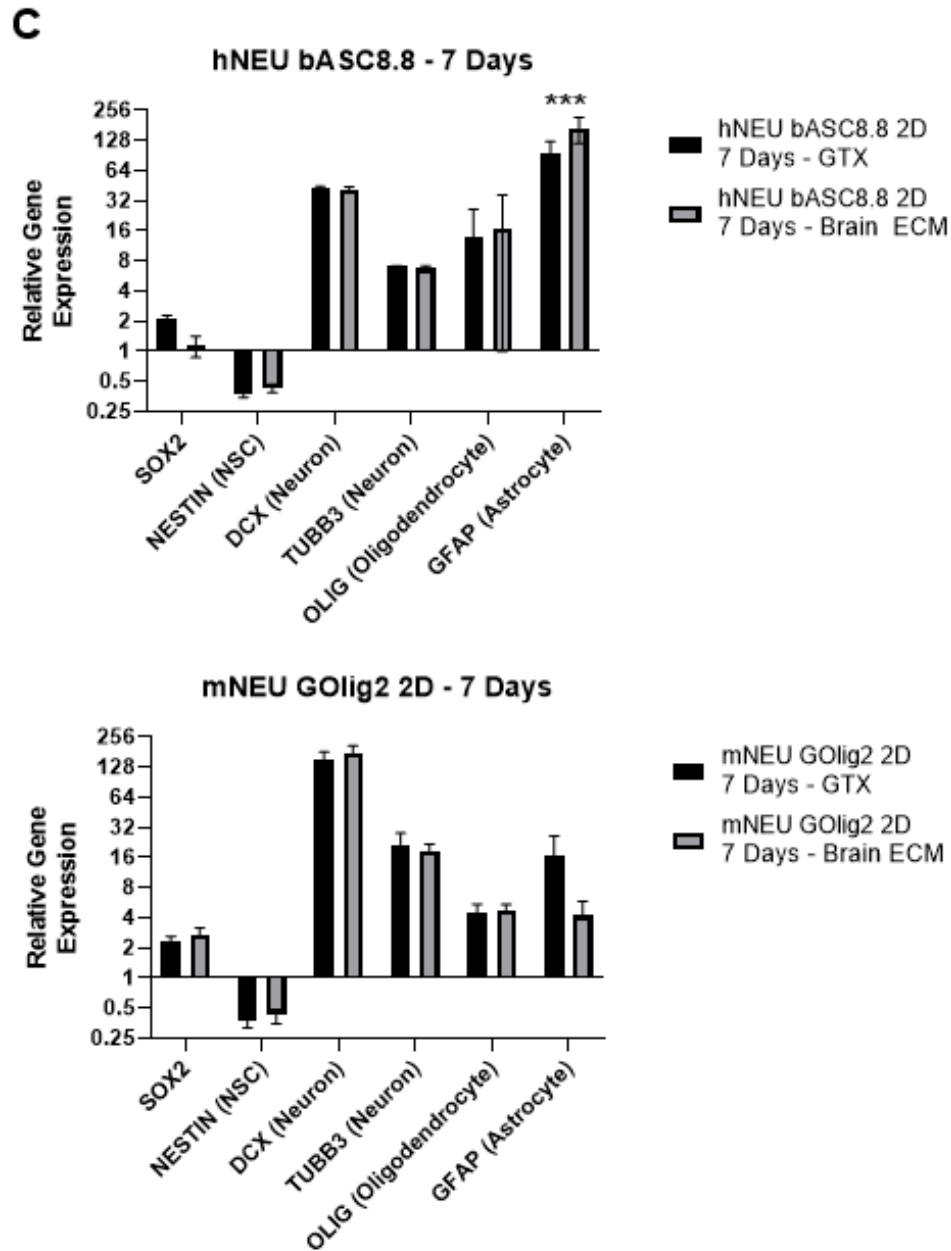
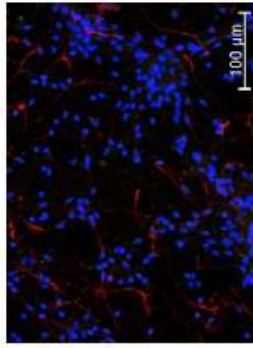


Figure 8: Short-term neural differentiation of human and mouse neural stem cells on Brain ECM coated plates. (A) Immunocytochemistry of Day 7 hNEU bASC3 grown on Geltrex® and Brain ECM coated plates. Cells differentiated on both substrates stained positively for NSC markers as well as neural markers (B) Immunocytochemistry of Day 7 mNEU GOlig2 grown on Geltrex® and Brain ECM coated plates. Cells differentiated on both substrates stained positively for NSC markers as well as neural markers. (C)

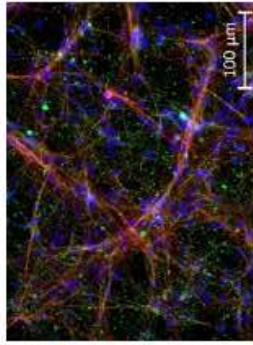
Relative gene expression of NSC and neural markers of hNEU bASC3 and mNEU GOlig2 differentiated for 7 days on Geltrex[®] and Brain ECM coated plates.

A hiNEU, Day 30 differentiation,
in 2D Geltrex coated plates

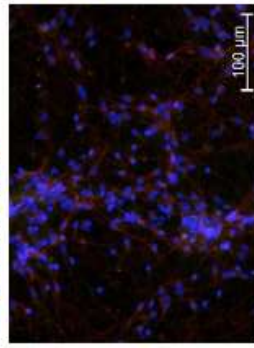
DAPI SOX2 Nestin



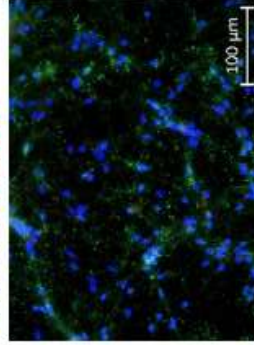
DAPI TUJ1 MAP2



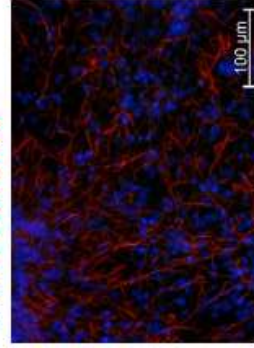
DAPI TH DCX



DAPI SYN1 BDNF

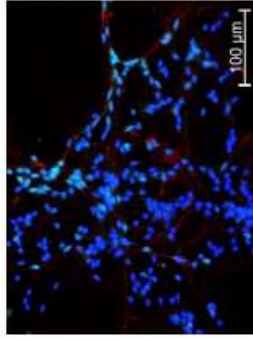


DAPI OLIG GFAP

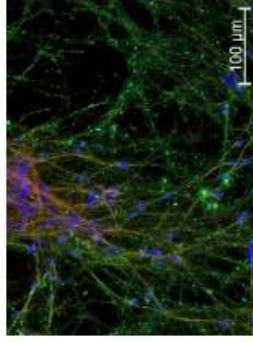


hiNEU, Day 30 differentiation,
in 2D Geltrex coated plates

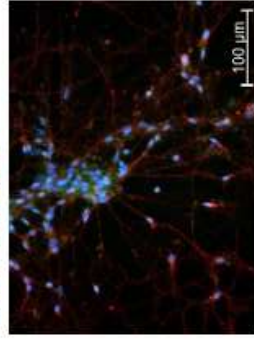
DAPI SOX2 Nestin



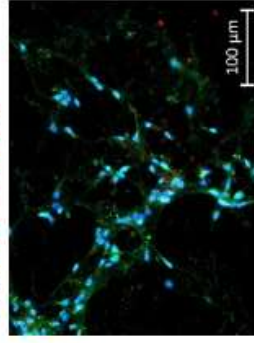
DAPI TUJ1 MAP2



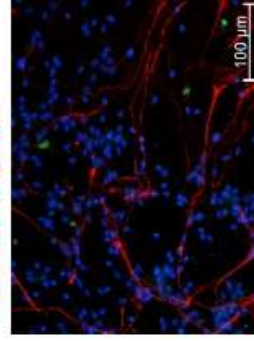
DAPI TH DCX



DAPI SYN1 BDNF



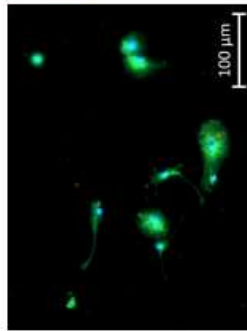
DAPI OLIG GFAP



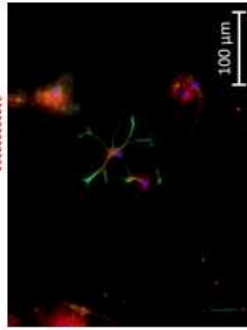
B

mNEU Golig2, Day 30, in 2D Geltrex coated plates

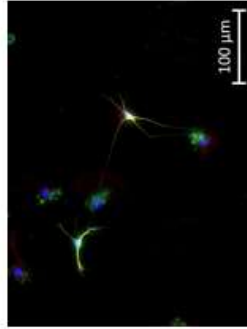
DAPI PAX3 SOX2



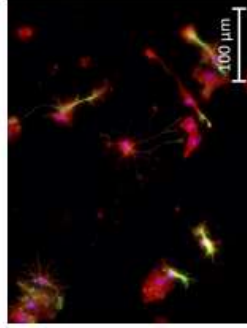
DAPI OLIG Nestin



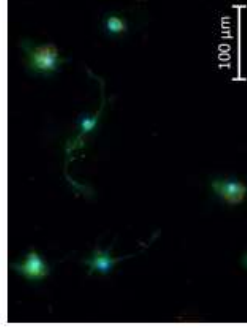
DAPI TUBB3 MAP2



DAPI GFAP DCX



DAPI SYN1 BDNF

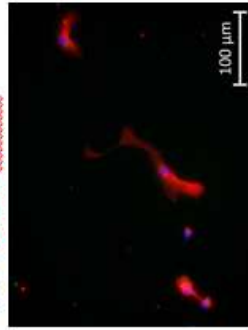


mNEU Golig2, Day 30, in 2D Brain ECM coated plates

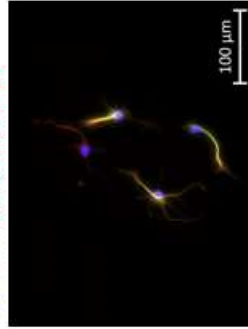
DAPI PAX3 SOX2



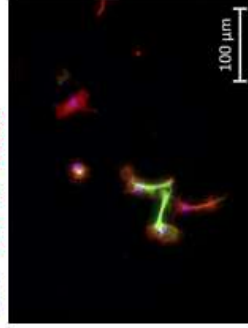
DAPI OLIG Nestin



DAPI TUBB3 MAP2



DAPI GFAP DCX



DAPI SYN1 BDNF



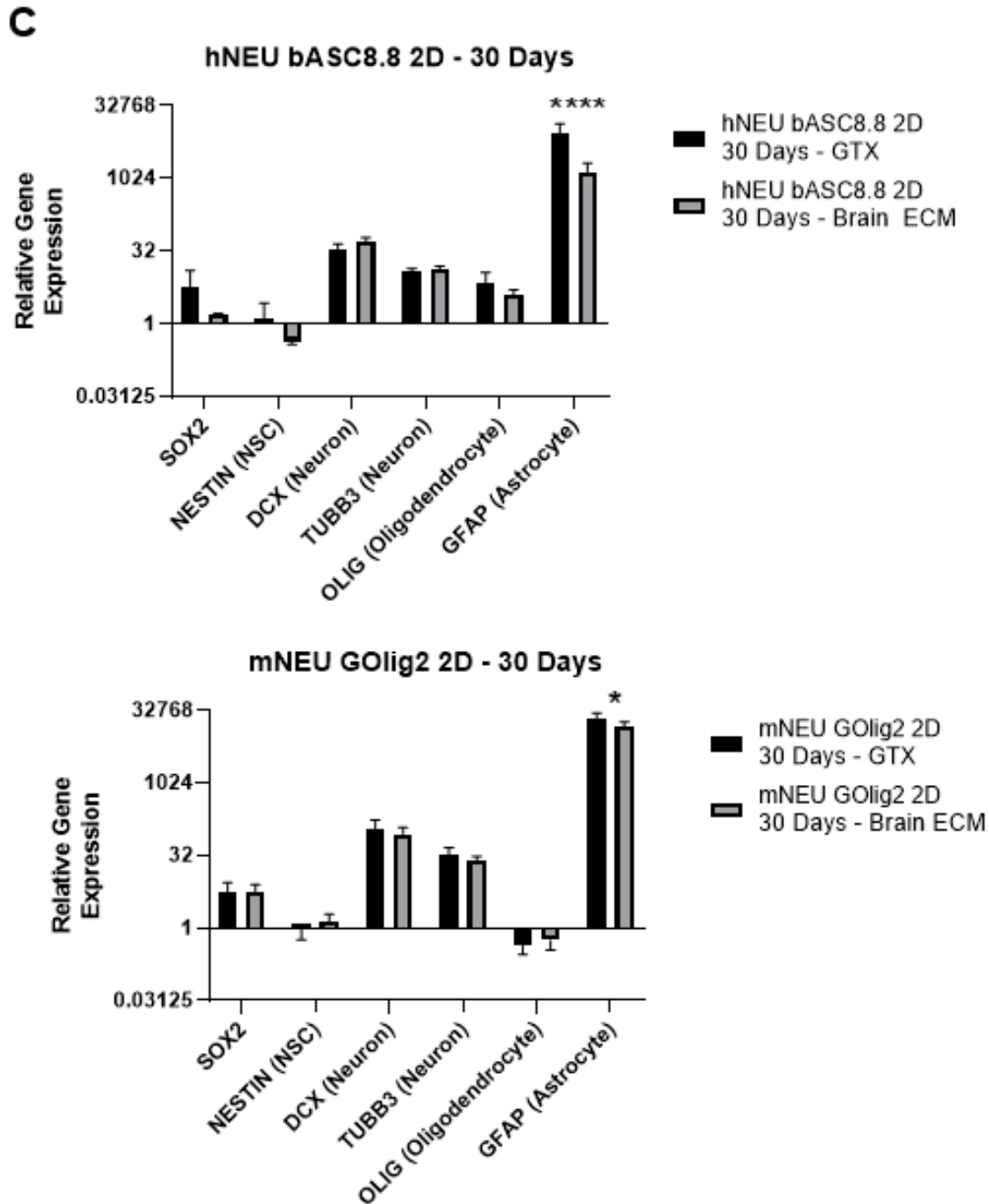


Figure 9: Long-term general neural differentiation of human and mouse NSC on the brain-derived substrate. (A) Immunocytochemistry of Day 30 hNEU bASC3 grown and differentiated on Geltrex and Brain ECM coated plates (B) Immunocytochemistry of Day 30 mNEU GOlig2 grown and differentiated on Geltrex and Brain ECM coated plates. (C) Relative gene expression of target genes of hNEU bASC3 and mNEU GOlig2 differentiated for 30 days on Geltrex and Brain ECM coated plates.

High-Throughput, Three-Dimensional Culture in Porcine Brain Matrix-Derived Substrate Promotes Differentiation Towards the Neural Lineage.

Three-dimensional cell culture methods allow us to perform studies with a higher degree of accuracy in representing true *in vivo* conditions, compared to two-dimensional cell culture. Seeding cells in three-dimensional conditions and allowing for their natural movement and organization within an environment representative of their tissue of origin, allows us to gain relevant insights concerning the role of the environment on the behaviour of stem and neural cells.

We tested the ability of the brain-derived substrate to sustain three-dimensional cell culture and/or promote differentiation of mouse embryonic stem cells. Traditional three-dimensional cell culture envisions either the manual injection of a cell solution within a three-dimensional substrate, or the mixture of cell solution with the substrate prior to gelling. Either method presents the drawback of not allowing for the precise placement of cells within the substrate, introducing new variables in the experimental setting. The application of the 3D bioprinter developed by our group for the controlled placement of cell in the environment, allowed for the reproducible injection of a controlled number of cells within the substrates. The system, depicted in Figure 10, was developed starting from a commercially available 3D printer model, and customized to allow the injection of a controlled number of cells at a pre-determined location within a three-dimensional substrate. The system allows for the definition of a large number of injection sites at once, enabling the performance of high throughput experiments with high automation and in few relatively simple steps. Figure 10 shows an example of how the 3D bioprinting system can be programmed for the injection of cells in a 10X10 grid pattern within the 8 wells of a chamber slide, producing a total of 800 injection sites in a single experiment.

Mouse embryonic stem cells of the line GOlig2 were injected into three-dimensional Geltrex® and brain ECM substrates and cultured for 14 days. The cells were cultured in mESC+LIF medium and were able to survive and proliferate in both substrates. The medium chosen allows maintenance of mouse embryonic stem cell state, without promoting maintenance of naïve state. Cell growth was followed throughout the 14-day period by monitoring the expression of the GFP character within the cell colonies. GFP expression was evaluated via fluorescence microscopy and was not observed in mESC

in monolayer culture, nor in clusters of cells on the day of printing (day 0). The GFP character became progressively visible with the prolonged incubation and growth of the cell colonies, indicating a degree of differentiation towards the neural lineage in cells grown in either Geltrex® or Brain ECM substrate. Figure 11 shows a visual representation of the increase in GFP character visible through fluorescence microscopy in mouse embryonic stem cells cultured over 14 days in Brain ECM substrate.

The figure also demonstrates the ability of our system to perform large scale experiments with a high degree of reproducibility. For each experiment performed within a well of a 24-well cell culture plate, cells were injected at 10 equidistant sites across 3 rows, for a total of 30 injection sites in a single well. Over the course of 14 days, each site developed into an individual and clearly distinguishable organoid, where growth was easily monitored. The coordinate-based 3D-bioprinting system allows us to adjust the injection parameters so that additional organoids could be printed within the same area. Furthermore, the system allows us to maintain the same set of environmental conditions across many organoids, ensuring for high reproducibility of individual experiments.

After the 14-day incubation period, samples of mESC colonies cultured on either substrate were fixed, and the differentiation state of the colonies was qualitatively evaluated via immunohistochemistry (IHC). H&E staining was performed on each section, and it revealed an altered morphology of mESC colonies grown in the brain matrix substrate versus Geltrex®. All mESC GOlig2 colonies developed within the Geltrex® substrate presented tightly packed cells with high nucleus-cytoplasm (N:C) ratio. Differently, mESC GOlig2 grown on tissue-specific substrate, also presented colonies with reduced cellular density and reduced N:C ratio, reported in Figure 12A. The latter is a measure of cellular differentiation state, with low ratio values indicating higher degree of cellular differentiation. Furthermore, the cellular morphology of mESC GOlig2 grown in brain substrate is suggestive of differentiation towards neuroglial cells, as it is possible to observe comparing such colonies to samples from the native pig brain cerebrum (Figure 12B).

To further investigate the differentiation potential of mESC Golig2 colonies within the two substrates, IHC was performed, and the following targets were selected: SOX1 (ectoderm), SOX17 (endoderm), Brachyury (BRY, mesoderm), GFP (associated with

OLIG2 expression and providing a positive control), GFAP (astrocyte marker) and CD44 (astrocyte-restricted precursor cell marker/ fibrous astrocyte marker). The stained sections revealed uniform expression of GFP and more prominent SOX17 expression in Geltrex® culture than brain ECM, while Brachyury and SOX1 staining were not evident in the assay (Figure 11B). Colonies grown in both substrates showed GFAP and CD44 expression, with no significant difference between substrates for the first marker and significantly elevated expression of CD44 in brain-derived substrates (data shown in Figure 12C). These findings, combined with the observation of altered cellular morphology, suggest that the presence of the brain-derived substrate directs mESCs towards commitment to the astrocyte lineage.

The differentiation state of the colonies in three-dimensional culture at day 3, 7 and 14 from injection, was also quantitatively characterized via qPCR (Figure 11C). The targets selected were SOX1, SOX17, HAND1 (mesoderm) and OLIG. The relative expression of each gene was calculated relatively to mESC GOlig2 cells grown in 2D conditions, with the same cell culture medium, and using the $2^{-\Delta\Delta Ct}$ method. The expression of germ layer markers followed comparable patterns throughout the three time periods. In both culture conditions, gene expression was decreased at day 3 and progressively increased through day 14. Gene expression changes were not statistically significant across the cell culture period (marked with an asterisk in the figure), or between the two culture substrates. The only exception was SOX17 expression, which was significantly higher in 14-day mESC GOlig2 cultured in Geltrex® substrate compared to brain ECM substrate. Olig2 expression showed low variability across the 14-day period and between culture substrates.

Next, we tested the ability of the brain-derived matrix to sustain cell growth and promote differentiation of mouse neural stem cells (mNSC) of the line GOlig2. mNSCs were injected into three dimensional Geltrex® and brain matrix derived substrates and allowed to incubate for a period of 14 days. The differentiation state of the cells was assessed throughout the incubation period by monitoring the expression of the GFP character of the cell line. The cells retained GFP expression throughout the 14-day incubation period, both in Geltrex® and brain matrix three-dimensional substrates. Figure 13A shows a visual representation of the GFP character visible through fluorescence

microscopy in mouse neural stem cells cultured for 14 days in Brain ECM substrate. The ability of the brain-derived substrate to maintain neural stem cells in culture, and whether it influences neural stem cell differentiation was evaluated qualitatively via IHC and quantitatively via qPCR, as reported in Figure 13. The targets chosen for IHC were GFP, SOX2, DCX, Beta III Tubulin and Nestin. SOX2, DCX and Nestin staining were present and comparable between the substrates. Beta III Tubulin staining was present to a higher extent in the Geltrex® culture compared to the brain ECM substrate. The targets chosen for gene expression analysis were SOX2, Nestin, DCX, Beta III Tubulin, GFAP and OLIG. The relative expression of each gene was calculated comparatively to mNSC GOlig2 cells grown in 2D conditions, within the same cell culture medium, and using the $2^{-\Delta\Delta Ct}$ method. The expression of the pluripotency marker SOX2 significantly varied over the incubation period to a comparable level across the two three-dimensional substrates chosen. The relative expression of Nestin was decreased to a non-significant extent in either substrate. Olig2 expression was decreased to a statistically significant extent over the 14 day-period, but not across substrates, likely indicative of the fact that the cells are beginning to differentiate. The relative expression of Beta III Tubulin and GFAP markers were increased by a statistically significant extent over the incubation period, with no significant difference between the two culture substrates, with exception of Beta III Tubulin showing higher expression levels at day 14 in Geltrex®, in line with what was observed in the IHC assay. Finally, DCX expression of NSC grown in either substrate significantly decreased over the incubation period compared to cells grown in monolayer culture.

The brain-derived hydrogel fabricated in our laboratory was revealed to be a suitable substrate for three-dimensional stem and neural cell culture models. The brain-specific substrate promoted survival of mouse embryonic stem cells and allowed for the formation of unique morphologies and gene expression patterns, similar to those that define neural support cells in the mature organism. The brain-derived hydrogels were also suitable for the maintenance of stem cells already committed to the neural lineage. Overall, we demonstrated that the application of our custom 3D bioprinter in combination with a brain tissue-specific substrate provides an excellent platform for the study of stem and neural cell physiology in a biomimetic environment.

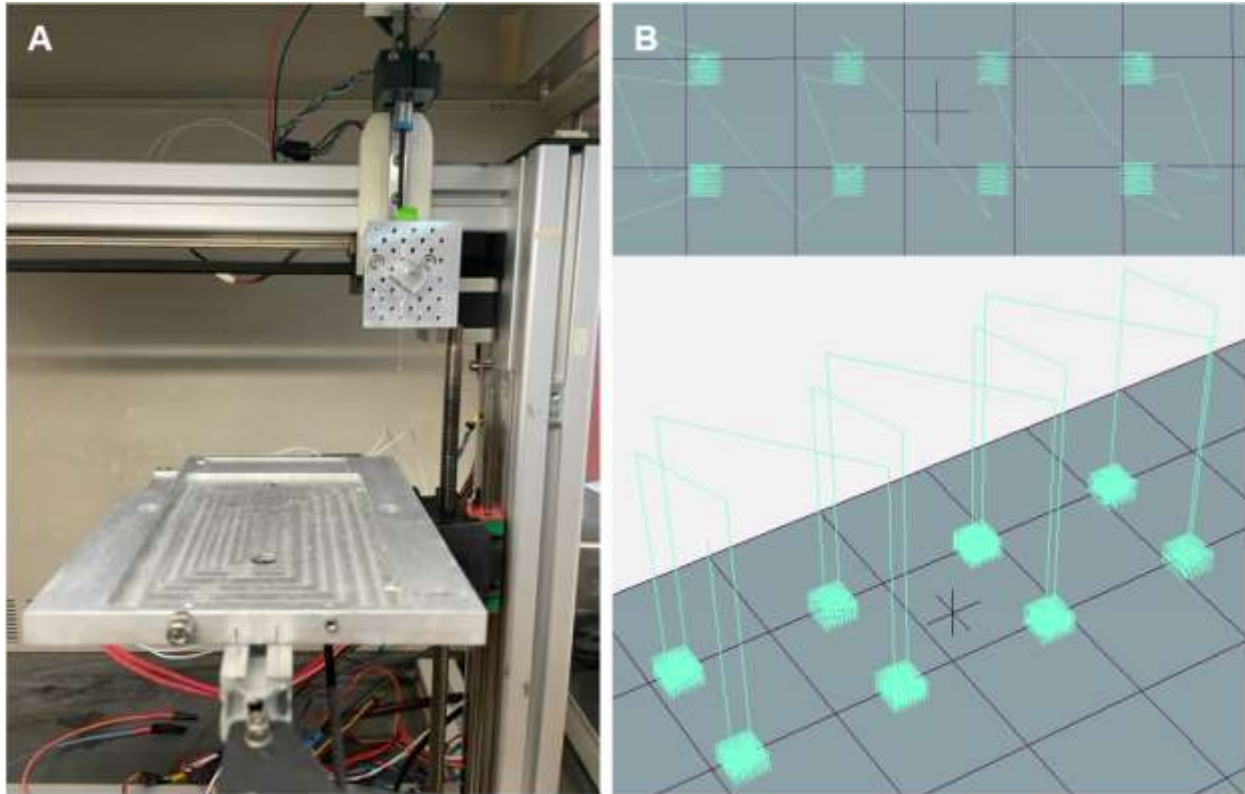
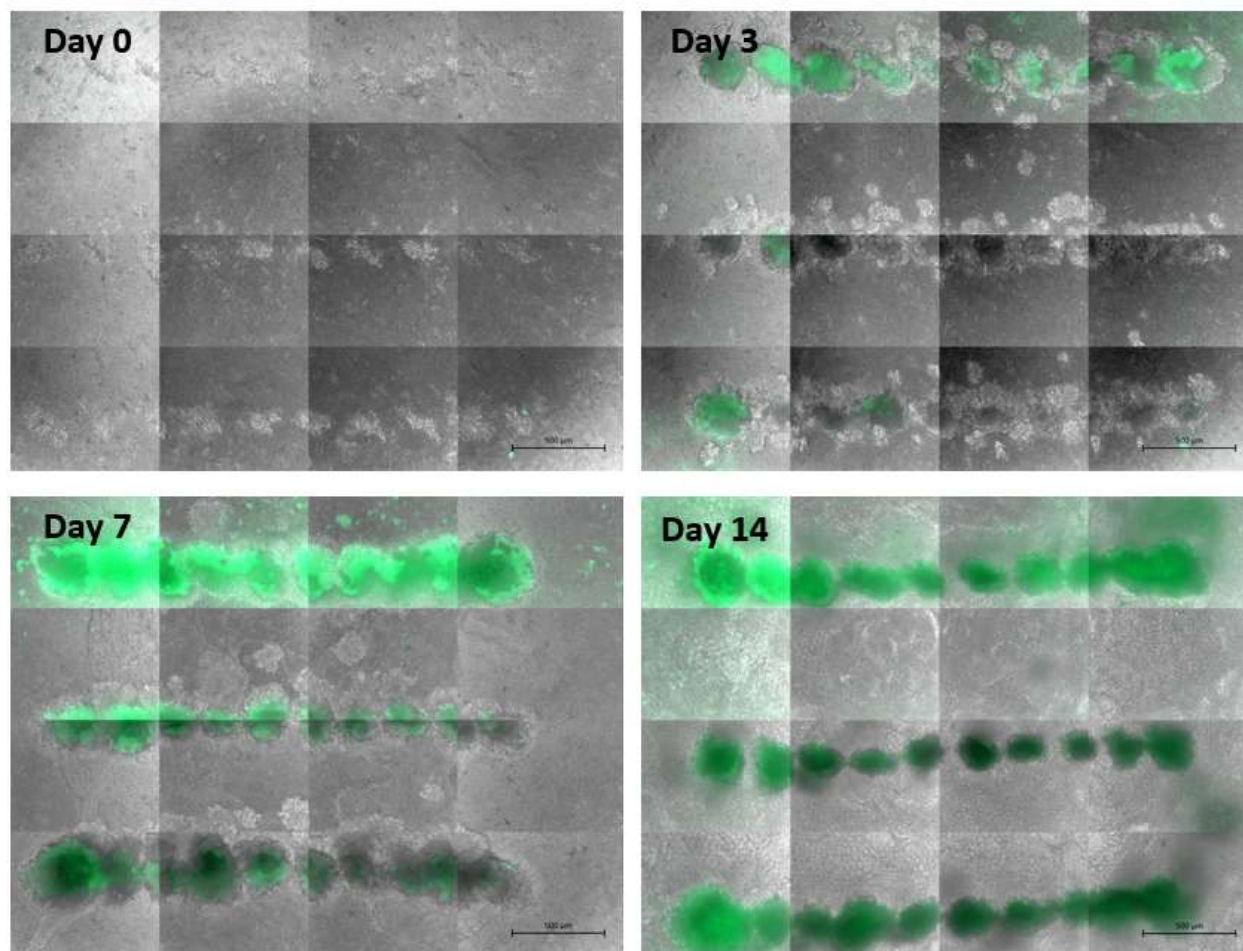


Figure 10: (A) 3D-bioprinting setup. A commercially available 3D printer was customized for biomedical research applications. A printing bed was designed to fit standard size cell culture plates and glass chamber slides. A printer head was designed for the placement of a micropipette pulled to the desired size, which allows for the controlled injection of cells within a three-dimensional substrate. (B) The 3D-bioprinting system is coordinate-based and allows for the performance of large-scale experiments while maintaining high reproducibility in the experimental conditions.

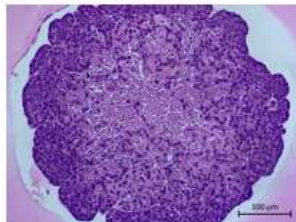
A mESC in 3D culture of BMX substrate at day 0, 3, 7 and 14



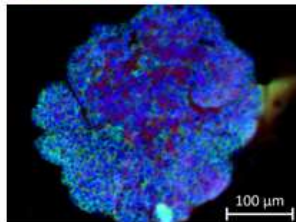
B

mESC Golig2, Day 14, in Geltrex

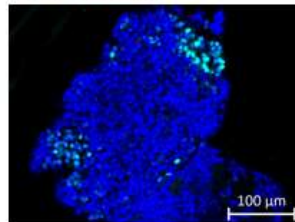
H&E



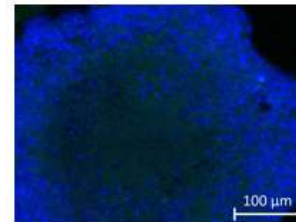
DAPI GFP SOX1



DAPI SOX17

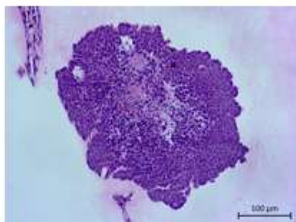


DAPI BRY

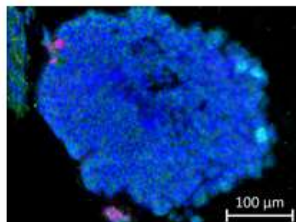


mESC Golig2, Day 14, in Brain ECM

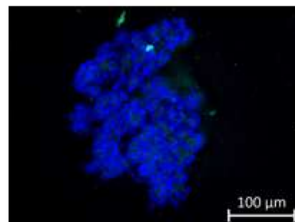
H&E



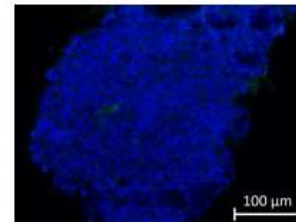
DAPI GFP SOX1



DAPI SOX17



DAPI BRY



C mESC GOlig2 cultured in 3D Geltrex® or Brain ECM substrates

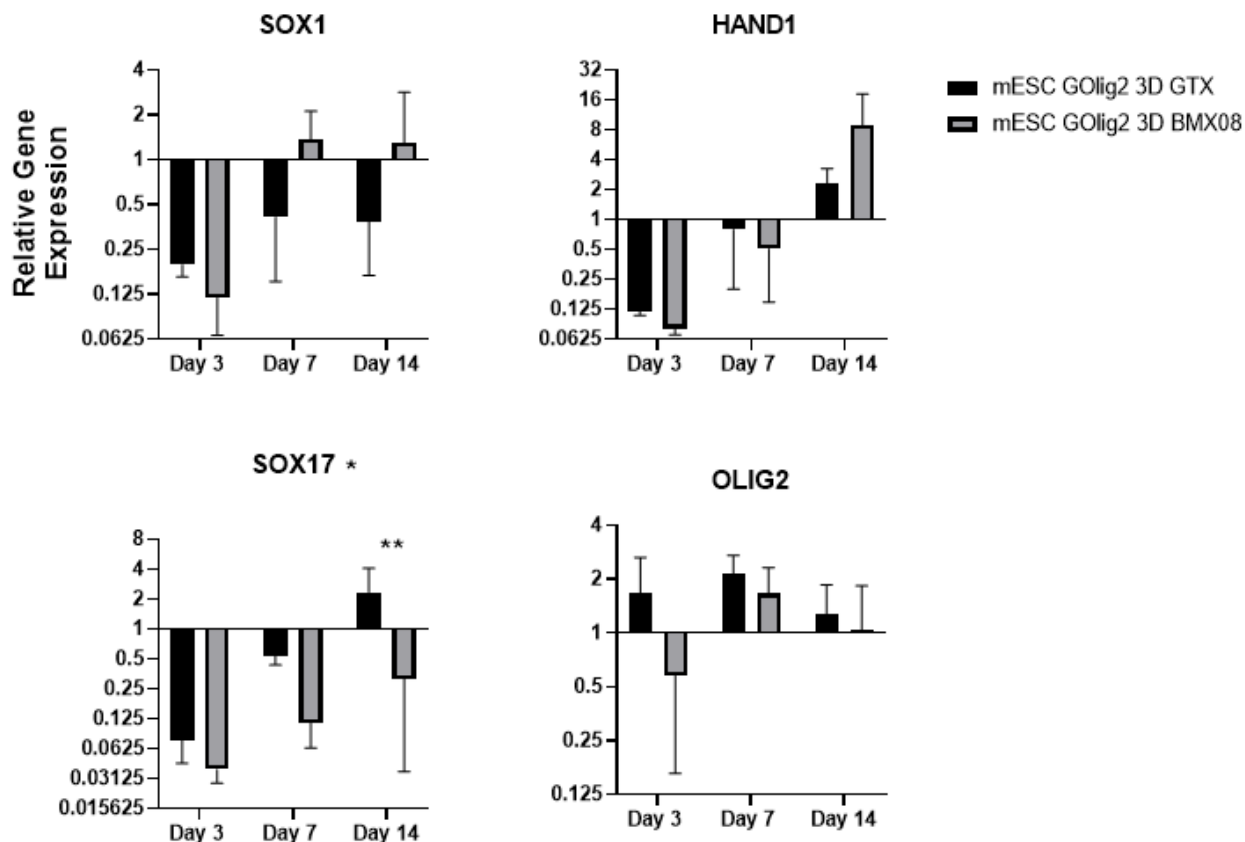
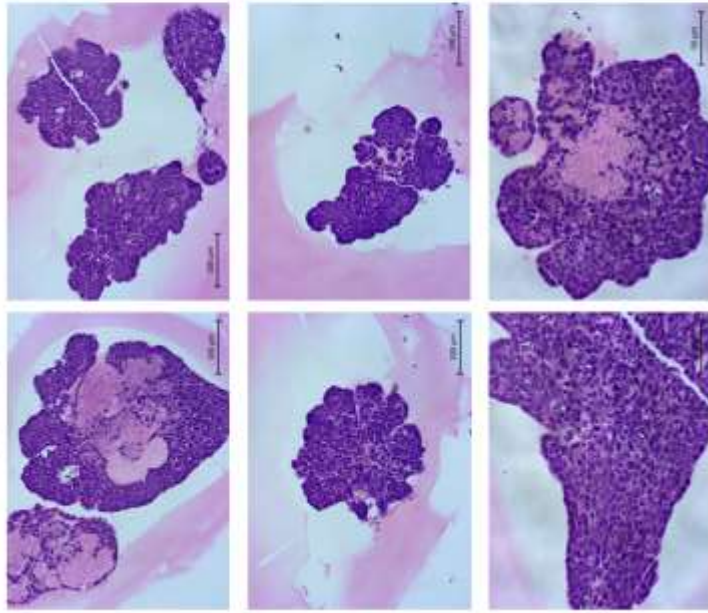
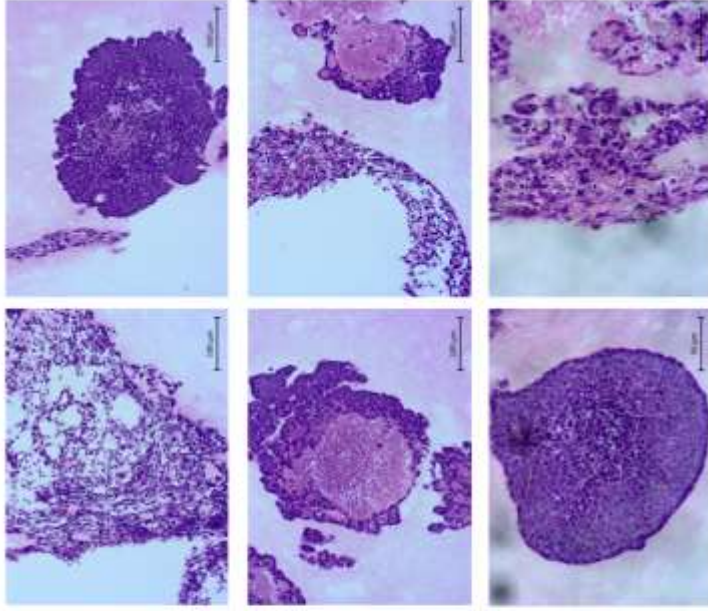


Figure 11: Three-dimensional cell culture of mouse embryonic stem cells in Brain ECM substrates. (A) mESC GOlig2 cells injected within Brain ECM substrates using a 3D bio-printer. Growth and expression of GFP character were evaluated at Day 0, 3 and 14 via fluorescence microscopy. (B) mESC GOlig2 cells injected in three-dimensional Geltrex® and Brain ECM substrates and cultured for 14 days in mESC+LIF medium. IHC was performed to evaluate the ability of the colonies to differentiate within each substrate and without the use of differentiation medium. (C) Relative gene expression of target genes of mESC GOlig2 cultured for 14 days in three-dimensional Geltrex® and Brain ECM substrates.

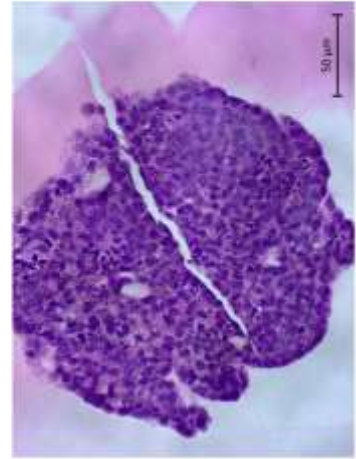
A mESC Golig2, Day 14, in Geltrex – HE Stain



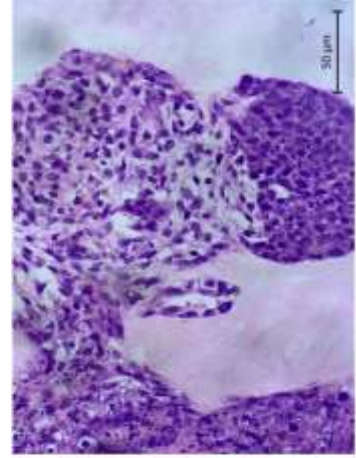
mESC Golig2, Day 14, in BMX08 – HE Stain



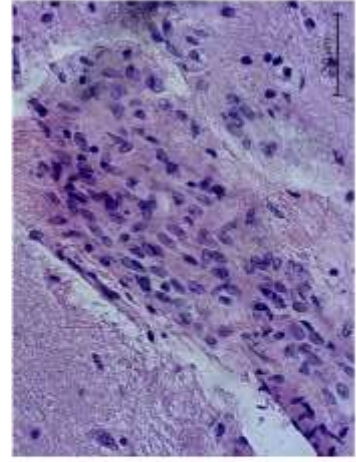
B mESC Golig2, Day 14, in Geltrex – HE Stain



mESC Golig2, Day 14, in BMX08 – HE Stain



Porcine Cerebrum – HE Stain



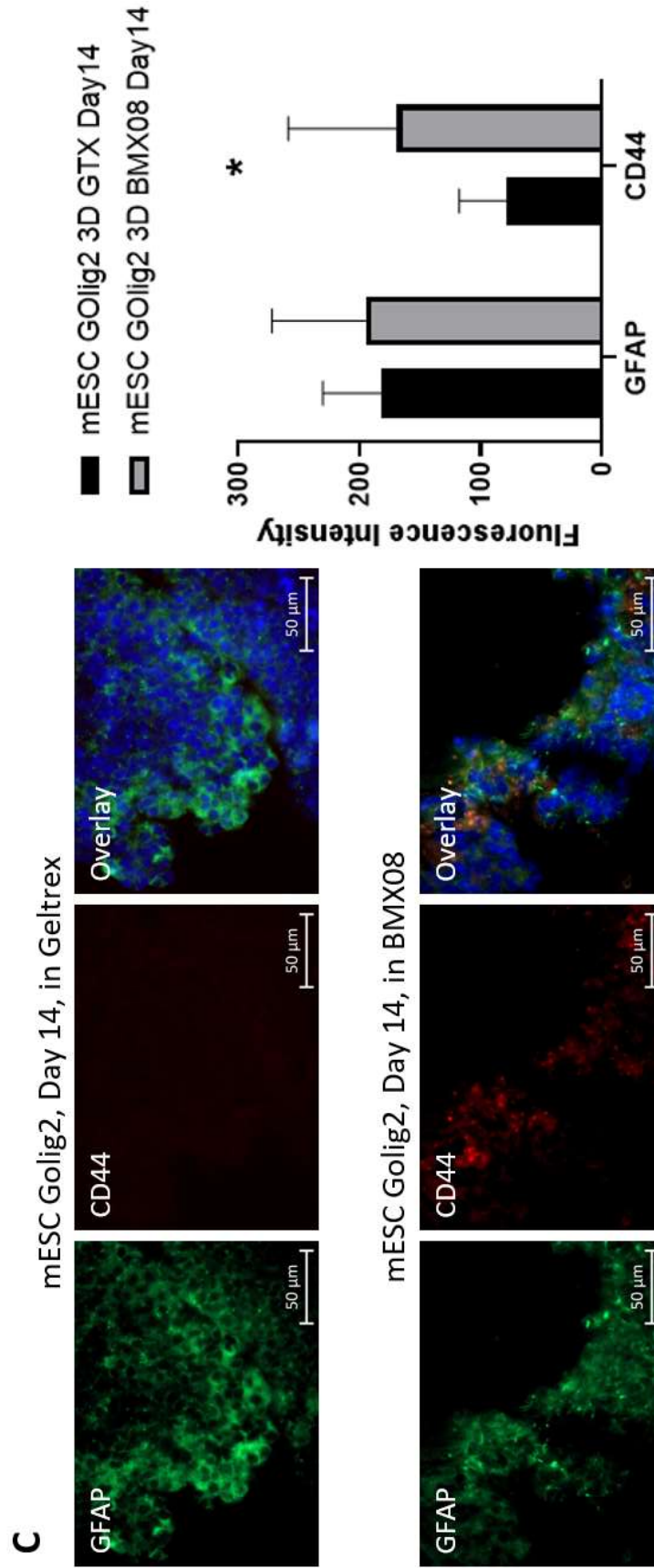
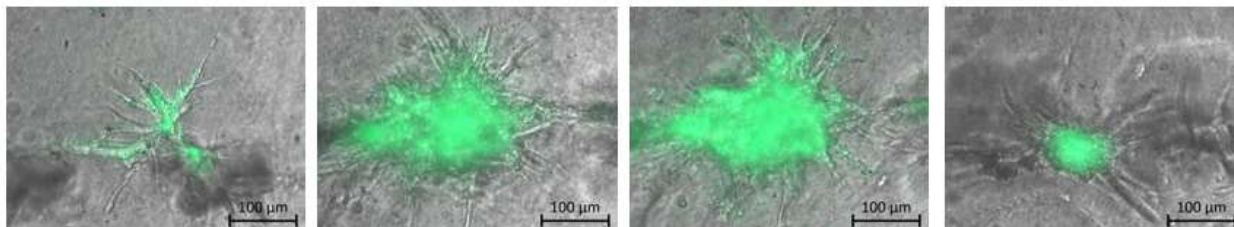
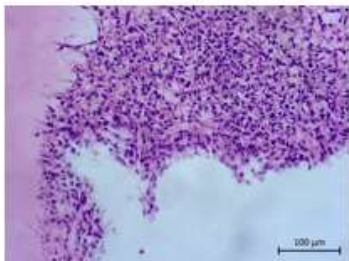


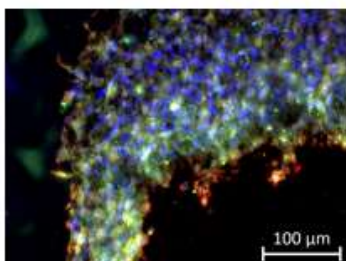
Figure 12: Neural organoids formation from mouse embryonic stem cells in Brain ECM three-dimensional substrates. (A) mESC GOlig2 cells injected within three-dimensional Geltrex[®] and Brain ECM substrates using a 3D bio-printer. Morphology of the cell colonies was evaluated after 14 days in culture. Colonies grown in Geltrex[®] uniformly presented with tightly packed cells with low N:C ratio, while colonies grown in Brain ECM substrate presented variable colony and cellular morphology. mESCs in brain substrate tended to form less tightly packed colonies and presented high N:C ratio. (B) Comparison of mESC colonies grown in Geltrex[®] and Brain ECM substrates versus a sample of porcine cerebrum prior to decellularization. The morphology of mESCs cultured in the brain-derived substrate closely resembles that of porcine brain resident cells. (C) Immunohistochemistry of mESC cultured on Geltrex[®] and Brain ECM substrates, with targets GFAP and CD44. Colonies on brain ECM substrates showed a statistically significant increase in CD44 expression compared to Geltrex[®].

A mNSC Golig2 in 3D culture of Brain ECM substrate, Day 14**B** mNSC Golig2, Day 14, in Geltrex

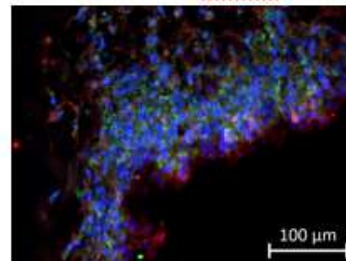
H&E



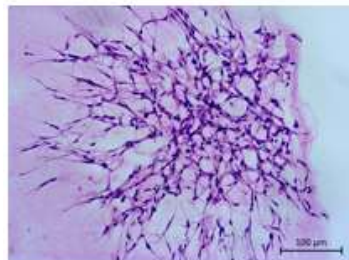
DAPI SOX2 DCX



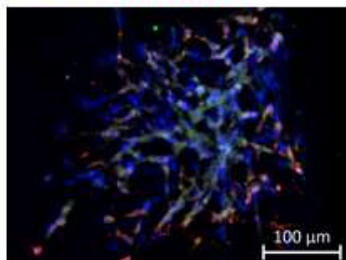
DAPI TUBB3 Nestin

mNSC Golig2, Day 14, in Brain ECM

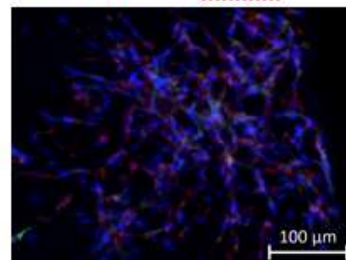
H&E



DAPI SOX2 DCX



DAPI TUBB3 Nestin



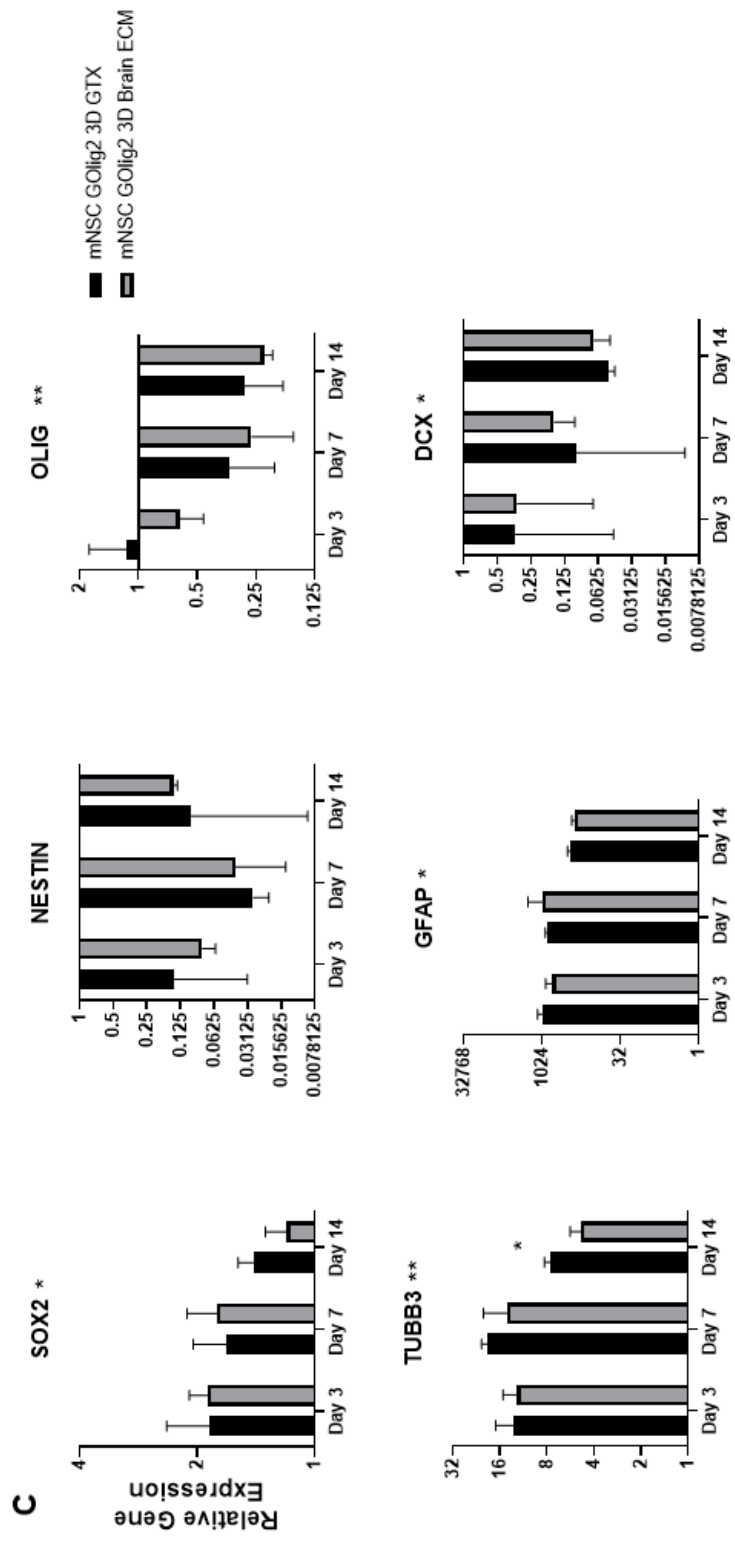


Figure 13: Three-dimensional cell culture of mouse neural stem cells in Brain ECM substrates. (A) mNSC GOlig2 cells injected within Brain ECM substrates using a 3D bio-printer. Growth and expression of GFP character were evaluated at day 0, 3 and 14 via fluorescence microscopy. The figure shows representative images of mNSC GOlig2 cells grown in Brain ECM substrate for 14 days. (B) mNSC GOlig2 cells injected in three-dimensional Geltrex® and Brain ECM substrates and cultured for 14 days in Stem Pro medium. IHC was performed to evaluate the ability of the colonies to differentiate within each substrate and without the use of differentiation medium. (C) Relative gene expression of target genes of mNSC GOlig2 cultured for 14 days in three-dimensional Geltrex® and Brain ECM substrates.

Porcine Brain Matrix-Derived Hydrogels are Biocompatible and Suitable for In Vivo Transplantation of Organoids Developed In Vitro.

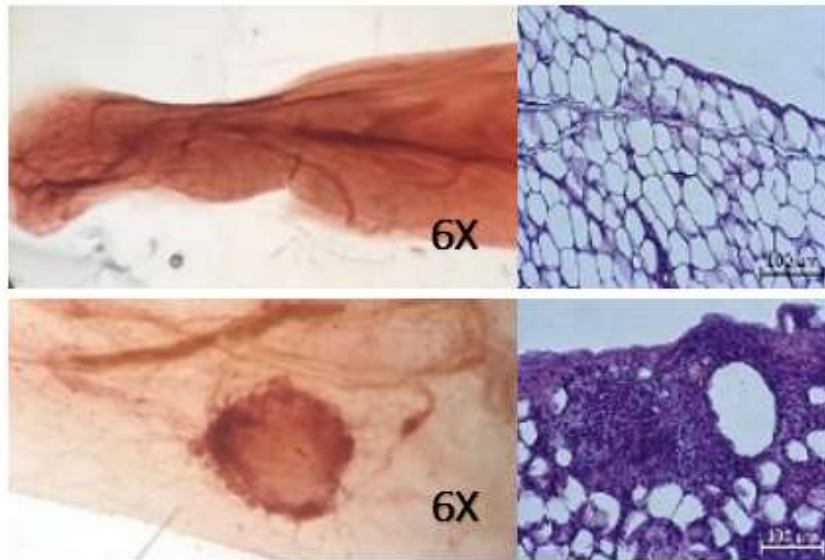
The development of a biocompatible tissue-specific substrate would open the doors to many potential *in vivo* applications. We tested the biocompatibility of our product by evaluating its ability to be transplanted *in vivo* without adverse effects. We also evaluated the suitability of our substrate to promote cell survival *in vivo*, as well as the sustainability of transplanting *in vitro* 3D-bioprinting generated neural organoids *in vivo*.

We first tested the biocompatibility of the brain-derived substrate and its ability to promote cell survival in mouse models. Human iPSCs and NSCs were diluted in either PBS or brain-derived matrix, injected into the cleared mammary fat pads of mice and allowed to incubate over a period of 10 weeks. All the mice survived and did not exhibit adverse effects throughout the experiment period, confirming that our brain tissue-specific substrate is biocompatible and suitable for *in vivo* applications. Mice that were injected with cell solution in PBS did not present any evident change in the morphology of the retrieved tissues. In contrast, 75% (6 out of 8) of the cleared fat pads that were injected with both cells and brain-derived substrates presented new growths following incubation. We concluded that the presence of our ECM-derived substrate was essential to create an environment in which human stem cells were able to survive and proliferate *in vivo*.

Next, we evaluated the potential of creating stem cell organoids *in vitro* and transplant them *in vivo* using three-dimensional brain-derived hydrogels as a vehicle. Organoids from mouse embryonic stem cells and mouse neural stem cells were generated by injecting each cell type within our brain-derived substrates and were kept in culture for a period of either 3 days (mESC) or 14 days (mNSC). Different incubation periods were chosen to accommodate the different proliferation rate of each cell line. Sections of the hydrogels containing stem cell organoids were cut and transplanted in the cleared mammary fat pad of live mice. The mice were monitored weekly over a period of 28 days, after which the injected tissues were retrieved for further analysis. To test whether the organoids were able to grow and proliferate following transplantation, we fixed the samples retrieved and performed immunostaining. The targets chosen for IHC assays performed on mESC GOlig2-derived organoids transplanted *in vivo* were GFP, SOX1, BRY and SOX17. Staining for all targets was observed in sections of tissue

injected with mouse embryonic stem cells grown in brain-derived ECM, while no obvious staining was observed in sections derived from tissue injected with Geltrex® cultures. The targets chosen for IHC assays performed on mNSC GOlig2-derived organoids transplanted *in vivo* were GFP, SOX2, DCX, Nestin and Beta III Tubulin. Staining for GFP, SOX2, Nestin and Beta III Tubulin was comparable in sections of tissue injected with cells grown on either substrate. DCX staining appeared increased in the presence of the brain-derived substrate.

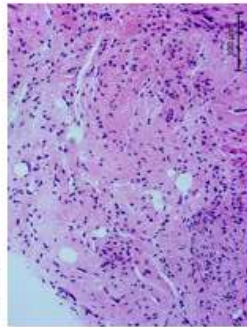
The brain-derived substrate generated in our laboratory was shown to be biocompatible and suitable for applications within mouse models. The presence of such a substrate was essential for the survival and proliferation of human pluripotent and neural stem cells at the site of injection in *in vivo* models. Finally, the brain ECM-derived hydrogels provide an excellent medium for the controlled formation of neural organoids *in vitro*, while at the same time allowing for their transplantation *in vivo*.

A

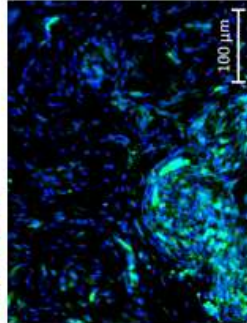
B

mESC Gollig2 in mESC +LIF medium – transplanted in vivo

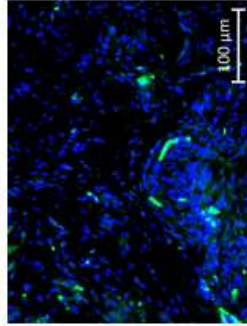
H&E



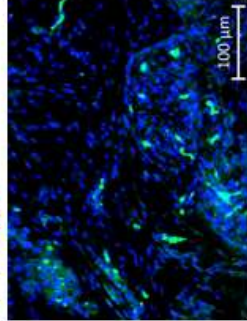
DAPI GFP



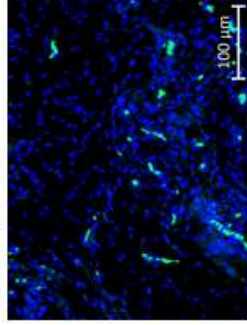
DAPI SOX1



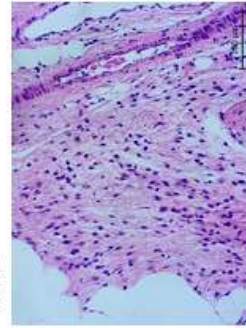
DAPI BRY



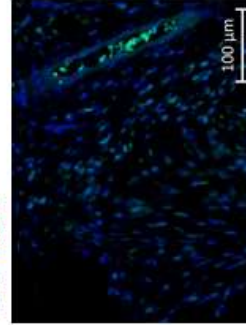
DAPI SOX17



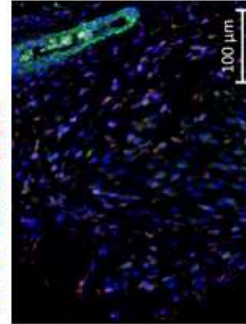
H&E



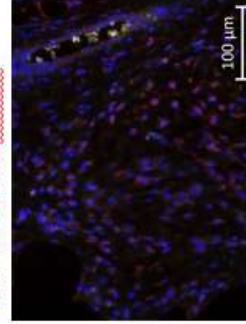
DAPI GFP



DAPI SOX2 DCX

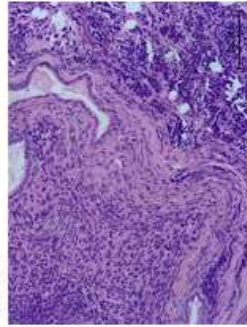


DAPI TUBB3 Nestin

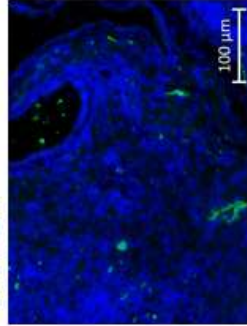


C

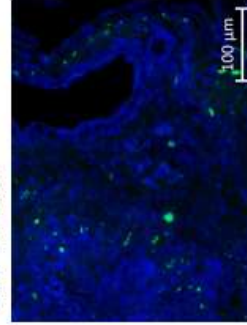
H&E



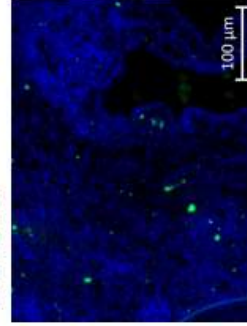
DAPI GFP



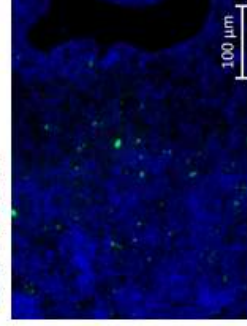
DAPI SOX1



DAPI BRY

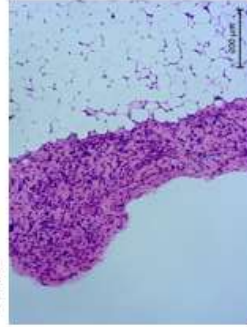


DAPI SOX17

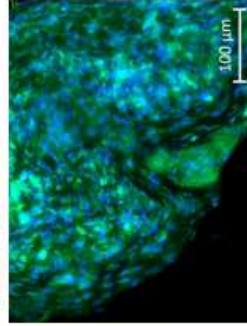


mESC Gollig2, Day 3 in GTX – transplanted in vivo

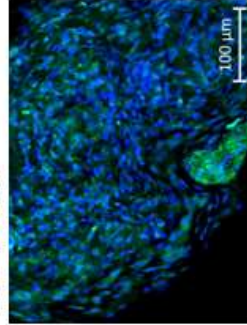
H&E



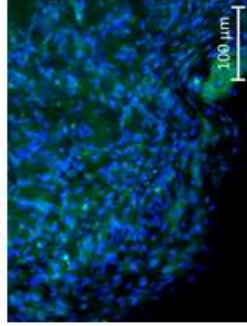
DAPI GFP



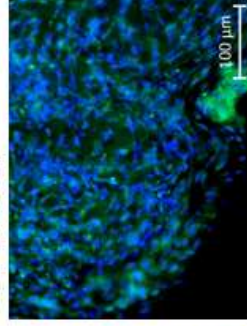
DAPI SOX1



DAPI BRY



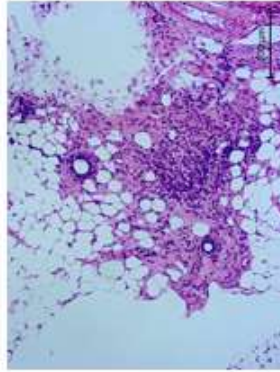
DAPI SOX17



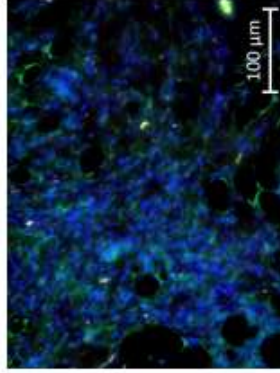
mESC Gollig2, Day 3 in Brain ECM – transplanted in vivo

D mNSC Golig2, Day 14, in Geltrex – transplanted in vivo

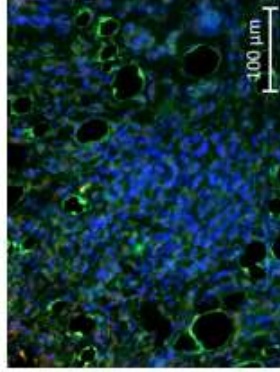
H&E



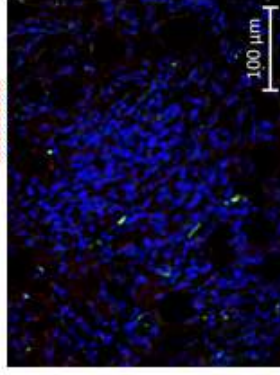
DAPI GFP



DAPI SOX2 DCX

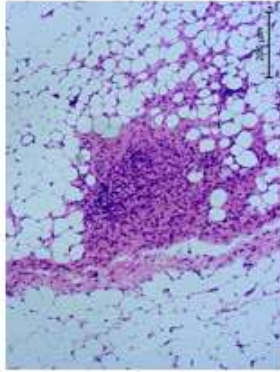


DAPI TUBB3 Nestin

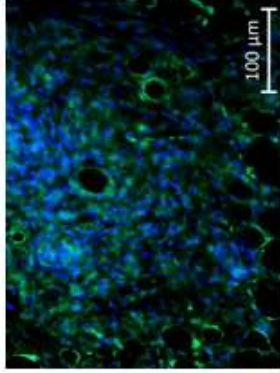


mNSC Golig2, Day 14, in Brain ECM – transplanted in vivo

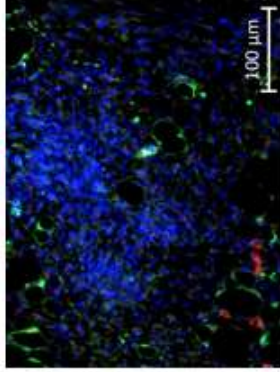
H&E



DAPI GFP



DAPI SOX2 DCX



DAPI TUBB3 Nestin

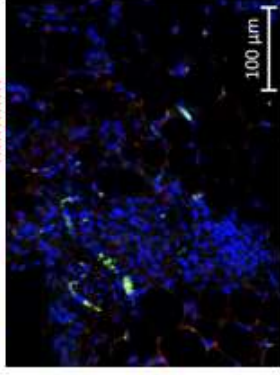


Figure 14: Biocompatibility of tissue-specific hydrogels and their ability to promote cell survival and proliferation *in vivo* was evaluated. (A) Human NSCs were injected in absence (top) or presence (bottom) of brain ECM. Mice were able to survive over the 10 weeks incubation period, indicating that our product is biocompatible and safe to use in murine models. (B) Mouse ESC and NSC were diluted in their respective culture media and were injected within the cleared mammary fat pad of mice. After a four-week incubation period, samples were retrieved and inspected for the presence of the injected cells. IHC revealed presence of mESC and mNSC after 28 days at the site of injection. (C) Mouse ESC were cultured for three days in three-dimensional Geltrex® or Brain ECM substrates in mESC+LIF medium. Cell colonies embedded in either substrate were then injected within the cleared mammary fat pads of mice and incubated over a four-week period. IHC revealed that colonies were able to survive and proliferate *in vivo*. (D) Mouse NSC were cultured for 14 days in three-dimensional Geltrex® or Brain ECM substrates in Stem Pro medium. Cell colonies embedded in either substrate were then injected within the cleared mammary fat pads of mice and incubated over a four-week period. IHC revealed that colonies were able to survive and proliferate *in vivo*.

Materials and Methods

Preparation of Porcine Brain ECM Scaffolds

Porcine brains were extracted from adult animals obtained from three sources. Two frozen porcine heads were purchased from Central Meats & Almost Catered (Chesapeake, VA). Two heads were purchased from Animal Biotech Industries, Inc (Danboro, PA). Two heads were provided by Dr. Christian Zemlin at the Frank Reidy Center for Bioelectrics, after the animals were sacrificed for the research purposes of his laboratory. Brains were carefully extracted and the blood-brain barrier, the meninges and the blood vessels were removed. The tissue was washed in sterile water to remove residual blood. Then, the tissue was cut into sections and washed in a 2% v/v solution of N-Lauryl Sarcosine (NLS) sodium salt solution (Sigma Aldrich) and 2X Antibiotic-Antimycotic (ABAM; Thermo Fisher). All washes were performed at room temperature in a temperature controlled orbital shaker (MaxQ 4000; Thermo Scientific). The supernatant was decanted every 24 hours and replaced with new decellularizing solution for 3-7 days (depending on the size of the tissue sample), until complete cell removal. The slurry was transferred to separate 50 mL conical centrifuge tubes and centrifuged at 35,000 x g for 5 minutes. The supernatant was carefully decanted to prevent the loss of ECM, and the product was resuspended and rinsed with ultrapure water. A total of ten washes were performed to ensure complete removal of the NLS solvent. Subsequently, the product was washed once with isopropyl alcohol for 24-48 hours to remove any liquid component. Finally, the product was washed an additional ten times with ultrapure water to remove any residual alcohol. The decellularized product was lyophilized using a FreeZone Triad Freeze Dryer (Labconco; Chapel Hill, NC). The ECM was then lyophilized through an enzymatic digestion process for 24-72 hours. The product was diluted in a 10 mg/mL solution of pepsin from porcine gastric mucosa (Sigma Aldrich) in 0.1M hydrochloric acid to a concentration of 5mg/mL. The acidic product was dialyzed using a 6-8 kDa dialysis tubing (Spectra Por; Spectrum Labs, Virginia Beach, VA) against a neutral PBS solution with 1X ABAM. Dialysis was performed at 4.0°C to prevent premature gelling. The product obtained was self-gelling when kept at 37.0°C.

Characterization of Total Residual Genomic DNA in Brain-Derived ECM

Native and decellularized porcine brain samples were characterized to determine the efficiency of the decellularization protocol. Samples from the unprocessed cerebrum, cerebellum, pons, midbrain, and medulla, as well as a sample of the decellularized product were fixed in 10% formalin for two hours and then preserved in 70% ethanol. The fixed samples were embedded in paraffin and sectioned at the EVMS Histology Laboratory (Eastern Virginia Medical School, Norfolk, VA). A section of each sample was stained with Hematoxylin and Eosin to determine their nuclear content.

The genomic DNA (gDNA) content of the native brain tissue and the final hydrogel products was determined using the Quant-iT™ PicoGreen® dsDNA Reagent Kit (Invitrogen). The gDNA content of each of the hydrogel batches was measured. The assay was performed following manufacturer's instructions, and fluorescence was measured using a Varioskan™ Lux microplate reader (Thermo Fisher Scientific).

Characterization of Protein Content in Brain-Derived ECM

The total protein concentration of the final brain ECM product was characterized using the DC™ Protein Assay (Bio-Rad Laboratories), which was performed following manufacturer's instructions. To perform this colorimetric assay, five serial dilutions of a bovine serum albumin protein standard (Bio-Rad Laboratories), as well as 1/10 dilutions of the brain-derived hydrogel batches, were prepared. The product concentration was measured spectrophotometrically using a Nanodrop 2000 (Thermo Fisher) and a wavelength of 750 nm.

Qualitative characterization of the hydrogels' protein content, compared to the commercially available Geltrex® matrix, was done performing polyacrylamide gel electrophoresis (PAGE) assay. A 7.5% polyacrylamide gel (Bio-Rad Laboratories) was inserted in a vertical electrophoresis cell (Bio-Rad Laboratories), and the cell's chambers were filled with 1X SDS Buffer, to obtain a continuous buffer system. Samples were prepared as a serial dilution of the brain matrix product, 100% to 6.5% concentration of product to sterile water. Geltrex® was diluted 1:100 in sterile water, for a final concentration of 1.57 mg/mL. Samples were diluted with Laemmli buffer to form a 1X solution, heated to about 100°C and incubated for 10 minutes. Equal amounts of each

sample were loaded into the polyacrylamide gel walls. The gel was resolved applying voltage at 5 V for five minutes, and then at 100 V until the ladder sample reached the lower portion of the gel. After completion of PAGE, the polyacrylamide gel was carefully removed from the chamber and washed with deionized water. A coomassie G-250 stain was prepared with 50% methanol, 10% acetic acid, 40% deionized water and 0.5% of coomassie brilliant blue G-250 dye (Amresco, Solon, OH), and used to wash the gel for 5 minutes. Successively, the gel was rinsed with deionized water, and a de-stain solution composed of 40% methanol, 10% acetic acid and 50% deionized water was applied overnight, until visible bands appeared on the gel. Imaging of the stained gels was performed with a myECL™ Imager (Thermo Fisher Scientific).

Generation and Culture of Human iPSC-Derived Neural Stem Cells

The wild-type human induced pluripotent stem cell (hiPSC) line is-bASC3 was previously generated in our laboratory from a human breast adipose tissue cell line. Cellular reprogramming and validation were performed using the CytoTune™ – iPS 2.0 Sendai Reprogramming Kit (Life Technologies) [109]. hiPSCs were adapted to feeder free conditions and cells were seeded on Geltrex® coated plates. All Geltrex® coatings were performed diluting the matrix 1:100 in cold DMEM, for a final concentration of 1.57 mg/mL, and incubated at 37.0°C for at least one hour. hiPSC cultures were maintained following the Maintenance of Human Pluripotent Stem Cells in mTeSR™1 technical manual (STEMCELL Technologies; Cambridge, MA). Cells were maintained in complete mTeSR™ Plus medium (STEM CELL Technologies), replenished daily. Upon reaching 70-90% confluency, cells were manually or enzymatically passaged. Enzymatic passage was performed using Dispase (STEMCELL Technologies) according to the manufacturer's suggested protocol. Pluripotency of the hiPSC colonies was confirmed using a Tra-160 live staining kit (Thermo Fisher).

Human neural stem cells (hNSCs) were generated from the is-bASC3 line using the STEMdiff™ Neural System Embryoid Body (EB) protocol (STEMCELL Technologies) and following manufacturer's instructions. Newly formed NSCs were cultured on Geltrex® coated plates and in complete StemPro® NSC Serum Free Medium (Thermo Fisher Scientific), which was completely replenished every other day. Cells were passaged upon

reaching 100% confluency, using TrypLE™ Express Enzyme (Thermo Fisher) according to the manufacturer's suggested protocol. The identity of the newly formed hNSCs was confirmed via immunocytochemistry, using the neural stem cell markers SOX2, NESTIN, PAX3 and PAX6.

Generation and Culture of Mouse ESC-Derived Neural Stem Cells

The wild-type mouse embryonic stem cell (mESC) reporter line G-Olig2 was purchased from ATCC®. mESCs were adapted to feeder-free conditions and cells were seeded on Geltrex® coated plates. Cells were cultured in mESC Cell Culture medium, containing Mouse ES Cell Basal Medium (ATCC), 15% Embryonic Stem Cell qualified FBS (Life Technologies), 1X Antibiotic-Antimycotic (Thermo Fisher), 55 µM β-Mercaptoethanol (Gibco). The medium was supplemented with 1000U/ml of Leukemia Inhibitory Factor (LIF) supplement (Millipore Sigma), 1µM MEK inhibitor PD0325901 (Millipore Sigma) and 5µM GSK3 inhibitor CHIR99021 (Millipore Sigma). Cell culture medium was completely replenished daily. Cells were passaged once the cells reached 70% confluency, using TrypLE™ Express Enzyme according to the manufacturer's suggested protocol. Pluripotency of the mESC colonies was confirmed using a SSEA-1 live staining kit (Esi Bio).

Mouse neural stem cells (mNSCs) were generated from the G-Olig2 line using the STEMdiff™ Neural System Embryoid Body (EB) protocol and following manufacturer's instructions. Newly formed NSCs were cultured on Geltrex® coated plates and in complete StemPro® NSC Serum Free Medium, which was completely replenished every other day. Cells were passaged upon reaching 100% confluency, using TrypLE™ Express Enzyme according to the manufacturer's suggested protocol. The identity of the newly formed mNSCs was confirmed via immunocytochemistry, using the neural stem cell markers SOX2, NESTIN, PAX3 and PAX6.

Neural Differentiation

Neural differentiation was achieved following previously published protocols [110, 111]. NSCs were cultured in complete StemPro® NSC Serum Free Medium until 50% confluent. Successively, the medium was replaced with Neurobasal™ Medium (Thermo

Fisher Scientific), supplemented with 2% B-27™ Supplement (50X) (Thermo Fisher Scientific), 0.5 mM GlutaMAX™, 1X ABAM, 500 nM purmorphamine (STEMCELL Technologies), 50 nM retinoic acid (STEMCELL Technologies). Partial (1/2) medium change was performed daily. At Day 15 of differentiation, the medium was substituted with neural maturation medium, constituted of Neurobasal™ Medium supplemented with 2% B-27™ Supplement (50X), 0.5 mM GlutaMAX™ and 1X ABAM. Cells were differentiated for up to 30 days. The ability of the cells to undergo neural differentiation onto different substrates was evaluated via qRT-PCR and immunocytochemistry assays. The targets of both assays were the following: PAX3 (ectoderm), SOX (pluripotency), NESTIN (neural stem cells), Doublecortin (neuron), MAP2 (neuron), β -III-Tubulin (neuron), SYN1 (mature neuron), GALC/OLIG (oligodendrocyte), GFAP (astrocyte), and BDNF.

2D Plating of Brain ECM for Cell Culture

The suitability of the porcine brain-derived matrix for two-dimensional cell culture was evaluated. Cell culture plates or glass coverslips were coated with a 0.1% polyethyleneimine (PEI; Sigma) solution in borate buffer pH 8.4 [112] and incubated at 37°C for one hour (200 μ L of PEI solution were used to coat wells of a 24 well plate or glass coverslips). Successively, the wells were washed three times with sterile water, for five minutes. Porcine derived hydrogels were diluted to a concentration of 0.3 mg/mL in cold DMEM/F12 and incubated overnight at 37°C (250 μ L of hydrogel solution were used to coat wells of a 24 well plate). The wells were then washed three times with sterile water for five minutes. Cells were then seeded, cultured, and differentiated following the previously described protocols.

Three-Dimensional Cell Culture in Brain ECM – Derived Substrates

The suitability of the porcine brain-derived ECM for three-dimensional cell culture was evaluated. 2mg/mL porcine ECM hydrogels were prepared diluting the tissue-derived hydrogel in Geltrex® and cell culture medium. Quantities were calculated so that the volume of Geltrex® would not exceed 50% of the total hydrogel volume, and the remaining 50% was constituted by porcine ECM diluted into cell culture medium. For example, to

prepare 250 μ L of 2mg/mL porcine ECM hydrogel, 125 μ L of Geltrex[®], 100 μ L of 5mg/mL porcine brain matrix and 25 μ L of cell culture medium were combined. Diluted ECM hydrogels were plated into wells of a cell culture plate and allowed to incubate overnight at 37.0°C to achieve gelation.

Cells were diluted in culture medium to a concentration of 10 million cells/mL and injected into the three-dimensional hydrogels, placing roughly 100 cells at each injection site. To do so, a 3D bio-printing system adapted in our laboratory was utilized [88]. Following placement of cells within the substrate, cell culture medium was added on each well, and samples were incubated at 37.0°C

Brain Scaffold In Vivo Biocompatibility

In vivo injections of the brain-derived matrix were performed in mice to assess the biocompatibility of the material. The ECM was then injected with human wild-type NSCs and hiPSCs to determine its ability to promote cell survival, proliferation, and differentiation *in vivo*. The endogenous epithelium of the inguinal mammary glands of sedated 3-week-old mice was removed, the brain-derived product was diluted 1:2 in DMEM/F12 and injected into the cleared mammary fat-pad. Consequently, 200,000 cells of either line were injected in the gel. Cells were also injected in the mice's mammary gland in absence of the brain-derived matrix, to provide a negative control. After ten weeks of incubation, the tissue was removed, fixed and embedded in paraffin for further analysis.

In Vivo Cell Culture Mediated by Brain-Derived Scaffolds

The ability of porcine brain-derived hydrogels to sustain cell proliferation and differentiation *in vivo* was evaluated. The endogenous epithelium of the inguinal mammary glands of sedated 3-week-old mice was removed, the brain-derived product was diluted 1:2 in DMEM/F12 and injected into the cleared mammary fat-pad. Consequently, 200,000 cells of both human neural stem cells and human induced pluripotent stem cells were injected into the gel. Cells were also injected in the mice's mammary gland in absence of the brain-derived matrix, to provide a negative control.

After ten weeks of incubation, the tissue was removed, fixed, and embedded in paraffin for further analysis.

Mouse embryonic and neural stem cells of the line GOlig2 were injected in three-dimensional brain derived or Geltrex[®] substrates and cultured over a period of 14 days. The endogenous epithelium of the inguinal mammary glands of sedated 3-week-old mice was removed, and cells embedded in the three-dimensional matrices were injected into the cleared mammary fat-pad. Cells were also injected in the mice's mammary gland in absence of the brain-derived matrix, to provide a negative control. After four weeks of incubation, the tissue was removed, fixed and embedded in paraffin for further analysis.

Nucleic Acid Extraction and Gene Expression Analysis

The differential gene expression of NSCs and neural cells grown and differentiated on two-dimensional and three-dimensional brain-derived substrates was measured. Gene expression data were obtained through RNA extraction and purification, cDNA synthesis, and Real-Time quantitative PCR assays.

Upon reaching the appropriate confluency level of the cultures, RNA extraction was performed using TRIzol[®] reagent (Thermo Fisher Scientific) following the manufacturer's protocol. The RNA phase was isolated through centrifugation. Next, the RNA was precipitated using 100% isopropanol, and washed using 75% ethanol. Finally, the isolated RNA was diluted in 22 μ L of nuclease-free water. Purity of the RNA samples was ensured by the performance of gDNA digestion using Deoxyribonuclease I, Amplification Grade (Thermo Fisher Scientific), following the manufacturer's protocol. RNA was then quantified using a NanoDrop 2000 (Thermo Fisher Scientific), and its concentration was determined based on the UV absorbance levels at 260 nm (A₂₆₀ nm). Quantification values were considered acceptable with 260/280 ratios >1.7, and 260/230 ratios > 1.8. The RNA product was then used to synthesize cDNA strands using the High-Capacity cDNA Reverse Transcription Kit (Thermo Fisher Scientific), as per manufacturer's protocol.

cDNA samples were amplified using TaqMan[®] Gene Expression Assay (Applied Biosystems) to quantify the original mRNA levels. Optimized primers and probes were provided for the specific target genes in analysis, and each probe presented a 5' terminal

reporter dye FAM (6-carboxyfluorescein) and a 3' terminal non-fluorescent quencher dye (NFQ-MGB). To perform the amplification, real-time quantitative PCR assays were performed using a StepOnePlus™ Real-Time PCR System (Applied Biosystems; Foster City, CA). Complete samples for the reactions comprised 1X TaqMan® Fast Advanced Master Mix, 1X TaqMan® Gene Expression Assay, and 50 ng of cDNA template, for a total final volume of 20µL. All PCR experiments comprised a total of 40 thermal amplification cycles, and each cycle consisted of 1 cycle of 2 minutes at 50°C, 1 cycles of 20 seconds at 95°C, and 40 cycles of 1 second at 95°C and 20 seconds at 60°C. All experiments were performed in triplicates, and each sample was sub-sampled three times, to ensure statistical significance of the results. Gene expression analysis was conducted using the $2^{-\Delta\Delta C_t}$ of the average Ct for each subsample. Statistical analysis and data graphical representation were performed with Prism 7 (GraphPad Software; La Jolla, CA).

Immunocytochemistry

Immunocytochemistry assays were performed to confirm the identity of newly generated neural stem cell lines, as well as to test the ability of the cells to survive and differentiate on the porcine brain-derived substrate. Samples were washed twice in 1X tris-buffered saline (TBS) for 5 minutes each – all the subsequent washes were performed for the same amount of time – and fixed in 10% formalin for 20 minutes. Samples were then washed with 1X TBS three times, incubated with 0.1% NP40 in TBS at room temperature for 10 minutes, and then blocked with 10% goat serum for 60 minutes. Primary antibodies were diluted in 1% goat serum according to the manufacturer's instructions, and following application they were incubated overnight at 4°C. Next, after washing the samples with TBS four times, Alexa Fluor™ 488 and 568 secondary antibodies (Thermo Fisher Scientific) diluted 1:1000 in 1% goat serum were added and the samples were incubated in the dark, at room temperature, for 60 minutes. Samples were newly washed in TBS four times, and nuclear stain was performed adding DAPI diluted 1:1000 in 1% goat serum. The samples were finally washed four times in TBS, and images were acquired with a Zeiss Axio microscope with a short-working distance 20X objective.

Immunohistochemistry

Three-dimensional cell culture samples were fixed with 10% formalin for one hour, incubated with 70% and 90% ethanol for one hour each and then preserved in 70% ethanol. Samples were embedded in paraffin and sectioned by Histoserv inc. (Germantown, MD). One section of each sample was stained with hematoxylin and eosin to define the nuclear content.

To perform immunofluorescence assays, sections were washed twice in xylenes (Thermo Fisher Scientific) for 8 minutes each, to remove the paraffin from the slides. Sections were rehydrated doing two 2 minutes washes in 100% ethanol, one 1-minute wash in 90% ethanol, one 1-minute wash in 70% ethanol, and one 1-minute wash in distilled water. Slides were rinsed in 1X TBS and transferred to preheated citrate buffer (antigen retrieval buffer) for 25 minutes. After cooling, the samples were rinsed twice in 1X TBS and washed in the same solution until cool. Samples were blocked with 10% goat serum and incubated for 60 minutes, at room temperature, in the dark. Primary antibodies were diluted in 1% goat serum according to the manufacturer's instructions, placed on the slides, and incubated overnight in humidified chambers, at 4°C. A negative control was performed by addition of 1% goat serum only. Next, slides were rinsed twice, and successively washed thrice in 1X TBS. Secondary antibodies were diluted 1:1000 in 1% goat serum, applied to the samples and incubated at room temperature, in the dark, for 60 minutes. Slides were washed with TBS and nuclear stain DAPI, diluted 1:1000 in 1% Goat Serum, was applied, and the samples were incubated for 5 minutes protected from light. Samples were finally washed thrice in 1X TBS and images were acquired with a Zeiss Axion Observer microscope at 10X or 20X magnification.

Image Analysis

Slides stained through immunohistochemistry were analyzed to evaluate the relative presence of the targets of interest. A negative control was obtained by substituting the overnight incubation with primary antibodies with incubation with 1% goat serum only. Images of the slides and the negative controls were taken with a Zeiss Axion Observer microscope ensuring maintenance of the same exposure times. Intensity values for each

channel were recorded in at least 3 locations where nuclear presence was detected via positive DAPI staining, in each image. Intensities values for sample images were calculated as the difference between the measured intensities and the average intensities of the respective channel in the negative control.

Statistical analysis and data graphical representation were performed with Prism 7 software. Specifically, t tests were used to evaluate differences between target expression between cells cultured in Geltrex® and brain-derived substrates.

Discussion

The cellular microenvironment has a fundamental role in establishing stem cell fate and regulating the behavior of differentiated cells. Such a notion is valid in the case of neural stem cells and their development into neurons and supportive cells of the nervous system. The components of the extracellular matrix that constitute the cellular environment are specific to each tissue and play a fundamental role in promoting the exchange of the cell-cell and cell-ECM signals necessary for the establishment of cell fate, proliferation, and motility. Current two- and three-dimensional cell culture methods often rely on the use of animal and tumor derived matrices or purified proteins to enable cell survival and proliferation. Such substrates have been critical in advancing our understanding of the physiology of stem and neural cells; however, they fail to accurately mimic the *in vitro* cellular environment. The use of a neural tissue-derived matrix establishes a highly biomimetic environment possessing a natural and specific combination of ECM proteins, and most suitable for the study of stem and neural cell behavior. This approach is being increasingly adopted in various areas of research for the study of tissue and cell-specific physiology, not only limited to the neural tissue.

In this study, we describe the application of a substrate produced from porcine brain tissue in combination with a 3D bioprinting platform for the establishment of a biomimetic cell culture system. Brains extracted from adult pigs were successfully decellularized and treated to produce self-gelling hydrogels. Characterization of the decellularized product revealed that no visible nuclear structures were present in the H&E staining of the tissue, and that the gDNA content of the final product was below 10 ug/mL. The product was further characterized to establish the hydrogels' total protein concentration, as well as compare it to the commercially available matrix Geltrex[®]. Calculating the protein concentration of the various batches was necessary to ensure uniformity and reproducibility when using the hydrogels as cell culture substrates. PAGE assay was utilized to qualitatively evaluate the hydrogels protein content. The specific bands observed suggested that the major components of Geltrex[®] were shared with the porcine-derived matrix, and that the latter presented an additional number of components that were not identified in this study. This finding was suggestive of the superiority of the tissue-specific matrix in accurately mimicking the *in vitro* neural environment.

After successful establishment of human and murine neural stem cell lines, the brain-derived product was tested for its suitability in promoting cell survival and proliferation, as well as its ability to promote cell differentiation. The ability of human and mouse NSCs to survive and proliferate on the brain-derived matrix was first tested, and Geltrex[®] coated plates were used as control. Cells were able to proliferate in two-dimensional cultures on brain ECM-coated plates, and no morphological differences were observed when using the new substrate. Gene expression analysis of NSCs cultured over two weeks on either substrate revealed that the brain specific substrate promotes expression of the early neuronal marker in the human model, while having a protective effect on the expression of the astrocyte marker in the mouse model. Whether the brain-derived substrate has an impact in the neuronal differentiation process at either a short or long term, was also investigated. We observed that human and mouse neural stem cells can successfully differentiate into neural cells while seeded on either substrate. No significant differences in the gene expression of germ layer, NSCs and neuronal markers were observed after 7 or 30 days of neural differentiation between cells seeded on either substrate. However, the brain ECM-derived substrate promoted higher expression of astrocyte markers in the short term, while having a protective effect in the long term, compared to Geltrex[®]. These results confirmed that the tissue-specific substrate generated in our laboratory can promote the survival, proliferation, and differentiation of neural stem cells in a two-dimensional culture system and that the presence of a brain-specific environment has an effect on the differentiation of human and mouse neural stem cells. The product also offers the advantage of providing an environment closely mimicking that of neural cells *in vitro*, and therefore providing a system with higher reliability for the study of cells of the neural lineage.

The three-dimensional organization of cells within a tissue is a factor that influences cell physiology *in vivo*. Establishing a reliable and highly biomimetic three-dimensional culture system for cells of the neural lineage is an important contribution and provides a reference for future research in the field. After determining the ability of our product to spontaneously form solid hydrogels when incubated at 37°C, we evaluated the performance of brain ECM -based substrates in the context of stem cell culture. To do so, we applied our 3D bioprinting system for the precise placement of cells within the three-

dimensional substrates. The 3D bioprinter was previously customized from a commercially available 3D bioprinter model as an improvement to traditional three-dimensional cell seeding methods. The system is coordinate-based and can be programmed to perform large scale experiments, with a high degree of reproducibility, and in one sitting. We first established the ability of mouse embryonic stem cells to survive in the tissue-specific three-dimensional environment. Cells of the line GOlig2 were selected as they are a reporter line in which GFP expression is associated with Olig gene expression. The fluorescent character of the cells makes for easier visualization of the cell colonies in 3D, as well as providing an insight on their differentiation state while they are maintained in culture. Next, we explored the potential to combine our 3D-bioprinting system with the tissue-specific substrate to efficiently produce neural organoids in three-dimensional cell cultures. We also investigated whether the three-dimensional culture conditions or the tissue-specific ECM promoted differentiation of cells cultured in mESC maintenance medium. Our system allowed us to successfully place a predetermined number of mESC in precise locations within the three-dimensional hydrogels, resulting in the formation of neural organoids at each injection site. Additionally, our system allowed for the performance of high throughput experiments while maintaining a high degree of repeatability of experimental conditions. No statistically significant change in the expression of Olig2 gene or germ layer markers was observed after incubation of the mESC over two weeks, with the exception of the endoderm marker. Throughout the incubation period within both 3D substrates its expression significantly increased, and at 14-days the colonies cultured in Geltrex[®] presented a significant increase in expression compared to brain ECM based substrates. Increased expression of the same marker in Geltrex[®] compared to the brain-derived substrate was also confirmed via ICC. This result indicated that the 3D conditions promoted a degree of differentiation towards endoderm compared to 2D conditions and that this was more significant in Geltrex[®] substrate. Immunohistochemistry analysis also revealed that the brain-derived substrate favors the differentiation of mESCs towards the astrocyte cell type, confirmed by staining for both GFAP and CD44 markers. Differentiation towards the neural lineage is also suggested by the development of unique morphologies of mESCs cultured within the tissue-specific substrate, comparable to those of resident cells of the porcine cerebrum. Overall, we

showed that three-dimensional cell culture conditions influence the propensity of mouse embryonic stem cells to spontaneously differentiate, and that the brain-derived substrate promotes differentiation towards the neural lineage also in a three-dimensional environment. We demonstrated that the combination of brain-specific substrates with 3D bioprinting technology is ideal to produce neural organoids in three-dimensional cell cultures and with high degrees of reproducibility.

The ability of the three-dimensional substrates to promote maintenance versus differentiation of stem cells was also evaluated in neural stem cells, already committed to a defined lineage. Mouse NSCs of the line GOlig2 were cultured in 3D Geltrex® and Brain ECM based hydrogels over a 14-day period and in NSC maintenance medium. Gene expression analysis revealed a statistically significant decrease in pluripotency and early neural differentiation gene expression. In contrast, expression of neuronal and astrocyte markers was significantly increased, with Geltrex® substrate favoring increase in neuronal markers expression. Overall, these results combined suggest that three-dimensional culture conditions alone and in absence of differentiation medium promote neural stem cell differentiation towards neuron and astrocyte cell types and at a comparable level in the presence or absence of brain ECM.

Finally, the potential of the tissue-specific substrate for *in vivo* applications was evaluated. We first demonstrated that the final hydrogel product is not only biocompatible, but also necessary for the survival of neural stem cells injected within the clear mammary fat pads of live mice. Next, we demonstrated that the neural organoids generated using the 3D bioprinting system can be transplanted *in vivo*. The cells can survive and maintain their cellular identity even after transplantation outside of their tissue of origin. This result constitutes a demonstration that our tissue specific cell culture system can have vast applications for the development of translational research techniques targeting an application within living organisms

Conclusion

The ability to create an artificial cell culture system that accurately mimics *in vivo* conditions, and that can be easily adopted, is an important step in the establishment of parameters that allow us to produce the most accurate research data. Stem cells' physiology and behavior are affected by their surrounding environment's structure and composition, and standard cell culture techniques lack the ability to efficiently reproduce them. Here we showed that combining our tissue-specific neural substrate with our 3D bioprinting system, we were able to optimize a three-dimensional cell culture system that promoted the growth and spontaneous differentiation of mouse stem cells towards the neural lineage as well as the formation of neural organoids. We also reported evidence demonstrating the important role that the cellular microenvironment plays in dictating stem cell behavior and differentiation. Our system holds great promise in future applications for the study of stem cell physiology as well as neural physiology and disease models.

CHAPTER III

ENGINEERING OF A BIOPRINTING SYSTEM FOR THE STUDY OF IMMOBILIZED-GROWTH FACTOR DRIVEN ASYMMETRICAL STEM CELL DIVISION

Introduction

The scientific community has made many great steps in the elucidation of the mechanisms that drive cellular physiology; however, this field of research is still defined by a myriad of unknowns. The lack of accessible systems that allow the performance of high throughput studies, at high resolution, and providing biomimetic conditions, is a limiting factor in the achievement of speedy progress.

Stem cell behavior is modulated by biomechanical and biochemical signaling between the cells and their environment; however, many of the molecular mechanisms that drive such changes are still unknown. Previously published work has demonstrated the potential of localized signals in the direction of an asymmetrical stem cell division process [26]. The authors showed that localization of WNT3A proteins on single mouse embryonic stem cells is sufficient to orient the mitotic division plane of stem cells, ultimately directing the asymmetrical division process. The results open the door to the design of many studies for the evaluation of the role of various individual proteins on the asymmetrical division process. With the appropriate setup, careful placement of localized growth factor can be used to direct asymmetrical division.

Studies that focus on the analysis of the behavior of single cells to understand cellular mechanisms are traditionally performed in two-dimensional conditions. In this configuration, if cells are not immobilized on the two-dimensional surface, challenges arise in determining a set of conditions that allow for cells to be seeded at very low density while enabling visualization of cellular behavior over time. The randomness that defines the process of plating cells in a monolayer culture, results in tedious experimental procedures and often low efficiency in achieving the desired conditions [26]. Alternatively, to perform single cell studies, micropatterning techniques can be utilized to immobilize cells within a confined area of the plate [113-115], or single cells can be isolated and seeded with the use of specialized equipment. Such methods either add a layer of complexity to the process, or they are not readily available or accessible by research

laboratories. The challenges associated with both these setups, prevents the easy performance of high-throughput studies.

The physical structure and mechanical properties of the environment in which the cells are growing, influence their physiology [48, 54, 57, 61, 116, 117]. The three-dimensional disposition of cells of specific tissues in an organism provides different stimuli to cells compared to two-dimensional cell culture plates. Ensuring a higher degree of biomimicry in experimental setups allows us to devise experiments that are more representative of the true cellular conditions, ensuring higher relevance of the data collected. The use of three-dimensional substrates for cell culture is an established technique in many laboratories [81, 86, 88, 90, 96]. The culture conditions are usually not permissive for single cell experiments, as cells are either seeded randomly by mixing of cell solution and hydrogel prior to gelation, or cells are injected within the solidified gels. Here we propose a 3D bioprinting based system for the performance of single cell and single cell – single bead resolution, high throughput studies in 2D or 3D cell culture conditions. Our group has previously adapted a commercially available 3D printer for biological applications, specifically for the injection of a selected number of cells within three-dimensional substrates [88, 94, 95, 108]. Here, we optimize the system to allow for the printing of single cells and single cell – single bead complexes in two-dimensional monolayer conditions and within thin three-dimensional hydrogels. We show that the setup is suitable for cell culture, for high throughput experiments and it allows for the study of cellular mechanisms at the single cell level. The use of re-purposed technology, along with the protocols provided, represent an accessible method for the performance of numerous types of alternative studies when the ability to easily manipulate experimental conditions is desired. In particular, by tethering microbeads to various proteins, the system developed can be applied to study the impact of any number of localized signals on stem cell processes. Moreover, the bioprinting system provides a platform that allows us to develop protocols for the manipulation and direction of asymmetrical stem cell division events *in vitro*. This concept was applied here to test the ability of WNT3A growth factors to direct asymmetrical division in mouse embryonic stem cells within a three-dimensional environment.

Materials and Methods

3D Bioprinting System

Our laboratory has previously adapted a commercially available “off-the-shelf” 3D printer into a functional 3D bio-printer. The printer was customized starting from the extrusion-based Felix 3.0 (FELIXrobotics, NL) model. The machine has listed print resolutions of 13 μm , 13 μm , and 0.39 μm for the x, y, and z axes. The print head, which functions for the controlled extrusion of plastic, was replaced with a deposition apparatus designed and 3D printed in the laboratory. The system is powered by a NEMA 17 hybrid bipolar stepping motor with an integrated threaded rod (Pololu, USA, itemno. 2268). Each step allows for the movement of the traveling nut by 40 μm , for a total movement by 8000 μm of linear travel during a total revolution. The deposition apparatus was designed to house a plunger, which in turns can fit into a glass microneedle and allow for the controlled release of fluid, much like in a syringe system. By immobilizing the microneedle while keeping the plunger connected to the moving printer head, release of fluid is achieved proportionally to the total movement of the traveling nut at any given time. The Felix 3.0’s motor driver is capable of using 1/16th microstepping routines, allowing the delivery of a cell solution with resolution of 2.5 nl. A depiction of the 3D bioprinting system is reported in Figure 15A.

The travel path of the print head during each experiment can be defined by the user using a Matlab interface. The software allows the user to select the characteristics of each printing experiment, modifying parameters such as location in the cell culture plate, number and disposition of the injection sites, and extrusion volume of cell solution, as well as correcting user operations that would place the needle tip outside the boundaries of the available print areas. The plotting locations and printing information are then automatically converted into a gCODE that, once imported into the 3D printer controller Repetier Host, provides the coordinates of each consecutive movement of the printer to achieve the desired print result.

The delivery of a cell solution within three-dimensional substrates using the 3D bioprinting system is mediated by micropipette needles cut to an optimal shape. Through computational modeling of fluid flow the optimal parameters for the fabrication of microneedles that can support bioprinting of mammalian cells were defined. Microneedles

are manufactured prior to each print using a Model P-1000 Flaming/Brown Micropipette Puller (Sutter Instruments; Novato, CA), using the parameters reported in Table 1. After pulling, the needles are manually cut to achieve a diameter of approximately 100 μm as well as a tapered shape. A representative figure of the needle shape is reported in Figure 15B.

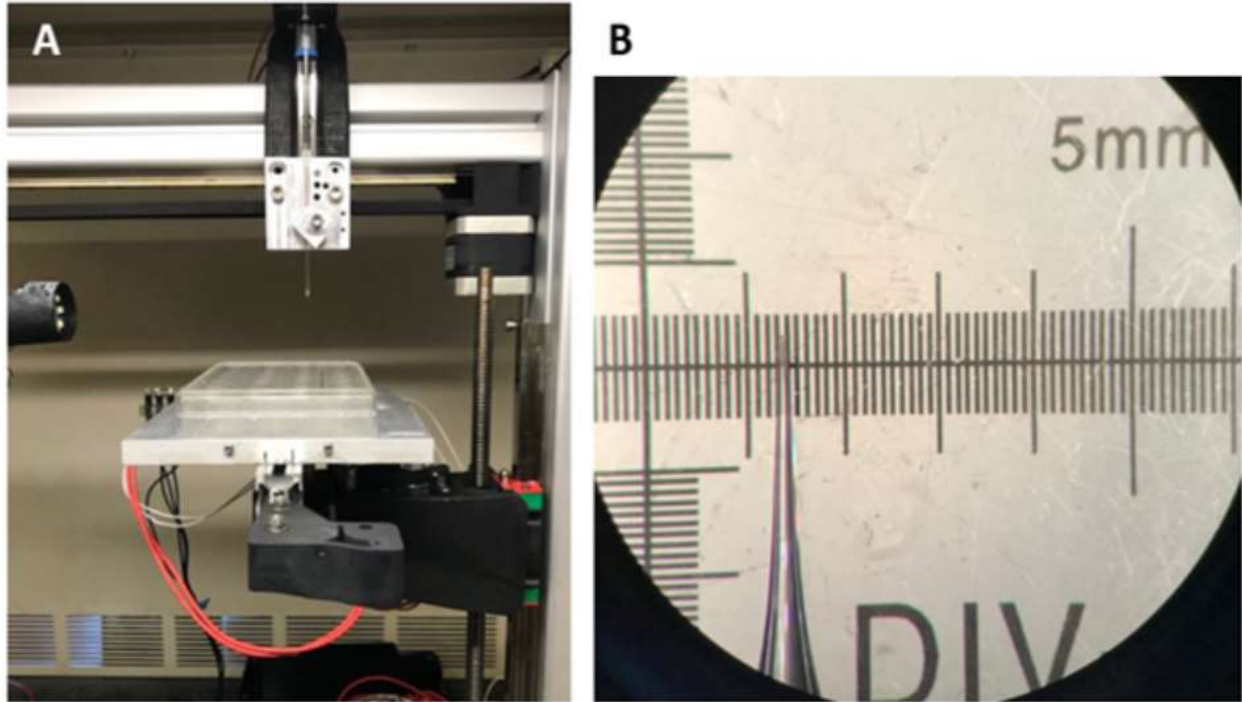


Figure 15: A) 3D-bioprinting setup. A 25-50 μL needle was filled with cell solution and mounted on the printer head. Printing substrates were previously prepared and allowed to solidify within a cell culture plate. Using coordinate-based commands, the system can inject a pre-determined amount of cell solution in a selected well and in an arbitrary pattern. B) Prior to printing, each needle is cut so that the needle tip diameter is approximately 100 μm .

Line	Heat	Pull	Velocity	Time	Pressure
1x1	530	30	22	75	550
2x1	520	30	21	250	
3x2	206	23	18	225	
4x4	510	20	14	150	

Table 1: Micropipette puller parameters adopted for the fabrication of consistent needles suitable for bioprinting of mammalian cells.

Conjugation of WNT3A Protein to Fluorescent Beads

To evaluate the use of protein-conjugated beads to study cellular processes within the context of the system that we propose, recombinant murine WNT3A proteins (amsbio) were immobilized to red FluoSpheres™ (Thermo Fisher).

The carboxylic acid groups were activated at room temperature for 30 minutes by EDAC (1-ethyl-3-(3-dimethylaminopropyl)-carbodiimide) and N-hydroxyl succinimide (50mg/ml each, dissolved in 50mM cold 2-(N-morpholino) ethanesulfonic acid (MES) buffer pH 6.0). After activation the beads were washed three times with MES. 20µg of WNT3A protein were immobilized to each mg of FluoSpheres™. The desired amount of protein was diluted in 50mM MES, to a final volume of 100µL and incubated at room temperature for 30 minutes. Glycine was then added to a final concentration of 100 mM and incubated at room temperature for 30 minutes to quench the reaction. The beads were washed one time with MES and twice with PBS. FluoSpheres™ were diluted in 2mM sodium azide in PBS and stored at -80.0 °C. By modifying the manufacturer's protocol and adding a freezing step at the end, we ensure the prolonged use of the conjugated beads, given that the proteins are unstable at 4°C over an extended period. Freezing the FluoSpheres™ leads to clumping of the beads and reduced overall yield of the conjugated beads.

The efficiency of the conjugation protocol was evaluated by antibody staining of the protein – conjugated beads. Beads were washed twice in 1X TBS and then incubated with WNT3A primary antibodies for 30 minutes, at room temperature, with slow tilt rotation. The beads were then washed again twice in 1X TBS and incubated for 30 minutes in secondary antibodies (Alexa Fluor 488) for 30 minutes, at room temperature, in the dark and with tilt rotation. Beads were then washed once in 1X TBS and resuspended in PBS for imaging. Fluorescent imaging was performed using a Zeiss Axio microscope with a short-working distance 20X objective.

Cell Culture

Mammary epithelial cells of the line MCF12a-RFP were plated and cultured in DMEM/F12 supplemented with 5% horse serum (Gibco), 20ng/mL human EGF (Millipore Sigma), 0.01 mg/mL bovine insulin (Millipore Sigma), 500 ng/mL hydrocortisone (Millipore

Sigma) and 1X Antibiotic-Antimycotic. All cells were maintained in a 5.0% CO₂ incubator at 37.0°C. The medium was replenished every 2-3 days until the cells reached 80% confluency and were ready for passage or freezing.

The wild-type mouse embryonic stem cell (mESC) Olig2 GFP reporter line G-Olig2 was purchased from ATCC. The SOX2 GFP reporter mouse embryonic stem cell line mESC SOX2-GFP was kindly donated by Dr. Konrad Hochedlinger's laboratory. mESCs were adapted to feeder-free conditions and cells were seeded on Geltrex[®] coated plates. All Geltrex[®] coatings were performed diluting 10 µL of stock solution in 1 mL of DMEM/F12. To prevent the substrate from solidifying prematurely, Geltrex[®] aliquots were prepared and stored at -80°C. Aliquots were retrieved and immediately thawed in medium. Diluted Geltrex[®] was allowed to spread evenly across each well of a cell culture plate and incubated at 37°C for at least one hour. Cells were cultured in mESC Cell Culture medium, containing Mouse ES Cell Basal Medium (ATCC), 15% Embryonic Stem Cell qualified FBS (Life Technologies), 1X Antibiotic-Antimycotic (Thermo Fisher), 55 µM β-Mercaptoethanol (Gibco). The medium was supplemented with 1000U/ml of Leukemia Inhibitory Factor (LIF) supplement (Millipore Sigma), 1µM MEK inhibitor PD0325901 (Millipore Sigma) and 5µM GSK3 inhibitor CHIR99021 (Millipore Sigma). The addition of MEK and GSK3 inhibitors allows the mESC to maintain a naïve state in feeder-free conditions. Cell culture medium was replaced daily, and the cells were passaged once the colonies reached 70% confluency. Cells were passaged using TrypLE™ Express Enzyme (Thermo Fisher) according to the manufacturer's suggested protocol. The pluripotency state of the cells was confirmed via positive SSEA-1 staining, and maintenance of naïve state was confirmed by the maintenance of domed morphology of the colonies.

Live Imaging of Cells and Beads in 3D Cell Culture

Live imaging of cells in culture provides a great tool to monitor cells throughout their incubation period if reporter cell lines are not available. We performed live staining via nuclear staining as well as via Alkaline Phosphatase live staining.

Nuclear staining was performed with Hoechst 33342 (Thermo Fisher) stain, according to manufacturer's instructions. The stain was diluted to a concentration of 1µg/mL in mESC cell culture medium. The cells printed within thin hydrogels, were incubated with the diluted stain, at 37°C, for 20 minutes. The incubation time was extended to allow the stain to fully penetrate the substrate and ensure maximum efficiency of the staining process. After incubation, the substrate was rinsed twice with FluoroBrite™ DMEM (Thermo Fisher) for 5 minutes. Successively, a thin layer of cell culture medium was added to coat the substrate and prevent drying during the imaging process.

Live staining was performed using Alkaline Phosphatase Live Stain (Thermo Fisher). A 1X solution was prepared using DMEM/F-12 and substrates were incubated with the diluted stain, at 37°C, for 30 minutes. After incubation, the substrate was rinsed twice with FluoroBrite™ DMEM (Thermo Fisher) for 5 minutes, and a thin layer of cell culture medium was added to coat the substrate and prevent drying during the imaging process.

Alternatively, characterization of printed cells throughout the incubation period can be achieved by using reporter cell lines, such as in the case of mESC-SOX2 cells.

Downstream Imaging Assays

The cell culture system that is proposed allows for the characterization of samples via immunocytochemistry. The performance of immunostaining allows us to assess the differential expression of genes of interest without requiring the removal of individual cells from their location within the substrate. The nature of three-dimensional cell culture poses a constraint to the use of immunocytochemistry protocols, which are traditionally designed for use on attached cells, as hydrogels are penetrable only to a very limited extent to the reagents required. It is for this reason that imaging studies of three-dimensional structures are performed on samples that are fixed, embedded in paraffin, cut onto slides and then stained via immunohistochemistry. Here we report an optimized protocol for the staining of single cells and colonies cultured into three-dimensional hydrogels. It is important to

note that the thickness of the hydrogels (defined in previous sections) is a fundamental parameter to preserve to ensure the success of this protocol.

After printing, samples were incubated at 37°C. The cell culture media was removed, and they were washed twice in 1X tris-buffered saline (TBS) for 5 minutes each. All subsequent washes were performed for the same amount of time. Samples were fixed and permeabilized with 100% methanol, cold, incubated for 20 minutes at -20°C. Samples were then washed with 1X TBS three times and then blocked with 10% goat serum for 60 minutes. Primary antibodies were diluted in 1% goat serum according to the manufacturer's suggested factor, and following application they were incubated overnight at 4.0°C. Next, after washing the samples with TBS four times, Alexa Fluor™ 488 and 568 secondary antibodies (Thermo Fisher Scientific) diluted 1:1000 in 1% goat serum were added and the samples were incubated in the dark, at room temperature, for 60 minutes. Samples were washed in TBS four times, and nuclear stain was performed adding DAPI diluted 1:1000 in 1% goat serum. The samples were finally washed two times in TBS, and images were acquired with a Zeiss Axio microscope with a short-working distance 20X objective.

As shown in Figure 16, the optimized incubation times allow for the immunostaining of cells cultured within 3D hydrogel substrates. Immunocytochemistry was performed on mESC GOlig2 cells printed into thin three-dimensional substrates and incubated over a 48-hour period. The cells were stained for pluripotency markers Oct4 and Nanog, and their continued expression after printing was confirmed.

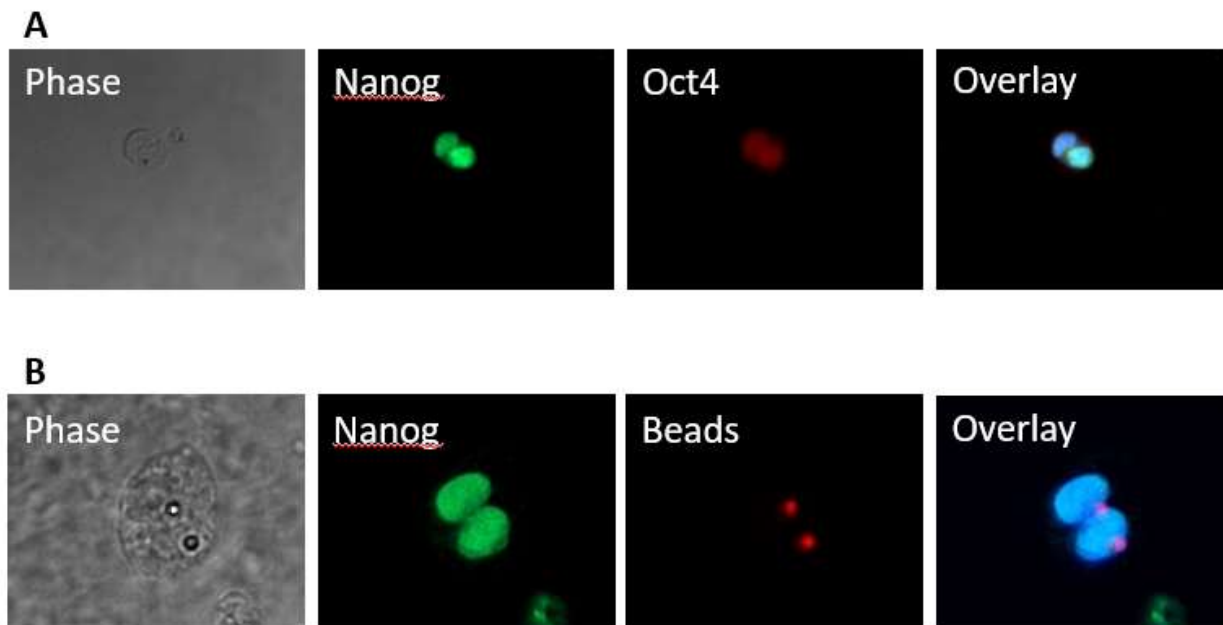


Figure 16: Our proposed protocol allows us to perform immunostaining on cells cultured in three-dimensional substrates (A) as well as cell-bead complexes (B).

Results

2D and 3D Bioprinting for Single Cell in Vitro Studies

The study of cellular mechanisms at the single cell level is hindered in part by the absence of efficient protocols for plating and culture of single cells, in a way that would allow for the performance of downstream assays. Our laboratory has previously developed an efficient system for the 3D bioprinting of cells into three-dimensional substrates, allowing for the culture of cells in a biomimetic setup as well as allowing for the formation of organoids *in vitro*. Here, we adapted the system to achieve printing of individual cells at each injection site, to allow for the performance of studies on single cells in an efficient manner and in a setup that allows us to follow the progress of each cell over time.

To achieve single cell printing, the following parameters were optimized: needle shape and diameter, concentration of the cell solution, and extrusion value. Based on the modeling previously performed to define the ideal needle shape for printing of mammalian cells into three-dimensional substrate, a tapered shape, and a needle tip diameter of 100 μm were preserved. This shape is ideal to allow the penetration of the needle within the three-dimensional gel while ensuring minimal structural damage to it. The diameter chosen allows for restricted cell flow to prevent the simultaneous release of multiple cells during the extrusion process, without mechanically damaging the cells.

The extrusion value is a parameter that defines the amount of cell solution released at each injection site by controlling the movement of the traveling nut, and in turn the plunger, within the printer's deposition apparatus. The number of cells deposited at each injection site is dependent on the volume of cell solution released, as well as its concentration. If the volume released is kept constant, a higher number of cells will be injected if the starting cell concentration is higher, and vice versa. Analogously, if the cell concentration is kept constant, a higher number of cells will be injected with a higher extrusion value, and vice versa. Knowing the resolution of the deposition apparatus, the extrusion value required for the deposition of a determinate number of cells could ideally be calculated relatively to the concentration of the cell solution utilized. However, due to mechanical error as well as cell variability within the needle, empirical determination of the ideal extrusion value for single cell injections was required. A relatively low cell

concentration of 300,000 cells/mL was chosen to prevent resuspended cells from quickly settling at the needle tip during printing and reducing the possibility of it getting clogged. Starting from this cell concentration, the ideal extrusion value was found to be $e = 0.009$. Figure 17 shows consistent single cell printing using the parameters described above.

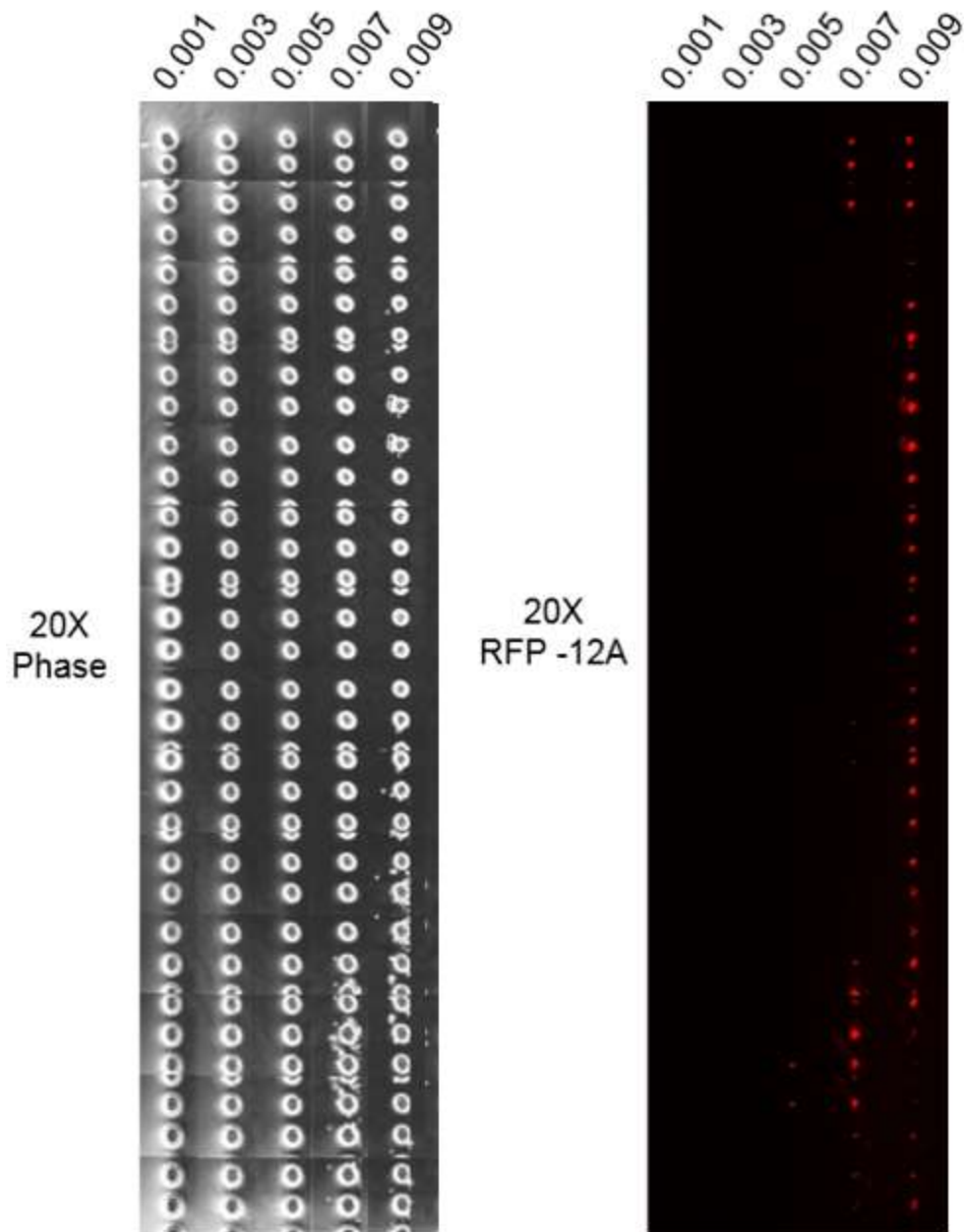


Figure 17: The extrusion value that allows for optimal single cell printing within three-dimensional hydrogels was experimentally determined.

Once the parameters for the achievement of single cell injections were determined, the system was optimized to allow for survival, proliferation, and imaging of the printed cells. The ability of cells to be cultured following the printing protocol enables the study of cellular processes over time.

Mouse embryonic stem cells of the line GOlig2 (mESC GOlig2) were utilized to optimize the protocol for printing single cells into three-dimensional substrates. 20 μ L of Geltrex[®] were placed in each well of an 8 well glass chamber slide and using a pipette tip it was gently spread to cover the entirety of the wells bottom. The coated plates were then incubated at 37°C for at least 10 minutes to allow the formation of solid hydrogels. The hydrogels were then covered with cell culture medium and incubated for at least 30 minutes, to allow the medium to completely soak the substrate. The 3D-bioprinter was programmed to print a matrix in each well of the chamber slide used, with equal spacing in each direction between injection sites. Matrix size and spacing can be adjusted to the needs of each specific experimental setting, allowing to produce upwards of 100 injection sites per well, facilitating high throughput experiments. After the print was concluded, cell culture medium supplemented with 10 μ M Y-27632 supplement was added to each well and the cells were incubated at 37°C. A modification of the protocol described above allows for the printing of individual cells in two-dimensional conditions. Embryonic stem cells are a cell type that cannot adhere to cell culture plates that have not been protein coated. In normal conditions, a Geltrex[®] dilution is prepared and placed on the culture plates and allowed to incubate at 37°C for at least an hour and removed immediately prior to cell plating. In order to print individual adhering cells into precise locations within the culture plate, the protocol described cannot be adopted. The residual Geltrex[®] solution remaining on the cell culture wells prior to plating, would prevent the deposition of precise droplets on the wells surface. Cohesive forces between the cell solution and the residual Geltrex[®] solution, which covers the entire surface of the cell culture well, would result in the dispersion of any deposited cell solution. This would prevent the ability to deposit cells in a predetermined precise location of the two-dimensional surface. To do so, it is necessary for the cell culture surface to be completely dry. In this situation, cohesive forces within the cell solution are stronger than the adhesion forces between the cell solution and the plate surface, allowing to maintain surface tension in the deposited

droplets, and preventing dispersion of the cell solution across the plate. To overcome this limitation, Geltrex[®] was diluted directly into the cell solution immediately prior to printing. This would ultimately allow for the deposition of Geltrex[®] coating only on the desired area, enabling the localization of cells in two dimensional conditions.

While the needle shape and cell concentration parameters were kept unaltered, the extrusion value was modified to suit the needs of two-dimensional cell plating. The optimal extrusion value for the consistent injection of a single cell, starting from a cell solution concentration of 300,000 cells/ml, was empirically determined. However, the ideal extrusion value of $e = 0.009$ results in the release of such a small volume of cell solution that is not suitable for transitioning from a three-dimensional substrate to a two-dimensional surface. Release of such a small volume would require the needle tip to get in contact with the culture plate surface at each injection site. This is not compatible with the precision of the printing system, as slight variability in the thickness of the cell culture plate along with mechanical error would most likely lead to damage of the glass needle tip during the printing process. Additionally, the release of such solution volume would result in rapid evaporation of the cell culture medium and death of the plated cells. Overall, the use of an extrusion value of $e = 0.009$ is not compatible with the performance of moderate or high throughput printing experiments and survival of the deposited cells in two-dimensional conditions. To overcome this limitation, we set to define the smallest extrusion value that was compatible with the release of adequate cell solution volume for the formation of a stable droplet and the performance of high throughput experiments. The value was empirically determined to be $e = 1$. As the cell solution concentration was left unaltered and the volume released was increased, so did the number of cells delivered at each site. To overcome this, the starting cell solution concentration can be adjusted, however maintenance of a cell concentration of 300,000 cells/ml was still suitable for clear visualization, distinction and following of individual cells. Immediately after printing, the deposited droplets were incubated at 37°C for 10-15 minutes, to promote Geltrex[®] and cells' deposition while avoiding evaporation of the cell culture medium. Then, the culture wells were filled with cell culture medium supplemented with 10 μ M Y-27632 supplement, gently released over the settled cells.

Both methods of single cell printing allowed for cell survival and proliferation, demonstrating that the 3D bioprinting system is a versatile tool that can be applied to 2D and 3D cell culture studies. A representative image of mouse embryonic stem cells printed in two and three-dimensions is shown in Figure 18. The figure is also an excellent example of how different substrates affect the morphology of cell colonies derived from a single cell. The nature of each system allows us to deposit cells in predefined patterns, such as grids, which facilitate the localization of the same cell of interest over the course of the experiment, a property that is enhanced when applied in combination with live cell staining. An example is provided in Figure 19, where single mouse embryonic stem cells printed into thin three-dimensional hydrogels can be easily identified thanks to live nuclear staining in combination with the visible printing pattern in the substrate.

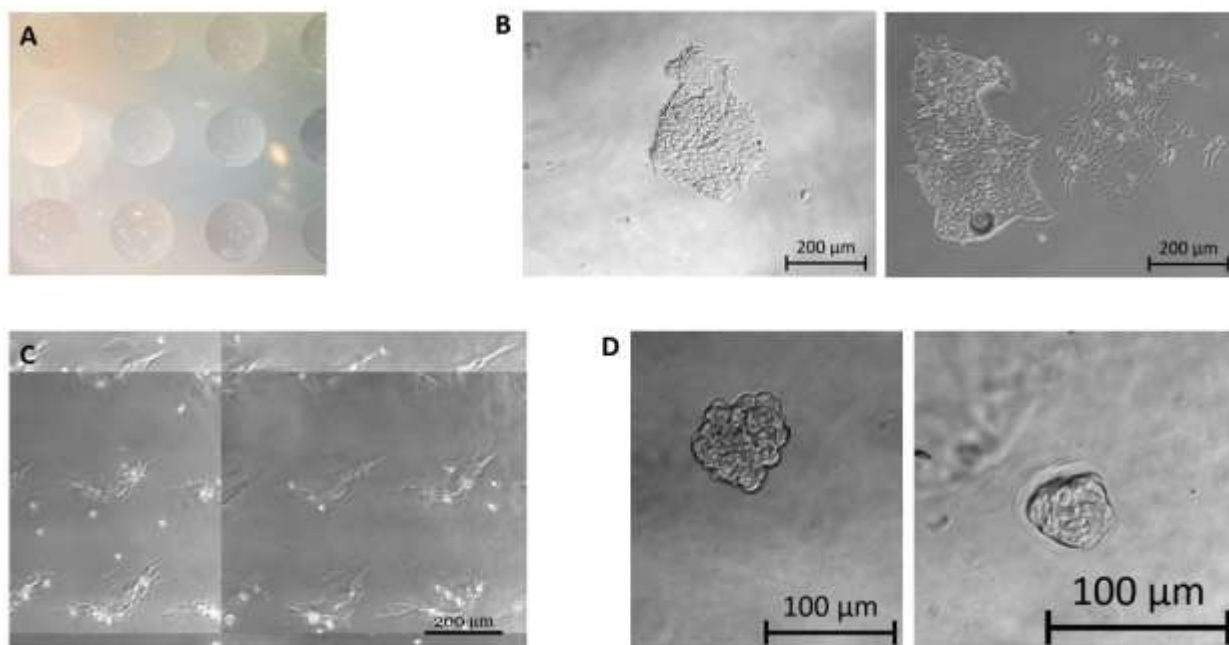


Figure 18: A) Droplets of cell solution and 10 μM Geltrex® deposited onto a glass chamber slide. The bioprinting system allows us to create clearly distinguished sites where a controlled number of cells is confined. B) Cells can survive and proliferate in monolayer cultures 48 hours following printing on two-dimensional surface. C) The bioprinting system allows for injection of a controlled number of cells within a three-dimensional substrate. D) Cells can survive and proliferate in three-dimensional cultures 48 hours following printing in three-dimensional substrate.

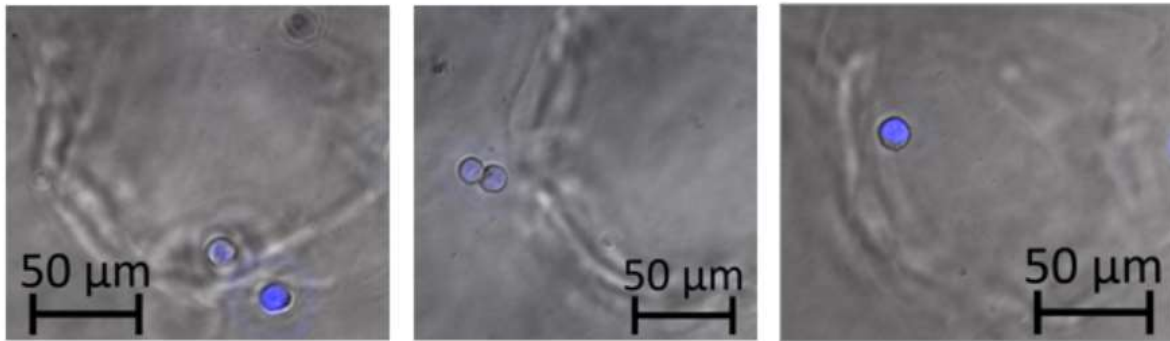


Figure 19: The 3D bioprinting system allows us to inject individual cells within a three-dimensional substrate. The figure shows mouse embryonic stem cells of the line G0lig2, which were stained with HOECHST nuclear stain prior to imaging.

Bioprinting of Single Cell and Single Beads Pairs

The use of localized proteins can be a valuable tool for the study of protein-mediated cell mechanisms. One method by which protein location can be controlled is by immobilization onto microbeads, which in turn can be easily visualized. To test the ability of our system to allow the study of protein-mediated processes, we conjugated WNT3A protein to red fluorescent beads. We chose to use WNT3A protein as it plays a key role in mouse embryonic stem cell physiology, and previous published data demonstrates the ability of bead immobilized WNT3A to bind to mouse ESCs [26]. The choice of using red fluorescent beads was dictated by the fact that they are very easily visualized via fluorescence microscopy. FluoSpheres™ were activated and conjugated to proteins following manufacturer's instructions. To confirm that the protein immobilization was successful, immunostaining targeting the WNT3A protein was performed. As reported in Figure 20A-C, fluorescence microscopy was used to confirm that the staining process was successful and WNT3A proteins were detected on the beads.

The 3D-bioprinting system, combined with the ability to deliver localized proteins, provide for a great opportunity to study cellular mechanisms at single cell resolution. To do so, we developed a modified printing protocol for the printing of single cells conjugated to single beads, with high resolution of individual complexes at each injection site. Mouse embryonic stem cells of the line GOlig2 (mESC GOlig2) and FluoSpheres™ conjugated to Wnt3a protein were utilized to optimize the protocol. Cells were cultured and resuspended to a concentration of 300,000 cells/mL in cell culture medium. In the meantime, a previously prepared 20 μ L aliquot of FluoSpheres™ solution, corresponding to about 600,000 beads, was allowed to thaw at room temperature. 200 μ L of the cell solution were added to the FluoSpheres™, very briefly vortexed, and allowed to incubate at 37°C with slow rotation, for at least 30 minutes. The incubation period allows for the protein conjugated beads to bind to cells in solution prior to injection in the 3D substrate, increasing the efficiency of printing of single cell-single beads complexes. Following the incubation period, the printing process proceeds as described previously. The proposed protocol allowed to achieve consistent single cell – single bead printing of mouse embryonic stem cells bound to WNT3A conjugated beads, as shown in Figure 20D-E. The efficiency of the printing protocol developed was calculated to be 5% in regard to the

injection of clearly identifiable single cell – single bead complexed within three-dimensional substrates. This result constitutes a significant improvement to previously published protocols [26], where the efficiency was highly variable, dependent on chance, and use of a very large bead/cell ratio was required to achieve meaningful results. The figure also shows that the cells were able to survive and proliferate following the printing process.

The ability to study a single cell or a single cell-single bead complex is a capability that greatly enhances the potential of the system we described. To identify and quantify the cells after printing, and evaluate their ability to proliferate over time, nuclear staining proved to be efficient. The use of Hoechst 33342 stain allows us to rapidly stain the cells' nuclei and visualize them in the three-dimensional environment. Extending the incubation time to 20 minutes, allows the dye to fully penetrate within the hydrogel and allows for maximum staining efficiency. The use of reporter cell lines is an ideal method to observe changes in gene expression over time relative to the experimental settings. Using a SOX2 reporter mouse embryonic stem cell line, referred to here as mESC SOX2GFP, in Figure 20D-E we show the ability to print and easily visualize reporter cell lines using a fluorescence microscope. An alternative method to using reporter cell lines is the use of live stains when possible. This allows us to characterize the cells over time, without requiring cell fixing. In Figure 20D-I, we show the ability to characterize cells using live stains.

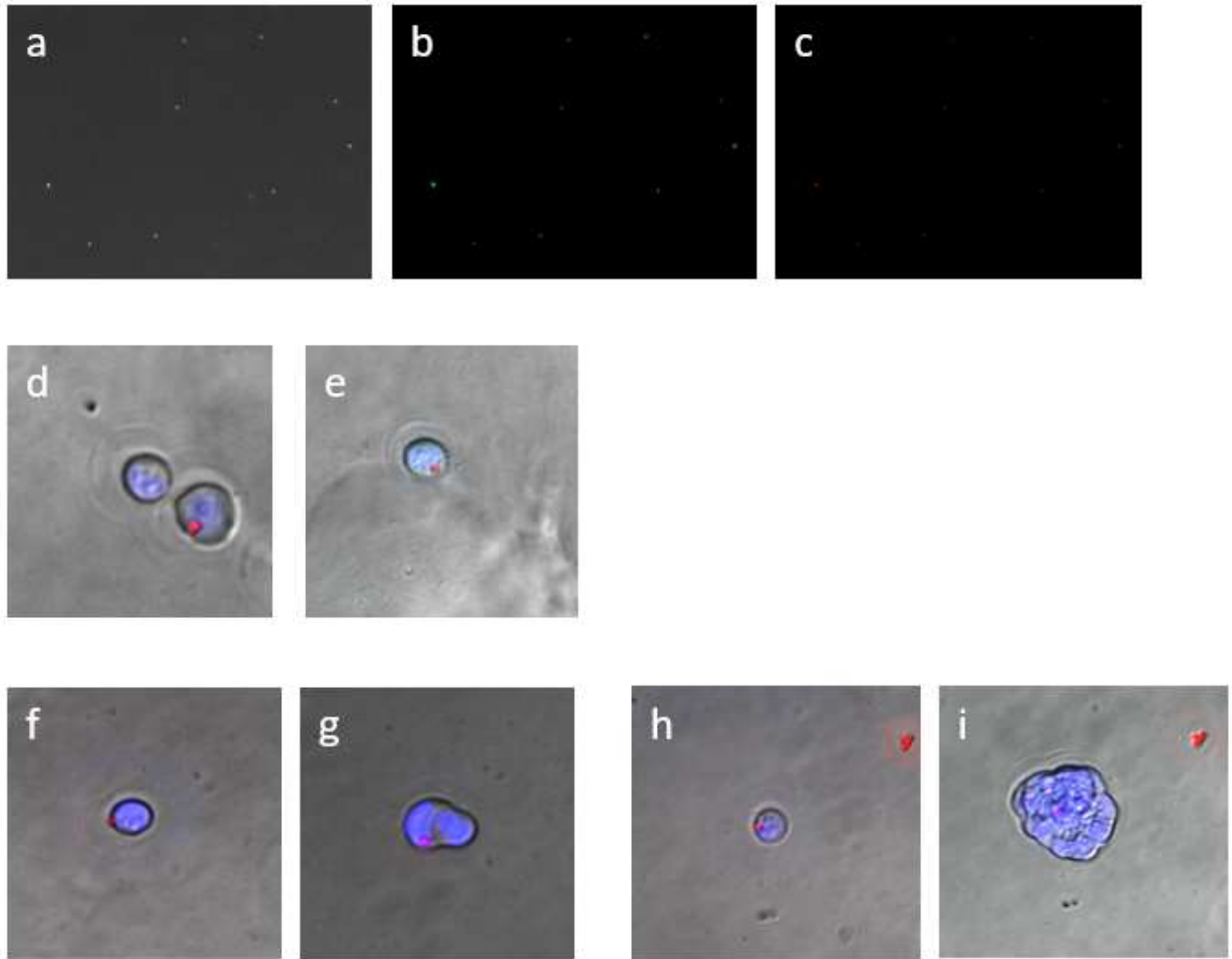


Figure 20: Red fluospheres were conjugated with WNT3A protein. Antibody staining against WNT3A protein (b) was performed to confirm that protein was successfully immobilized onto beads (a-c). Protein-conjugated beads are bound to cells in solution, and single-cell and single-bead complexes are printed into three-dimensional substrates (d, e). The complexes can survive and proliferate in these culture conditions over time (f-g, h-i).

Localized WNT3A is Not Sufficient to Promote Asymmetrical Division in Three-Dimensional Conditions

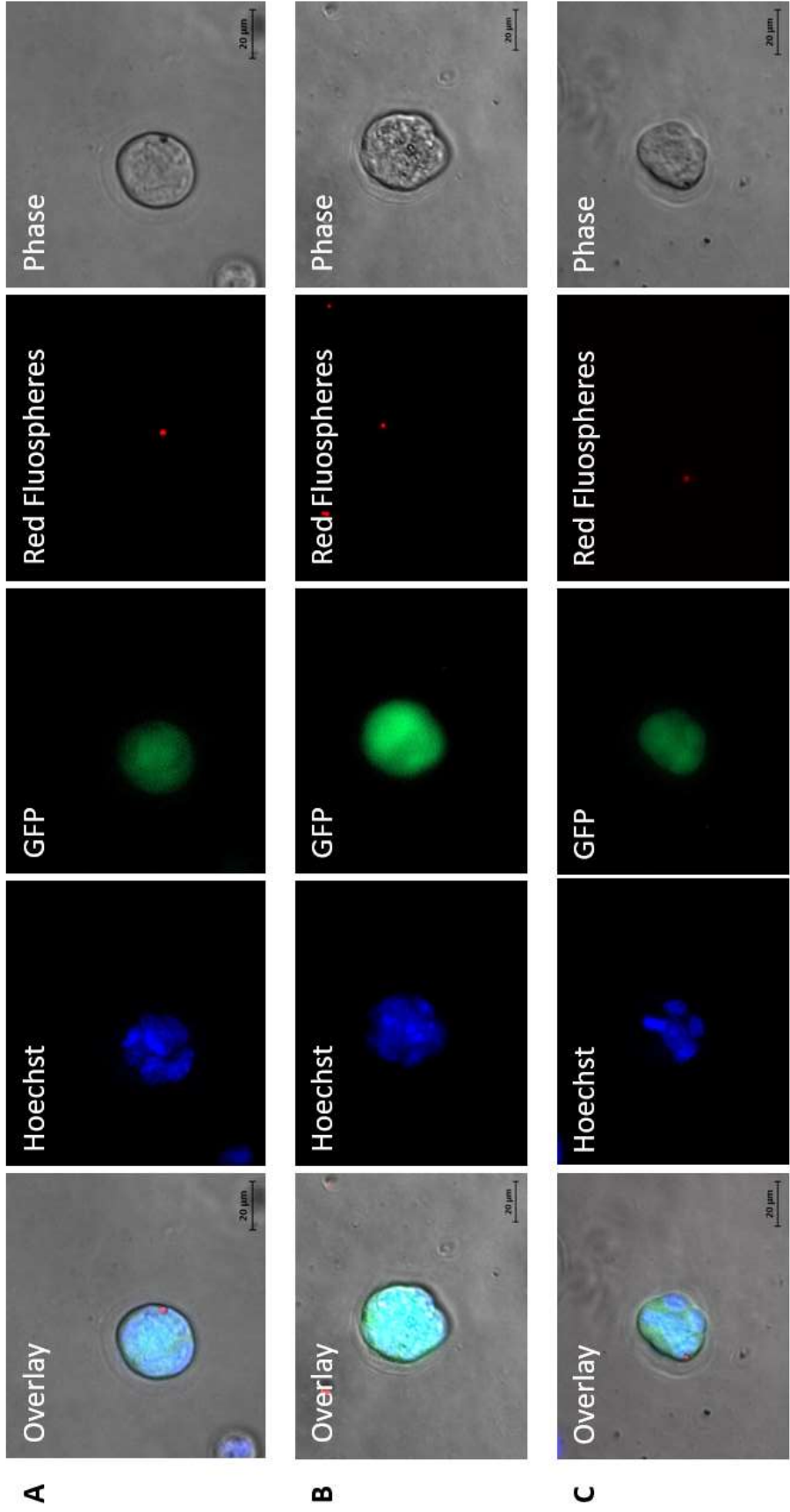
Habib et al., in a study published in 2013, demonstrated the ability of localized WNT3A signaling to direct asymmetrical division in mouse embryonic stem cells [26]. The authors showed that WNT3A proteins conjugated to microbeads promoted the maintenance of undifferentiated state when bound to mESCs. The study was performed with cells in two-dimensional cell culture, and the attachment of protein-conjugated beads to stem cells was driven by chance. This system presented two major drawbacks: the efficiency of achieving single cell and single bead complexes was extremely low, and the visualization of the complexes over time was very labor intensive as there is no efficient way to mark their location on the cell culture surface.

Here, we set forth to apply our 3D bioprinting system for the printing of single mESC SOX2 cells bound to WNT3A conjugated beads, and evaluate whether three-dimensional culture conditions allowed to replicate the results presented by Habib et al. Single cell – single bead printing was successfully achieved on Geltrex hydrogels, relying on the protocols described above. Our system allowed to overcome the limitations encountered by Habib et al in their experimental design. We produced sites with single cells and single beads by in 5% of the injection sites, and each single cell and single bead pair of interest was easily followed throughout the 48 hours incubation period, thanks to the performance of injections in a grid pattern.

In contrast to what reported by Habib et al, differential expression of SOX2 GFP marker in cells either in contact or not in contact with WNT3A conjugated beads was not observed in three-dimensional culture conditions (shown in Figure 21A-C). After 48 hours, stem cells underwent multiple cell division events, forming highly compact colonies that expressed the GFP marker uniformly.

One explanation behind the different outcomes of the two studies is given by the fact that the microenvironment of the stem cells was significantly different in the two setups. It is not possible to state with certainty what effects this change poses on the mechanisms associated with the expression of pluripotency genes. However, there are noticeable differences in morphology and gene expression patterns in mESC SOX2 cells cultured for 48 hours in two- versus three-dimensional conditions. Firstly, the three-

dimensional substrate promotes the growth of the cell colonies in a round and tightly packed conformation, such that cells can only be distinguished from one another with the aid of nuclear staining, as shown in Figure 21A-C. In contrast, attached cell colonies tend to grow in width, and individual cells can be easily visualized. Secondly, gene expression analysis of mESC SOX2 in the two culture conditions shows that after 48 hours of incubation, the colonies display differences in the pattern of expression of germ layer markers (Figure 21D). Gene expressions were calculated relatively to mESC cultured in 2D conditions and in mESC+LIF medium supplemented with GSK3 and MEK inhibitors. Specifically, in three-dimensional conditions, a significant increase in the expression of mesoderm gene marker HAND1 was detected, suggesting that the two conditions are permissive of cell differentiation to different levels. Additionally, no changes in the pluripotency marker expression (SOX2) were detected in cells cultured in three-dimensional hydrogels, consistent with the maintenance of the SOX2-GFP marker.



A

B

C

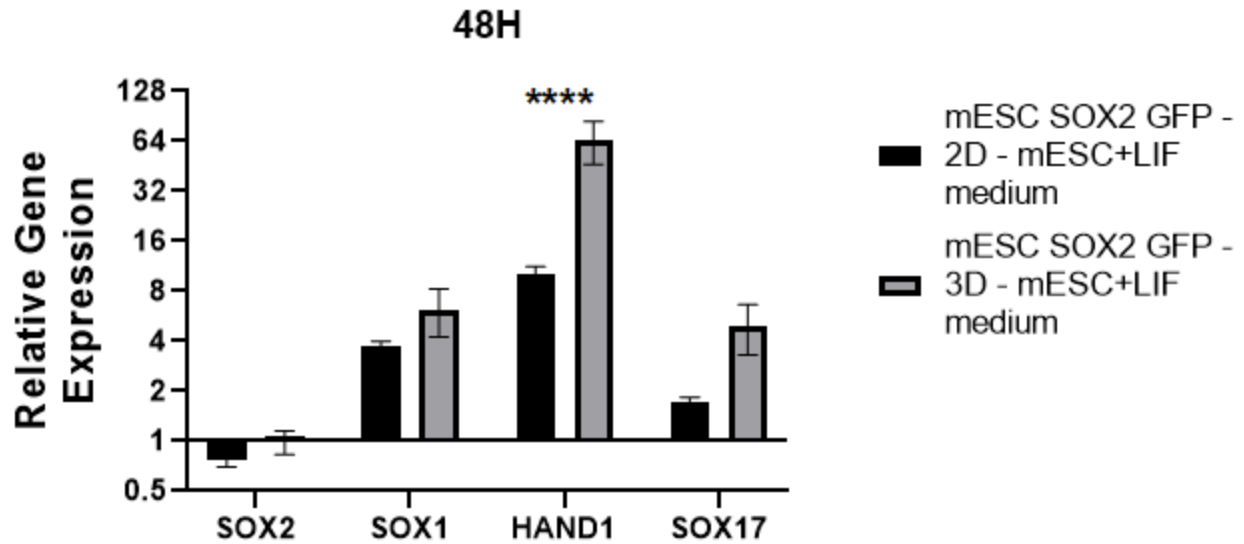


Figure 21: (A-C) mESC SOX2GFP single cells bound to a single WNT3A conjugated bead were printed into thin three-dimensional hydrogels and allowed to incubate for 48 hours. The cells were able to form new colonies, but loss of the pluripotent marker (SOX2-GFP) was not detected. (D) Gene expression analysis of pluripotency and germ layer markers was performed on mESC SOX2GFP cells cultured in 2D and 3D conditions with mESC+LIF medium for 48 hours. Differences in the gene expression patterns were detected.

Discussion

Many of the molecular mechanisms that drive stem cell physiology and differentiation remain to be elucidated. The design of experiments to attempt to resolve some of the unanswered questions on the matter is challenging. Efficient and accessible methods for the study of mechanisms at the single cell resolution are not readily available. Here, we presented an optimized 3D bioprinting system for the study of single cell mechanisms in biomimetic conditions and with high efficiency.

An off-the-shelf model of extrusion-based 3D printer was previously purchased in our laboratory and customized to allow for the controlled injection of cells within three-dimensional substrates. Optimization of the parameters of needle shape and diameter, cell solution concentration, extrusion value, and substrate preparation were performed to achieve consistent delivery of individual cells into two-dimensional and three-dimensional substrates. The system described allowed for the consistent delivery of individual cells under either culture condition, as well as providing the opportunity to perform high throughput experiments in an automated way. The methodology presented here allowed for printed cells survival and proliferation over time, providing multiple alternatives ways to examine cells of interest with ease at different time points.

The importance of localized biochemicals signal and the role they play in dictating the mechanisms of asymmetrical stem cell division is a concept surrounded by much uncertainty. Localization of transcription factors by conjugation to microbeads is a technique that has been adopted to allow for the easy visualization of proteins relatively to individual cells. This method allows us to evaluate the effects of transcription factors of interest on the processes of cell division and differentiation, however current experimental designs are still limited by the need to rely on chance for the formation of cell-bead complexes, as well as their random placing within the culture plate. The system we described here relies on the use of the 3D bioprinting system for the delivery of previously bound cells and beads complexes within three dimensional substrates. Our system greatly increases the efficiency of the formation and delivery of such complexes within a single experiment compared to previously published protocols. Additionally, the coordinate-based injection system that directs the motion of the bioprinter allows us to deliver cells and beads in a precise pattern that is clearly definable following printing,

improving the experimental design by facilitating the study of the same complex of interest over time.

Finally, the system was applied to evaluate whether immobilized WNT3A protein can direct mouse embryonic stem cell asymmetrical division in three dimensional conditions. Conjugation of the WNT3A protein to red fluorescent microspheres as well as the highly efficient printing of single cell and single bead complexed were achieved. The single cells in culture were able to undergo multiple division events within the 48 hours period taken into consideration, and WNT3A conjugated beads maintained their original location. Our data shows that, in three-dimensional cell culture conditions, localized Wnt3A proteins are not sufficient to regulate asymmetrical division in mouse embryonic stem cells. A possible explanation behind our finding is given by the significant differences between the two- and three-dimensional cellular microenvironments. The disposition of the stem cells within these two setups drastically changes the amount and type of interactions that stem cells have with each other and with the culture substrate. This has the potential to affect physiological changes in the cells in culture, as suggested by our evaluation of the colony morphology and gene expression patterns of cells grown in either condition.

Conclusion

The development of highly efficient methods for the study of the mechanisms of stem cell physiology at the single cell level is highly warranted. The system we proposed here is a customization of an off-the-shelf model of 3D bioprinter, highly accessible to research laboratories. We described protocols to enable the delivery of single cells or single cells and single beads complexes within two or three-dimensional substrates. The methods we propose enable the localization of individual cells with high efficiency, the ability to perform high throughput experiments, while being permissive of common downstream analysis assays. Overall, the system proposed represents an excellent solution to overcome some of the limitations in the study of cellular processes at the single cell level and holds great promise in its application in the study of stem cell physiology.

CHAPTER V

DISCUSSION

The cellular microenvironment has been shown to play an essential role in the definition of cellular physiology and behavior. Stem cells are a type of cell that have the potential to generate new stem or differentiated cell types. It is speculated that the processes of stem cell fate determination and differentiation are highly influenced by microenvironmental cues. Factors such as the histological organization and cellular composition of the *in vivo* resident tissues, as well as biomechanical and biochemical cues from the environment all play a role in establishing stem cell physiology and behavior. Currently, techniques for the efficient study of the mechanisms that drive stem cell differentiation and fate determination at the cellular level are not available.

This dissertation addressed the gaps in current research methodologies and developed ideal techniques for the study of microenvironmental control on stem cell mechanisms in highly accurate environments and with high precision. Here, these needs were addressed first with the development of a novel 3D bioprinting system integrated with tissue-specific substrates. The setup proposed is ideal for the study of the effects of the microenvironment provided by the extracellular matrix on stem cell differentiation potential. Secondly, the bioprinting system was engineered to achieve an ideal setup for the study of stem cell mechanisms at a single cell resolution, with particular focus on an immobilized growth-factor driving asymmetrical stem cell division. The system provides an accessible platform for the performance of experiments with high reproducibility, high precision and in a highly biomimetic cellular environment.

Effects of a Brain Extracellular Matrix-Derived 3D Cell Culture System on Stem Cell Culture and Differentiation

The extracellular matrix is a major constituent of cellular microenvironment and plays an important role in the regulation of cellular behavior and the establishment of stem cell fate. It is a three-dimensional architectural network comprised of proteins and macromolecules secreted by the tissue resident cells, and its composition is variable across different tissues. These notions are valid in the context of the central nervous

system, where the extracellular matrix plays a role in the regulation of neural stem cell behavior and their development into neural or supportive cells of the nervous system.

In this dissertation, we describe the application of brain tissue specific extracellular matrix, in combination with a custom 3D bioprinting system, for the establishment of a highly biomimetic two- and three-dimensional cell culture system. This system provides ideal conditions for the culture of embryonic and neural stem cells and the study of how a tissue specific microenvironment can influence stem cell fate determination *in vitro*.

We described the fabrication of porcine brain extracellular matrix-derived hydrogels, able to spontaneously solidify upon incubation at 37°C. We confirmed that the brain-specific substrate suitable to promote survival and proliferation of stem and neural cell lines in two- and three-dimensional cell culture conditions. We first investigated whether the brain-specific environment promoted neural stem cell differentiation in two-dimensional conditions. We demonstrated that, in comparison to commercially available matrices, the brain-derived substrate promoted the expression of early neuronal markers in stem cell cultures, and earlier expression of astrocyte markers in neural differentiation cultures. Next, our custom 3D bioprinting system was applied for the establishment of three-dimensional stem cell cultures. This enabled the study of the impact of the tissue-specific extracellular matrix on stem cell differentiation in a three-dimensional *in vitro* context. The bioprinting system allowed to deliver a controlled number of cells, in precise locations of the three-dimensional substrates, enabling the performance of automated high-throughput experiments that ensured repeatability and consistency across injections. We demonstrated that our cell culture system promotes cell survival and proliferation of embryonic and neural stem cells in three-dimensional cell culture conditions and provides an excellent platform for the study of stem cell differentiation in this context. The system allows for the formation of neural organoids starting from injected stem cells, with both the three-dimensional conditions and the tissue-specific environment contributing to the expression of neural character. Additionally, we demonstrated that the three-dimensional organoids obtained with this optimized system are suitable for transplantation into *in vivo* models, where the organoids survive and continue developing. The 3D bioprinting system described in this dissertation provides an excellent tool for research laboratories to create an ideal cell culture system that mimics true *in vivo* cellular

conditions. Hydrogel substrates can be generated from the matrix of virtually any tissue and applied to our system for the study of cellular behavior and impact of the ECM microenvironment in the context of different tissues. Modulation of the ECM is a staple of many disease conditions; the system described here has enormous potential for an application studying the changes in the extracellular matrix as well as its impact on cellular mechanisms that characterize disease conditions. Traditionally, protocols for the establishment of organoid cultures entail several steps and the establishment of large numbers of organoids at once is hindered by the high level of maintenance required. Here, we demonstrated that our 3D bioprinting method, in combination with tissue-specific three-dimensional substrates, is an optimal setup for organoid formation. The three-dimensional disposition and the ability of cells to spontaneously organize render organoids an ideal system for the performance of *in vitro* studies, which use can be hindered by the complexity of their establishment. Our system provides an accessible platform for easy and high throughput formation of organoids, paving the way for their establishment as a cell culture standard.

Overall, we developed a versatile system that combines the properties of 3D bioprinting technology and tissue-specific environments and has vast potential applications for the creation of stem cell models and the study of cellular mechanisms in healthy and disease conditions.

Adaptation of a 3D Bioprinter System to Enable the Study of Cellular Mechanisms at a One-Cell Resolution

Biochemical signaling plays an important role in stem cell fate determination. Growth factors such as Wnt3a have been shown to be able to direct asymmetrical stem cell division by orienting the plane of cell division. Localization of such protein has been demonstrated to promote maintenance of pluripotency in contrast to a differentiated state in *in vitro* experimental settings. The study of how localized signals can direct asymmetrical stem cell division and differentiation is hindered by the absence of optimal research methodologies.

In this dissertation, we describe the engineering of a 3D bioprinter based model for the consistent delivery of single cells and single cell - single bead complexes to enable

the study of cellular physiology at single cell resolution, as well as the study of growth factor directed asymmetrical division. With the aid of an optimized 3D bioprinting system, we were able to achieve consistent delivery of individual cells onto two- and three-dimensional substrates. Cells were able to survive and proliferate under both plating conditions. We also optimized a system for the conjugation of transcription factors onto fluorescent beads with consequent binding to individual cells, allowing for the consistent delivery of single cell – single bead complexes with high efficiency. Additionally, the unique properties of the 3D bioprinter allow us to establish the localization of sites of interest with ease, greatly simplifying the task of following the progress of individual cells over time.

The system we proposed has incredible potential to enable the study of the molecular processes that drive stem cell physiology at a single cell resolution. The accessibility of the system, combined with the demonstrated high efficiency of achieving single cell and single beads injections enables the potential to design a wide variety of experiments. Expanding the project that we described in this dissertation, the bioprinting system is an optimal platform for the study of the effects of different individual growth factors on the stem cell asymmetrical division process and in different species. Adult stem cells have unique characteristics that allow them to best maintain local tissue homeostasis, and they present unique response to stimuli. Studies comparing the responses of each cell type to the same environmental stimuli can be easily performed with the system we devised. Its demonstrated high-throughput potential allows us to design large experiments to collect statistically significant results at once. The potential of the platform described in this dissertation expands beyond the study of stem cell physiology. The way in which the microenvironment modulates cell physiology and behavior can be evaluated in the context of different somatic cell types and across different species; the cellular response to exposure to drugs versus placebo can be studied, and the behavior of individual cells in diseased versus healthy conditions can be observed.

REFERENCES

- [1] K.C. Clause, L.J. Liu, K. Tobita, Directed stem cell differentiation: the role of physical forces, *Cell Commun Adhes* 17(2) (2010) 48-54.
- [2] J. Wang, C.D. Wang, N. Zhang, W.X. Tong, Y.F. Zhang, S.Z. Shan, X.L. Zhang, Q.F. Li, Mechanical stimulation orchestrates the osteogenic differentiation of human bone marrow stromal cells by regulating HDAC1, *Cell death & disease* 7(5) (2016) e2221-e2221.
- [3] O. Chaudhuri, L. Gu, D. Klumpers, M. Darnell, S.A. Bencherif, J.C. Weaver, N. Huebsch, H.P. Lee, E. Lippens, G.N. Duda, D.J. Mooney, Hydrogels with tunable stress relaxation regulate stem cell fate and activity, *Nat Mater* 15(3) (2016) 326-34.
- [4] S.R. Chastain, A.K. Kundu, S. Dhar, J.W. Calvert, A.J. Putnam, Adhesion of mesenchymal stem cells to polymer scaffolds occurs via distinct ECM ligands and controls their osteogenic differentiation, *J Biomed Mater Res A* 78(1) (2006) 73-85.
- [5] D.L. Myser, R.J. Duronio, Cell cycle: To differentiate or not to differentiate?, *Current Biology* 10(8) (2000) R302-R304.
- [6] G. Kolios, Y. Moodley, Introduction to stem cells and regenerative medicine, *Respiration* 85(1) (2013) 3-10.
- [7] M.P. De Miguel, S. Fuentes-Julián, Y. Alcaina, Pluripotent stem cells: origin, maintenance and induction, *Stem Cell Rev Rep* 6(4) (2010) 633-49.
- [8] F.D. Houghton, Energy metabolism of the inner cell mass and trophectoderm of the mouse blastocyst, *Differentiation* 74(1) (2006) 11-8.
- [9] S. Mitalipov, D. Wolf, Totipotency, pluripotency and nuclear reprogramming, *Adv Biochem Eng Biotechnol* 114 (2009) 185-99.
- [10] D. Klein, Lung Multipotent Stem Cells of Mesenchymal Nature: Cellular Basis, Clinical Relevance, and Implications for Stem Cell Therapy, *Antioxid Redox Signal* 35(3) (2021) 204-216.
- [11] V.K. Singh, A. Saini, M. Kalsan, N. Kumar, R. Chandra, Describing the Stem Cell Potency: The Various Methods of Functional Assessment and In silico Diagnostics, *Front Cell Dev Biol* 4 (2016) 134.

- [12] R.G. Hawley, A. Ramezani, T.S. Hawley, Hematopoietic stem cells, *Methods Enzymol* 419 (2006) 149-79.
- [13] C.J. Eaves, Hematopoietic stem cells: concepts, definitions, and the new reality, *Blood* 125(17) (2015) 2605-13.
- [14] G.-Y. Chu, Y.-F. Chen, H.-Y. Chen, M.-H. Chan, C.-S. Gau, S.-M. Weng, Stem cell therapy on skin: Mechanisms, recent advances and drug reviewing issues, *Journal of Food and Drug Analysis* 26(1) (2018) 14-20.
- [15] P.C. Sachs, P.A. Mollica, R.D. Bruno, Tissue specific microenvironments: a key tool for tissue engineering and regenerative medicine, *Journal of Biological Engineering* 11 (2017) 34.
- [16] R.D. Bruno, G.H. Smith, Reprogramming non-mammary and cancer cells in the developing mouse mammary gland, *Semin Cell Dev Biol* 23(5) (2012) 591-8.
- [17] Z.G. Venkei, Y.M. Yamashita, Emerging mechanisms of asymmetric stem cell division, *J Cell Biol* 217(11) (2018) 3785-3795.
- [18] A. Vertii, P.D. Kaufman, H. Hehnlly, S. Doxsey, New dimensions of asymmetric division in vertebrates, *Cytoskeleton (Hoboken)* 75(3) (2018) 87-102.
- [19] S. Vora, B.T. Phillips, Centrosome-Associated Degradation Limits β -Catenin Inheritance by Daughter Cells after Asymmetric Division, *Curr Biol* 25(8) (2015) 1005-16.
- [20] C. Chen, Y.M. Yamashita, Centrosome-centric view of asymmetric stem cell division, *Open Biol* 11(1) (2021) 200314-200314.
- [21] S.J. Morrison, A.C. Spradling, Stem cells and niches: mechanisms that promote stem cell maintenance throughout life, *Cell* 132(4) (2008) 598-611.
- [22] R. Nusse, Wnt signaling and stem cell control, *Cell Res* 18(5) (2008) 523-7.
- [23] B.T. MacDonald, K. Tamai, X. He, Wnt/beta-catenin signaling: components, mechanisms, and diseases, *Dev Cell* 17(1) (2009) 9-26.
- [24] N. Bengoa-Vergniory, R.M. Kypta, Canonical and noncanonical Wnt signaling in neural stem/progenitor cells, *Cell Mol Life Sci* 72(21) (2015) 4157-72.
- [25] D. ten Berge, D. Kurek, T. Blauwkamp, W. Koole, A. Maas, E. Eroglu, R.K. Siu, R. Nusse, Embryonic stem cells require Wnt proteins to prevent differentiation to epiblast stem cells, *Nat Cell Biol* 13(9) (2011) 1070-5.

- [26] S.J. Habib, B.C. Chen, F.C. Tsai, K. Anastassiadis, T. Meyer, E. Betzig, R. Nusse, A localized Wnt signal orients asymmetric stem cell division in vitro, *Science* 339(6126) (2013) 1445-8.
- [27] A. Gajos-Michniewicz, M. Czyz, WNT Signaling in Melanoma, *International journal of molecular sciences* 21(14) (2020) 4852.
- [28] R. Schofield, The relationship between the spleen colony-forming cell and the haemopoietic stem cell, *Blood Cells* 4(1-2) (1978) 7-25.
- [29] T.H. Cheung, T.A. Rando, Molecular regulation of stem cell quiescence, *Nat Rev Mol Cell Biol* 14(6) (2013) 329-40.
- [30] H. Clevers, STEM CELLS. What is an adult stem cell?, *Science* 350(6266) (2015) 1319-20.
- [31] S. Lympieri, F. Ferraro, D.T. Scadden, The HSC niche concept has turned 31. Has our knowledge matured?, *Ann N Y Acad Sci* 1192 (2010) 12-8.
- [32] J. Voog, D.L. Jones, Stem cells and the niche: a dynamic duo, *Cell Stem Cell* 6(2) (2010) 103-15.
- [33] F. Ferraro, C.L. Celso, D. Scadden, Adult stem cells and their niches, *Adv Exp Med Biol* 695 (2010) 155-68.
- [34] A.D. Theocharis, D. Manou, N.K. Karamanos, The extracellular matrix as a multitasking player in disease, *Febs j* 286(15) (2019) 2830-2869.
- [35] N.K. Karamanos, A.D. Theocharis, Z. Piperigkou, D. Manou, A. Passi, S.S. Skandalis, D.H. Vynios, V. Orian-Rousseau, S. Ricard-Blum, C.E.H. Schmelzer, L. Duca, M. Durbeej, N.A. Afratis, L. Troeberg, M. Franchi, V. Masola, M. Onisto, A guide to the composition and functions of the extracellular matrix, *The FEBS Journal* 288(24) (2021) 6850-6912.
- [36] B. Yue, Biology of the extracellular matrix: an overview, *J Glaucoma* 23(8 Suppl 1) (2014) S20-S23.
- [37] B. Sun, The mechanics of fibrillar collagen extracellular matrix, *Cell Reports Physical Science* 2(8) (2021) 100515.
- [38] J. Casale, J.S. Crane, *Biochemistry, Glycosaminoglycans, StatPearls, Treasure Island (FL), 2022.*

- [39] R.V. Iozzo, L. Schaefer, Proteoglycan form and function: A comprehensive nomenclature of proteoglycans, *Matrix Biol* 42 (2015) 11-55.
- [40] B.J. Rybarczyk, S.O. Lawrence, P.J. Simpson-Haidaris, Matrix-fibrinogen enhances wound closure by increasing both cell proliferation and migration, *Blood* 102(12) (2003) 4035-4043.
- [41] J. Halper, M. Kjaer, Basic Components of Connective Tissues and Extracellular Matrix: Elastin, Fibrillin, Fibulins, Fibrinogen, Fibronectin, Laminin, Tenascins and Thrombospondins, in: J. Halper (Ed.), *Progress in Heritable Soft Connective Tissue Diseases*, Springer Netherlands, Dordrecht, 2014, pp. 31-47.
- [42] C. Bonnans, J. Chou, Z. Werb, Remodelling the extracellular matrix in development and disease, *Nat Rev Mol Cell Biol* 15(12) (2014) 786-801.
- [43] J.F. Bateman, R.P. Boot-Handford, S.R. Lamandé, Genetic diseases of connective tissues: cellular and extracellular effects of ECM mutations, *Nat Rev Genet* 10(3) (2009) 173-83.
- [44] K.H. Vining, D.J. Mooney, Mechanical forces direct stem cell behaviour in development and regeneration, *Nat Rev Mol Cell Biol* 18(12) (2017) 728-742.
- [45] J.-L. Maître, H. Turlier, R. Illukkumbura, B. Eismann, R. Niwayama, F. Nédélec, T. Hiragi, Asymmetric division of contractile domains couples cell positioning and fate specification, *Nature* 536(7616) (2016) 344-348.
- [46] N. Desprat, W. Supatto, P.A. Pouille, E. Beaurepaire, E. Farge, Tissue deformation modulates twist expression to determine anterior midgut differentiation in *Drosophila* embryos, *Dev Cell* 15(3) (2008) 470-477.
- [47] Y. Yang, S. Beqaj, P. Kemp, I. Ariel, L. Schuger, Stretch-induced alternative splicing of serum response factor promotes bronchial myogenesis and is defective in lung hypoplasia, *J Clin Invest* 106(11) (2000) 1321-30.
- [48] J.R. Hove, R.W. Köster, A.S. Forouhar, G. Acevedo-Bolton, S.E. Fraser, M. Gharib, Intracardiac fluid forces are an essential epigenetic factor for embryonic cardiogenesis, *Nature* 421(6919) (2003) 172-7.
- [49] S.M. Nauli, F.J. Alenghat, Y. Luo, E. Williams, P. Vassilev, X. Li, A.E. Elia, W. Lu, E.M. Brown, S.J. Quinn, D.E. Ingber, J. Zhou, Polycystins 1 and 2 mediate mechanosensation in the primary cilium of kidney cells, *Nat Genet* 33(2) (2003) 129-37.

- [50] N.C. Nowlan, P. Murphy, P.J. Prendergast, A dynamic pattern of mechanical stimulation promotes ossification in avian embryonic long bones, *J Biomech* 41(2) (2008) 249-58.
- [51] J. Tang, R. Peng, J. Ding, The regulation of stem cell differentiation by cell-cell contact on micropatterned material surfaces, *Biomaterials* 31(9) (2010) 2470-6.
- [52] Q. Jiao, X. Li, J. An, Z. Zhang, X. Chen, J. Tan, P. Zhang, H. Lu, Y. Liu, Cell-Cell Connection Enhances Proliferation and Neuronal Differentiation of Rat Embryonic Neural Stem/Progenitor Cells, *Front Cell Neurosci* 11 (2017) 200-200.
- [53] J.S. Park, J.S. Chu, A.D. Tsou, R. Diop, Z. Tang, A. Wang, S. Li, The effect of matrix stiffness on the differentiation of mesenchymal stem cells in response to TGF- β , *Biomaterials* 32(16) (2011) 3921-3930.
- [54] A.J. Engler, S. Sen, H.L. Sweeney, D.E. Discher, Matrix Elasticity Directs Stem Cell Lineage Specification, *Cell* 126(4) (2006) 677-689.
- [55] M. Sun, G. Chi, J. Xu, Y. Tan, J. Xu, S. Lv, Z. Xu, Y. Xia, L. Li, Y. Li, Extracellular matrix stiffness controls osteogenic differentiation of mesenchymal stem cells mediated by integrin $\alpha 5$, *Stem Cell Research & Therapy* 9(1) (2018) 52.
- [56] K. Saha, A.J. Keung, E.F. Irwin, Y. Li, L. Little, D.V. Schaffer, K.E. Healy, Substrate Modulus Directs Neural Stem Cell Behavior, *Biophysical Journal* 95(9) (2008) 4426-4438.
- [57] O. Chaudhuri, L. Gu, D. Klumpers, M. Darnell, S.A. Bencherif, J.C. Weaver, N. Huebsch, H.-p. Lee, E. Lippens, G.N. Duda, D.J. Mooney, Hydrogels with tunable stress relaxation regulate stem cell fate and activity, *Nature Materials* 15(3) (2016) 326-334.
- [58] N. Datta, H.L. Holtorf, V.I. Sikavitsas, J.A. Jansen, A.G. Mikos, Effect of bone extracellular matrix synthesized in vitro on the osteoblastic differentiation of marrow stromal cells, *Biomaterials* 26(9) (2005) 971-977.
- [59] N. Datta, Q.P. Pham, U. Sharma, V.I. Sikavitsas, J.A. Jansen, A.G. Mikos, In vitro generated extracellular matrix and fluid shear stress synergistically enhance 3D osteoblastic differentiation, *Proc Natl Acad Sci U S A* 103(8) (2006) 2488-93.
- [60] E.K.F. Yim, M.P. Sheetz, Force-dependent cell signaling in stem cell differentiation, *Stem Cell Research & Therapy* 3(5) (2012) 41.

- [61] R. McBeath, D.M. Pirone, C.M. Nelson, K. Bhadriraju, C.S. Chen, Cell shape, cytoskeletal tension, and RhoA regulate stem cell lineage commitment, *Dev Cell* 6(4) (2004) 483-95.
- [62] H. Lv, L. Li, M. Sun, Y. Zhang, L. Chen, Y. Rong, Y. Li, Mechanism of regulation of stem cell differentiation by matrix stiffness, *Stem cell research & therapy* 6(1) (2015) 103-103.
- [63] L. Przybyla, J. Voldman, Probing embryonic stem cell autocrine and paracrine signaling using microfluidics, *Annu Rev Anal Chem (Palo Alto Calif)* 5 (2012) 293-315.
- [64] B. Greber, H. Lehrach, J. Adjaye, Fibroblast growth factor 2 modulates transforming growth factor beta signaling in mouse embryonic fibroblasts and human ESCs (hESCs) to support hESC self-renewal, *Stem Cells* 25(2) (2007) 455-64.
- [65] R.H. Xu, T.L. Sampsel-Barron, F. Gu, S. Root, R.M. Peck, G. Pan, J. Yu, J. Antosiewicz-Bourget, S. Tian, R. Stewart, J.A. Thomson, NANOG is a direct target of TGFbeta/activin-mediated SMAD signaling in human ESCs, *Cell Stem Cell* 3(2) (2008) 196-206.
- [66] X. Lim, S.H. Tan, W.L. Koh, R.M. Chau, K.S. Yan, C.J. Kuo, R. van Amerongen, A.M. Klein, R. Nusse, Interfollicular epidermal stem cells self-renew via autocrine Wnt signaling, *Science* 342(6163) (2013) 1226-30.
- [67] A. Pardo-Saganta, P.R. Tata, B.M. Law, B. Saez, R.D. Chow, M. Prabhu, T. Gridley, J. Rajagopal, Parent stem cells can serve as niches for their daughter cells, *Nature* 523(7562) (2015) 597-601.
- [68] M. Gnecci, Z. Zhang, A. Ni, V.J. Dzau, Paracrine mechanisms in adult stem cell signaling and therapy, *Circ Res* 103(11) (2008) 1204-19.
- [69] T. Kinnaird, E. Stabile, M.S. Burnett, C.W. Lee, S. Barr, S. Fuchs, S.E. Epstein, Marrow-derived stromal cells express genes encoding a broad spectrum of arteriogenic cytokines and promote in vitro and in vivo arteriogenesis through paracrine mechanisms, *Circ Res* 94(5) (2004) 678-85.
- [70] A.M. Hocking, N.S. Gibran, Mesenchymal stem cells: paracrine signaling and differentiation during cutaneous wound repair, *Exp Cell Res* 316(14) (2010) 2213-9.
- [71] G. Belenguer, P. Duart-Abadia, A. Jordán-Pla, A. Domingo-Muelas, L. Blasco-Chamarro, S.R. Ferrón, J.M. Morante-Redolat, I. Fariñas, Adult Neural Stem Cells Are

Alerted by Systemic Inflammation through TNF- α Receptor Signaling, *Cell Stem Cell* 28(2) (2021) 285-299.e9.

[72] D. Drummond-Barbosa, Stem cells, their niches and the systemic environment: an aging network, *Genetics* 180(4) (2008) 1787-97.

[73] A. Arvidsson, T. Collin, D. Kirik, Z. Kokaia, O. Lindvall, Neuronal replacement from endogenous precursors in the adult brain after stroke, *Nat Med* 8(9) (2002) 963-70.

[74] K. Takahashi, K. Tanabe, M. Ohnuki, M. Narita, T. Ichisaka, K. Tomoda, S. Yamanaka, Induction of pluripotent stem cells from adult human fibroblasts by defined factors, *Cell* 131(5) (2007) 861-72.

[75] K. Tanabe, K. Takahashi, S. Yamanaka, Induction of pluripotency by defined factors, *Proc Jpn Acad Ser B Phys Biol Sci* 90(3) (2014) 83-96.

[76] N. Malik, M.S. Rao, A review of the methods for human iPSC derivation, *Methods Mol Biol* 997 (2013) 23-33.

[77] J.A. Thomson, J. Itskovitz-Eldor, S.S. Shapiro, M.A. Waknitz, J.J. Swiergiel, V.S. Marshall, J.M. Jones, Embryonic stem cell lines derived from human blastocysts, *Science* 282(5391) (1998) 1145-7.

[78] K. Duval, H. Grover, L.H. Han, Y. Mou, A.F. Pegoraro, J. Fredberg, Z. Chen, Modeling Physiological Events in 2D vs. 3D Cell Culture, *Physiology (Bethesda)* 32(4) (2017) 266-277.

[79] M. Ravi, V. Paramesh, S.R. Kaviya, E. Anuradha, F.D. Solomon, 3D cell culture systems: advantages and applications, *J Cell Physiol* 230(1) (2015) 16-26.

[80] R. Edmondson, J.J. Broglie, A.F. Adcock, L. Yang, Three-dimensional cell culture systems and their applications in drug discovery and cell-based biosensors, *Assay Drug Dev Technol* 12(4) (2014) 207-18.

[81] S.R. Caliari, J.A. Burdick, A practical guide to hydrogels for cell culture, *Nat Methods* 13(5) (2016) 405-14.

[82] C.S. Hughes, L.M. Postovit, G.A. Lajoie, Matrigel: a complex protein mixture required for optimal growth of cell culture, *Proteomics* 10(9) (2010) 1886-90.

[83] E. Polykandriotis, A. Arkudas, R.E. Horch, U. Kneser, To matrigel or not to matrigel, *Am J Pathol* 172(5) (2008) 1441; author reply 1441-2.

- [84] T. Hartung, Thoughts on limitations of animal models, *Parkinsonism Relat Disord* 14 Suppl 2 (2008) S81-3.
- [85] M. Jucker, The benefits and limitations of animal models for translational research in neurodegenerative diseases, *Nat Med* 16(11) (2010) 1210-4.
- [86] P. Kc, Y. Hong, G. Zhang, Cardiac tissue-derived extracellular matrix scaffolds for myocardial repair: advantages and challenges, *Regen Biomater* 6(4) (2019) 185-199.
- [87] S. Croce, A. Peloso, T. Zoro, M.A. Avanzini, L. Cobianchi, A Hepatic Scaffold from Decellularized Liver Tissue: Food for Thought, *Biomolecules* 9(12) (2019) 813.
- [88] P.A. Mollica, E.N. Booth-Creech, J.A. Reid, M. Zamponi, S.M. Sullivan, X.L. Palmer, P.C. Sachs, R.D. Bruno, 3D bioprinted mammary organoids and tumoroids in human mammary derived ECM hydrogels, *Acta Biomater* 95 (2019) 201-213.
- [89] P.M. Crapo, C.J. Medberry, J.E. Reing, S. Tottey, Y. van der Merwe, K.E. Jones, S.F. Badylak, Biologic scaffolds composed of central nervous system extracellular matrix, *Biomaterials* 33(13) (2012) 3539-47.
- [90] J.A. DeQuach, S.H. Yuan, L.S. Goldstein, K.L. Christman, Decellularized porcine brain matrix for cell culture and tissue engineering scaffolds, *Tissue Eng Part A* 17(21-22) (2011) 2583-92.
- [91] C.J. Medberry, P.M. Crapo, B.F. Siu, C.A. Carruthers, M.T. Wolf, S.P. Nagarkar, V. Agrawal, K.E. Jones, J. Kelly, S.A. Johnson, S.S. Velankar, S.C. Watkins, M. Modo, S.F. Badylak, Hydrogels derived from central nervous system extracellular matrix, *Biomaterials* 34(4) (2013) 1033-40.
- [92] M.T. Wolf, K.A. Daly, E.P. Brennan-Pierce, S.A. Johnson, C.A. Carruthers, A. D'Amore, S.P. Nagarkar, S.S. Velankar, S.F. Badylak, A hydrogel derived from decellularized dermal extracellular matrix, *Biomaterials* 33(29) (2012) 7028-7038.
- [93] Y. Zhang, Y. He, S. Bharadwaj, N. Hammam, K. Carnagey, R. Myers, A. Atala, M. Van Dyke, Tissue-specific extracellular matrix coatings for the promotion of cell proliferation and maintenance of cell phenotype, *Biomaterials* 30(23-24) (2009) 4021-8.
- [94] J.A. Reid, X.-L. Palmer, P.A. Mollica, N. Northam, P.C. Sachs, R.D. Bruno, A 3D bioprinter platform for mechanistic analysis of tumoroids and chimeric mammary organoids, *Scientific Reports* 9(1) (2019) 7466.

- [95] J.A. Reid, P.A. Mollica, G.D. Johnson, R.C. Ogle, R.D. Bruno, P.C. Sachs, Accessible bioprinting: adaptation of a low-cost 3D-printer for precise cell placement and stem cell differentiation, *Biofabrication* 8(2) (2016) 025017.
- [96] K. Duval, H. Grover, L.-H. Han, Y. Mou, A.F. Pegoraro, J. Fredberg, Z. Chen, Modeling Physiological Events in 2D vs. 3D Cell Culture, *Physiology* 32(4) (2017) 266-277.
- [97] A. Khoruzhenko, 2D- and 3D-cell culture, 2011.
- [98] R.D. Bruno, J.M. Fleming, A.L. George, C.A. Boulanger, P. Schedin, G.H. Smith, Mammary extracellular matrix directs differentiation of testicular and embryonic stem cells to form functional mammary glands in vivo, *Sci Rep* 7 (2017) 40196.
- [99] A.D. Theocharis, S.S. Skandalis, C. Gialeli, N.K. Karamanos, Extracellular matrix structure, *Advanced Drug Delivery Reviews* 97 (2016) 4-27.
- [100] E. Vorotnikova, D. McIntosh, A. Dewilde, J. Zhang, J.E. Reing, L. Zhang, K. Cordero, K. Bedelbaeva, D. Gourevitch, E. Heber-Katz, S.F. Badylak, S.J. Braunhut, Extracellular matrix-derived products modulate endothelial and progenitor cell migration and proliferation in vitro and stimulate regenerative healing in vivo, *Matrix Biology* 29(8) (2010) 690-700.
- [101] F. Ferraro, C.L. Celso, D. Scadden, ADULT STEM CELLS AND THEIR NICHEs, *Advances in experimental medicine and biology* 695 (2010) 155-168.
- [102] W. Yan, W. Liu, J. Qi, Q. Fang, Z. Fan, G. Sun, Y. Han, D. Zhang, L. Xu, M. Wang, J. Li, F. Chen, D. Liu, R. Chai, H. Wang, A Three-Dimensional Culture System with Matrigel Promotes Purified Spiral Ganglion Neuron Survival and Function In Vitro, *Mol Neurobiol* (2017).
- [103] G. Sun, W. Liu, Z. Fan, D. Zhang, Y. Han, L. Xu, J. Qi, S. Zhang, B.T. Gao, X. Bai, J. Li, R. Chai, H. Wang, The Three-Dimensional Culture System with Matrigel and Neurotrophic Factors Preserves the Structure and Function of Spiral Ganglion Neuron In Vitro, *Neural Plast* 2016 (2016) 4280407.
- [104] A.N. Cho, Y. Jin, S. Kim, S. Kumar, H. Shin, H.C. Kang, S.W. Cho, Aligned Brain Extracellular Matrix Promotes Differentiation and Myelination of Human-Induced Pluripotent Stem Cell-Derived Oligodendrocytes, *ACS Appl Mater Interfaces* 11(17) (2019) 15344-15353.

- [105] Y. Wu, J. Wang, Y. Shi, H. Pu, R.K. Leak, A.K.F. Liou, S.F. Badylak, Z. Liu, J. Zhang, J. Chen, L. Chen, Implantation of Brain-Derived Extracellular Matrix Enhances Neurological Recovery after Traumatic Brain Injury, *Cell Transplant* 26(7) (2017) 1224-1234.
- [106] D. Sood, D.M. Cairns, J.M. Dabbi, C. Ramakrishnan, K. Deisseroth, L.D. Black, 3rd, S. Santaniello, D.L. Kaplan, Functional maturation of human neural stem cells in a 3D bioengineered brain model enriched with fetal brain-derived matrix, *Sci Rep* 9(1) (2019) 17874.
- [107] P.A. Mollica, E.N. Booth-Creech, J.A. Reid, M. Zamponi, S.M. Sullivan, X.-L. Palmer, P.C. Sachs, R.D. Bruno, 3D bioprinted mammary organoids and tumoroids in human mammary derived ECM hydrogels, *Acta Biomaterialia* 95 (2019) 201-213.
- [108] J.A. Reid, P.A. Mollica, R.D. Bruno, P.C. Sachs, Consistent and reproducible cultures of large-scale 3D mammary epithelial structures using an accessible bioprinting platform, *Breast Cancer Res* 20(1) (2018) 122.
- [109] P.A. Mollica, M. Zamponi, J.A. Reid, D.K. Sharma, A.E. White, R.C. Ogle, R.D. Bruno, P.C. Sachs, Epigenetic alterations mediate iPSC normalization of DNA-repair expression and TNR stability in Huntington's disease, *Journal of Cell Science* (2018).
- [110] J.T. Dimos, K.T. Rodolfa, K.K. Niakan, L.M. Weisenthal, H. Mitsumoto, W. Chung, G.F. Croft, G. Saphier, R. Leibel, R. Goland, H. Wichterle, C.E. Henderson, K. Eggan, Induced pluripotent stem cells generated from patients with ALS can be differentiated into motor neurons, *Science* 321(5893) (2008) 1218-21.
- [111] M. Ehrlich, S. Mozafari, M. Glatza, L. Starost, S. Velychko, A.L. Hallmann, Q.L. Cui, A. Schambach, K.P. Kim, C. Bachelin, A. Marteyn, G. Hargus, R.M. Johnson, J. Antel, J. Sternecker, H. Zaehres, H.R. Scholer, A. Baron-Van Evercooren, T. Kuhlmann, Rapid and efficient generation of oligodendrocytes from human induced pluripotent stem cells using transcription factors, *Proc Natl Acad Sci U S A* 114(11) (2017) E2243-E2252.
- [112] E. Deneault, S.H. White, D.C. Rodrigues, P.J. Ross, M. Faheem, K. Zaslavsky, Z. Wang, R. Alexandrova, G. Pellecchia, W. Wei, A. Piekna, G. Kaur, J.L. Howe, V. Kwan, B. Thiruvahindrapuram, S. Walker, A.C. Lionel, P. Pasceri, D. Merico, R.K.C. Yuen,

- K.K. Singh, J. Ellis, S.W. Scherer, Complete Disruption of Autism-Susceptibility Genes by Gene Editing Predominantly Reduces Functional Connectivity of Isogenic Human Neurons, *Stem Cell Reports* 11(5) (2018) 1211-1225.
- [113] M. Molina-Calavita, M. Barnat, S. Elias, E. Aparicio, M. Piel, S. Humbert, Mutant huntingtin affects cortical progenitor cell division and development of the mouse neocortex, *J Neurosci* 34(30) (2014) 10034-40.
- [114] S. Yu, D. Liu, T. Wang, Y.Z. Lee, J.C.N. Wong, X. Song, Micropatterning of polymer substrates for cell culture, *J Biomed Mater Res B Appl Biomater* 109(10) (2021) 1525-1533.
- [115] N.F. Huang, B. Patlolla, O. Abilez, H. Sharma, J. Rajadas, R.E. Beygui, C.K. Zarins, J.P. Cooke, A matrix micropatterning platform for cell localization and stem cell fate determination, *Acta Biomater* 6(12) (2010) 4614-21.
- [116] D.M. Cohen, C.S. Chen, Mechanical control of stem cell differentiation, *StemBook*, Cambridge (MA), 2008.
- [117] M.C. Cramer, S.F. Badylak, Extracellular Matrix-Based Biomaterials and Their Influence Upon Cell Behavior, *Ann Biomed Eng* 48(7) (2020) 2132-2153.

VITA

Martina Zamponi**Education:**

Ph.D. in Biomedical Engineering, August 2022, Old Dominion University, Norfolk, VA

M.S. in Biomedical Engineering, August 2018, Old Dominion University, Norfolk, VA

B.S in Biology, August 2017, Old Dominion University, Norfolk, VA

Certifications:

Molecular Laboratory Technologist – MB(ASCP)

Publications

Zamponi, M., Mollica P.A., Sachs, P.C., Bruno, R.D. Effects of a brain extracellular matrix-derived 3D cell culture system on stem cell culture and differentiation. (Submitted)

Zamponi, M., Mollica P.A., Bruno, R.D., Sachs P.C. A high-throughput 3D bioprinting system for the study of asymmetrical stem cell division at single cell resolution. (In Progress)

Zamponi, M., Tardif-Kunk, M, Mollica, P.A. Applied picosecond pulsed electric fields affect the pluripotency state of human induced pluripotent stem cells. (In Progress)

Zamponi, M., Petrella, A. R., Mollica, P.A. Picosecond Pulsed Electric Fields and Promise in Neurodegeneration Research. In Press. *Bioelectricity*

Peter A Mollica, PhD; Elizabeth Creech; **Martina Zamponi, MS**; John A Reid, PhD; Shae M Sullivan; Robert D Bruno, PhD (2018) 3D bioprinted growth of mammary organoids and tumoroids in human mammary derived ECM hydrogels. In Press. *Acta Biomaterialia*

Petrella, R. A., Mollica, P. A., **Zamponi, M.**, Xiao, S., Bruno, R. D., and Sachs P. C. Picosecond pulsed electric fields up-regulate SOX2 gene expression in mesenchymal stem cells. In Press. *IEEE Journal of Electromagnetics, RF and Microwaves in Medicine and Biology*

Petrella, R. A., Mollica, P. A., **Zamponi, M.**, Reid, J. A., Ogle, R.C., Xiao, S., Bruno, R. D., and Sachs, P. C. 3D bioprinter applied picosecond pulsed electric fields for targeted manipulation of proliferation and lineage specific gene expression in neural stem cells. In Press. *Journal of Neural Engineering*

Mollica, P. A., **Zamponi, M.**, Reid, J. A., Sharma, D. K., White, A. E., Ogle, R. C., Bruno, R. D., and Sachs, P. C. (2018) Epigenetic alterations mediate pluripotency-induced normalization of DNA-repair and TNR stability in Huntington's disease. In Press. *Journal of Cell Science*